NASA/CR—2003-212359 MTI 95TM5



Users' Manual for Computer Code SPIRALI

Incompressible, Turbulent Spiral Grooved Cylindrical and Face Seals

Jed A. Walowit
Jed A. Walowit, Inc., Clifton Park, New York

Wilbur Shapiro
Mechanical Technology, Inc., Latham, New York

Restriction changed to Unclassified/Unlimited on July 27, 2005, by authority of the NASA Glenn Research Center, Structures Division.

Export Administration Regulations (EAR) Notice

This document contains information within the purview of the Export Administration Regulations (EAR), 15 CFR 730–774, and is export controlled. It may not be transferred to foreign nationals in the U.S. or abroad without specific approval of a knowledgeable NASA export control official, and/or unless an export license/license exception is obtained/available from the Bureau of Industry and Security, United States Department of Commerce. Violations of these regulations are punishable by fine, imprisonment, or both.

October 2005

The NASA STI Program Office . . . in Profile

Since its founding, NASA has been dedicated to the advancement of aeronautics and space science. The NASA Scientific and Technical Information (STI) Program Office plays a key part in helping NASA maintain this important role.

The NASA STI Program Office is operated by Langley Research Center, the Lead Center for NASA's scientific and technical information. The NASA STI Program Office provides access to the NASA STI Database, the largest collection of aeronautical and space science STI in the world. The Program Office is also NASA's institutional mechanism for disseminating the results of its research and development activities. These results are published by NASA in the NASA STI Report Series, which includes the following report types:

- TECHNICAL PUBLICATION. Reports of completed research or a major significant phase of research that present the results of NASA programs and include extensive data or theoretical analysis. Includes compilations of significant scientific and technical data and information deemed to be of continuing reference value. NASA's counterpart of peer-reviewed formal professional papers but has less stringent limitations on manuscript length and extent of graphic presentations.

- TECHNICAL MEMORANDUM. Scientific and technical findings that are preliminary or of specialized interest, e.g., quick release reports, working papers, and bibliographies that contain minimal annotation. Does not contain extensive analysis.

- CONTRACTOR REPORT. Scientific and technical findings by NASA-sponsored contractors and grantees.

- CONFERENCE PUBLICATION. Collected papers from scientific and technical conferences, symposia, seminars, or other meetings sponsored or cosponsored by NASA.

- SPECIAL PUBLICATION. Scientific, technical, or historical information from NASA programs, projects, and missions, often concerned with subjects having substantial public interest.

- TECHNICAL TRANSLATION. English-language translations of foreign scientific and technical material pertinent to NASA's mission.

Specialized services that complement the STI Program Office's diverse offerings include creating custom thesauri, building customized databases, organizing and publishing research results . . . even providing videos.

For more information about the NASA STI Program Office, see the following:

- Access the NASA STI Program Home Page at ***http://www.sti.nasa.gov***

- E-mail your question via the Internet to help@sti.nasa.gov

- Fax your question to the NASA Access Help Desk at 301–621–0134

- Telephone the NASA Access Help Desk at 301–621–0390

- Write to:
 NASA Access Help Desk
 NASA Center for AeroSpace Information
 7121 Standard Drive
 Hanover, MD 21076

NASA/CR—2003-212359 MTI 95TM5



Users' Manual for Computer Code SPIRALI

Incompressible, Turbulent Spiral Grooved Cylindrical and Face Seals

Jed A. Walowit
Jed A. Walowit, Inc., Clifton Park, New York

Wilbur Shapiro
Mechanical Technology Inc., Latham, New York

Restriction changed to Unclassified/Unlimited on July 27, 2005, by authority of the NASA Glenn Research Center, Structures Division.

Export Administration Regulations (EAR) Notice

This document contains information within the purview of the Export Administration Regulations (EAR), 15 CFR 730–774, and is export controlled. It may not be transferred to foreign nationals in the U.S. or abroad without specific approval of a knowledgeable NASA export control official, and/or unless an export license/license exception is obtained/available from the Bureau of Industry and Security, United States Department of Commerce. Violations of these regulations are punishable by fine, imprisonment, or both.

Prepared under Contract NAS3–25644

National Aeronautics and
Space Administration

Glenn Research Center

October 2005

Document History

The source and executable files for the CFD Seal Analysis Industrial Codes, of which this is a part, were released as LEW–16582 in 1998. This report was originally published by Mechanical Technology, Inc., in March 1995.

Document Availability Change Notice

NASA/CR—2003-212359

Users' Manual for Computer Code SPIRALI Incompressible, Turbulent Spiral Grooved Cylindrical and Face Seals

Jed A. Walowit and Wilbur Shapiro

This document was published in July 2003 with the restriction Export Administration Regulations (EAR). It was changed to Unclassified/Unlimited July 27, 2005, by authority of the NASA Glenn Research Center, Structures Division.

Per the STI Program Office and Code I at Headquarters, you may modify copies in your possession. The restriction notice on the cover, title page, and Report Documentation Page should be boldly crossed out and the above statement printed clearly above or below it.

Trade names or manufacturers' names are used in this report for identification only. This usage does not constitute an official endorsement, either expressed or implied, by the National Aeronautics and Space Administration.

This work was sponsored by the Low Emissions Alternative Power Project of the Vehicle Systems Program at the NASA Glenn Research Center.

Available from

NASA Center for Aerospace Information
7121 Standard Drive
Hanover, MD 21076

National Technical Information Service
5285 Port Royal Road
Springfield, VA 22100

Available electronically at http://gltrs.grc.nasa.gov

Table of Contents

List of Figures v

Nomenclature vii

1. Introduction 1

2. Formulation and Method of Solution 3
 - Formulation of bulk flow equations for turbulent lubrication 3
 - Boundary and continuity conditions 7
 - Narrow groove theory for spiral groove seals 9
 - Development of first and second order equations for small displacements 17
 - Solution to first order flow equations 19
 - Solution to second order flow equations 20
 - Forces, moments and dynamic coefficients 23
 - Determination of power loss and flow 27

3. Description of Computer Code SPIRALI 29
 - Input description for SPIRALI 32
 - Description of output from SPIRALI 34

4. Sample Problems 36

5. Verification 49

6. Operating Environment 63

7. Error Messages 64

8. References 66

APPENDIX A: Application to Parallel and Helical Grooved Seals 69

List of Figures

Figure 1 Coordinate system for spiral groove analysis. 4

Figure 2 Velocities and forces on a differential element in the θ direction. 5

Figure 3 Jump in film thickness.. 7

Figure 4 Examples of degrees of film formation in groove 10

Figure 5 Schematic of spiral groove parameters, global and local pressures, Case a 11

Figure 6 Schematic of spiral groove parameters, global and local pressures, Case b 12

Figure 7 Parameters for characterizing quadratic film variation. 30

Figure 8 Flow diagram for overall logic used in computations 31

Figure 9 Namelist defaults 35

Figure 10 Schematic of cylindrical seal for cases 1 - 5 37

Figure 11 Stator with inward pumping grooves for cases 6 - 8 43

Nomenclature

[A]	apparent mass matrix, see Eq. (90)
[B]	damping matrix, see subscripts below for definitions of components
[$\tilde{B}$]	dimensionless stiffness matrix, see Eq. (89) for component scale factors
C	clearance (cylindrical seal) or reference film thickness (face seal)
e_x, e_z	displacements of center of seal in x,z directions, see Fig. 1
$\tilde{e}_x, \tilde{e}_z$	dimensionless displacements, e_x/C, e_z/C
$\tilde{e}_{x0}, \tilde{e}_{z0}$	dimensionless displacement amplitudes, see Eq. (60)
F	function defining derivatives, see Eqs. (56)-(58)
f	shear factor (¼ friction factor)
f_a	shear factor at surface (a), see Eq. (4)
f_b	shear factor at surface (b), see Eq. (5)
H	first order film thickness
$\tilde{H}$	dimensionless film thickness, H/C
H_{BRL}	film change defining quadratic "barreling", see Fig. 5
H_r	first order film thickness over ridges
H_{TAP}	film change defining linear taper, see Fig. 5
h	film thickness
$\tilde{h}$	dimensionless film thickness, h/C
h′	second order film thickness
$\tilde{h}'$	dimensionless film thickness, h′/C
h_g	film thickness over grooves, see Fig. 4
$\tilde{h}_g$	dimensionless film thickness, h_g/C
h_r	film thickness over ridges, see Fig. 4
$\tilde{h}_r$	dimensionless film thickness, h_r/C
[I]	unit diagonal matrix of order N
I_c	cylindrical seal flag parameter, I_c=1 for cylindrical seal, I_c=0 for face seal
I_f	face seal flag parameter, I_f=1 for face seal, I_f=0 for cylindrical seal
I_ω	rotating groove flag parameter, I_ω=1 for grooves on rotor, I_ω=0 for grooves on stator
I	unit imaginary number, $\sqrt{-1}$
$\vec{i}, \vec{j}$	unit vectors in θ,s directions
$\Im(Z)$	imaginary part of complex number, Z
J_k	see Eq. (64)
[K]	stiffness matrix, see subscripts below for definitions of components
[$\tilde{K}$]	dimensionless stiffness matrix, see Eq. (88) for component definitions
[K^0]	stiffness matrix, [K] at Ω=0

$[k]$	derivative matrix used in numerical solution, see Eq. (58) for definitions of components
L	seal length, see Fig. 1
M_x, M_y	applied moments about x, y axes
$\tilde{M}_x, \tilde{M}_y$	dimensionless moments, $M_x/(p_0 r_0^3)$, $M_y/(p_0 r_0^3)$
m_a	exponent in shear factor power law relationship for surface(a), $f_a = n_a R_a^{m_a}$
m_b	exponent in shear factor power law relationship for surface(a), $f_b = n_b R_b^{m_b}$
m_0	exponent for shear factor power law based on Blasius relationship, see Eq. (7)
N	order of system of ordinary differential equations, see Eqs. (56)-(58)
N_g	number of grooves
n_a	coefficient in shear factor power law relationship for surface(a), $f_a = n_a R_a^{m_a}$
n_b	coefficient in shear factor power law relationship for surface(a), $f_b = n_b R_b^{m_b}$
n_0	coefficient for shear factor power law based on Blasius relationship, see Eq. (7)
$\vec{n}_\beta$	unit vector normal to grooves, see Fig. 4
P	first order pressure
$\bar{P}$	dimensionless pressure, P/p_0
$\tilde{P}_{g,\theta}$	dimensionless first order local tangential pressure gradient over grooves see Eq. (94)
p	pressure
$\tilde{p}$	dimensionless pressure, p/p_0
p'	second order pressure
$\tilde{p}'$	dimensionless pressure, p'/p_0
p_0	reference pressure
$\tilde{p}^*$	dimensionless parameter, $\mu V_0 r_0/(4C^2 p_0)$
p_J	pressure at upstream side of jump in film thickness
p_J'	second order pressure at upstream side of jump in film thickness
$\hat{p}_k$	component of second order pressure, $\tilde{p}'$, associated with δ_k, see Eq. (65)
$\hat{p}_k^+, \hat{p}_k^-$	complex, second order, dimensionless component pressures, see Eqs. (66)-(67)
$\overline{p}_k^+, \overline{p}_k^-$	complex S dependent factors of $\tilde{p}_k$ and $\hat{p}_k$ respectively, see Eq. (67)
p_{ex}	pressure at exit side of seal
p_{in}	pressure at inlet side of seal
$\tilde{p}_{ex}, \tilde{p}_{in}$	dimensionless pressures, p_{ex}/p_0, p_{in}/p_0
$p_{g,\theta}, p_{g,s}$	local pressure gradients over grooves in tangential ($p_{g,\theta}$) and transverse ($p_{g,s}$) directions
$\tilde{p}_{g,\theta}, \tilde{p}_{g,s}$	dimensionless local pressure gradients $r_0 p_{g,\theta}/p_0$, $r_0 p_{g,s}/p_0$, see Eqs. (24)-(25)
$p_{r,\theta}, p_{r,s}$	local pressure gradients over ridges in tangential ($p_{r,\theta}$) and transverse ($p_{r,s}$) directions
$\tilde{p}_{r,\theta}, \tilde{p}_{r,s}$	dimensionless local pressure gradients $r_0 p_{r,\theta}/p_0$, $r_0 p_{r,s}/p_0$, see Eqs. (26)-(27)
$\wp$	power loss
$\tilde{\wp}$	dimensionless power loss, $\wp/(C_p r_0 \omega^2)$
Q	volumetric flow rate in transverse (s) direction

$\tilde{q}_{g\theta}, \tilde{q}_{gs}$	dimensionless flow components over grooves, $\tilde{u}_g \tilde{h}_g$, $\tilde{v}_g \tilde{h}_g$
$\tilde{q}_{r\theta}, \tilde{q}_{rs}$	dimensionless flow components over ridges, $\tilde{u}_r \tilde{h}_r$, $\tilde{v}_r \tilde{h}_r$
q_n	flow rate in $\vec{n}_\beta$ direction relative to spiral groove motion
$\tilde{q}_n$	dimensionless flow rate normal to spiral grooves, $q_n/(h_0 V_0)$
R	Reynolds number, see Eq. (9)
R^*	characteristic inertia parameter, $2CR/r_0$
R_a	local Reynolds number associated with surface (a), see Eq. (6)
R_b	local Reynolds number associated with surface (b), see Eq. (6)
r	radial coordinate, taken as r_0 for cylindrical seal
$\tilde{r}$	dimensionless coordinate, r/r_0 taken as 1 for cylindrical seal
r_0	reference radius, taken as outside radius for face seal and shaft radius for cylindrical seal
$\Re(Z)$	real part of complex number, Z
S	dimensionless coordinate, s/r_0
S_J	dimensionless coordinate s_j/r_0
S_L, S_R	dimensionless boundary coordinates s_L/r_0, s_R/r_0
S_{in}, S_{ex}	dimensionless coordinates s_{in}/r_0, s_{ex}/r_0
s	transverse coordinate, s = r for a face seal and s = z for a cylindrical seal
s_J	s coordinate at jump in film thickness
s_L	left boundary coordinate, inside radius for face seal and s_L = -L/2 for cylindrical seal
s_R	right boundary coordinate, $s_R = r_0$ for face seal and s_R = L/2 for cylindrical seal
s_{ex}	s coordinate at exit from seal
s_{in}	s coordinate at inlet to seal
t	time
$\tilde{t}$	dimensionless time, $V_0 t/r_0$
$\vec{t}_\beta$	unit vector tangent to grooves, see Fig. 4
U	first order tangential (θ) velocity component
$\tilde{U}$	dimensionless velocity, U/V_0
u	tangential (θ) velocity component
$\tilde{u}$	dimensionless velocity, u/V_0
u'	second order tangential (θ) velocity component
$\tilde{u}'$	dimensionless velocity u'/V_0
$\vec{u}$	fluid velocity vector
$\vec{u}_a$	velocity of surface a, see Fig. 2
$\vec{u}_b$	velocity of surface b, see Fig. 2
u_g, u_r	tangential velocity over grooves (u_g), ridges (u_r)
$\tilde{u}_g, \tilde{u}_r$	dimensionless velocity components u_g/V_0, u_r/V_0
u_{in}	tangential velocity component at inlet side of seal

$\tilde{u}_{in}$	dimensionless velocity, u_{in}/V_0
$\hat{u}_k$	component of $\tilde{u}'$, associated with δ_k, see Eq. (65)
$\hat{u}_k^+, \hat{u}_k$	complex, second order, dimensionless component tangential velocities, see Eqs. (66)-(67)
$\overline{u}_k^+, \overline{u}_k$	complex S dependent factors of $\hat{u}_k$ and $\hat{u}_k$ respectively, see Eq. (67)
V	first order transverse (s) velocity component
$\tilde{V}$	dimensionless velocity, V/V_0
V_0	reference velocity
v	transverse (s) velocity component
$\tilde{v}$	dimensionless velocity component, v/V_0
v'	second order transverse (s) velocity component
$\tilde{v}'$	dimensionless velocity v'/V_0
v_g, v_r	transverse velocity over grooves (v_g), ridges (v_r)
$\tilde{v}_g, \tilde{v}_r$	dimensionless velocity components v_g/V_0, v_r/V_0
v_J	s velocity component at upstream side of jump in film thickness
$\tilde{v}_J$	dimensionless velocity v_J/V_0
v_J'	second order s velocity component at upstream side of jump in film thickness
$\tilde{v}_J'$	dimensionless velocity v_J'/V_0
$\hat{v}_k$	component of $\tilde{v}'$, associated with δ_k, see Eq. (65)
$\hat{v}_k^+, \hat{v}_k$	complex, second order, dimensionless component transverse velocities, see Eqs. (66)-(67)
$\overline{v}_k^+, \overline{v}_k$	complex S dependent factors of $\hat{v}_k$ and $\hat{v}_k$ respectively, see Eq. (67)
W_z	first order axial load applied to face seal
$\tilde{W}_z$	dimensionless load, $W_z/(p_0 r_0^2)$
w_x, w_y, w_z	applied loads in x, y, z directions
$\tilde{w}_x, \tilde{w}_y, \tilde{w}_z$	dimensionless loads, $w_x/(p_0 r_0^2)$, $w_y/(p_0 r_0^2)$, $w_z/(p_0 r_0^2)$
x, y, z	coordinate variables, see Fig. 1
$\{Y\}$	column vector of independent variables at old grid point, see Eqs. (56)-(58)
$\{Y^{new}\}$	column vector of independent variables at new grid point, see Eqs. (56)-(58)
α	groove to pitch ratio, $\Delta\theta_g/(\Delta\theta_g+\Delta\theta_r)$
β	spiral groove angle, angle between grooves and surface velocity
Δh	jump in film thickness (downstream - upstream)
$\Delta\tilde{h}$	dimensionless jump in film thickness, $\Delta h/C$
Δp	jump in pressure at s_J, $p-p_J$
$\Delta\tilde{p}$	dimensionless jump in pressure, $\Delta p/p_0$
$\Delta\tilde{p}'$	dimensionless second order jump in pressure at S_J, $(p'-p_J')/p_0$
$\Delta p_g, \Delta p_r$	spiral grv. downstream - upstream pressure jump at entrance to grooves, (Δp_g) or ridges, (Δp_r)
$\Delta\tilde{p}_g, \Delta\tilde{p}_r$	dimensionless spiral groove pressure jumps, $\Delta p_g/p_0$, $\Delta p_r/p_0$
ΔS	variable increment between grid points used in numerical solutions, see Eqs. (57)-(58)

$\Delta\theta$	circumferential extent of groove-ridge pair, see Fig. 4
$\Delta\theta_g$	circumferential extent of groove, see Fig. 4
$\Delta\theta_r$	circumferential extent of ridge, see Fig. 4
δ	groove depth, h_g-h_r
$\tilde{\delta}$	dimensionless groove depth, δ/C
δ_k	dimensionless component film displacements, see Eqs. (59)-(61)
δ_k^+, δ_k^-	complex dimensionless component displacements associated with $+\tilde{\Omega}$ and $-\tilde{\Omega}$ resp., see Eq. (63)
ϵ_k	set of amplitudes, see Eq. (64)
ζ	loss coefficient due to contraction
η_k	see Eq. (64)
θ	angular coordinate, see Fig. 1
λ	correction factor applied to $\tilde{\tau}_c$, see Eq. (94)
μ	viscosity
ξ	loss coefficient, see Eq. (18)
ρ	density
τ	tangential shear stress
$\tilde{\tau}$	dimensionless shear stress, $r\tau/(Cp_0)$
τ_a	tangential shear stress, surface (a)
$\tilde{\tau}_a$	dimensionless shear stress, $r_0\tau_a/(Cp_0)$
$\vec{\tau}_a$	shear traction vector for surface (a), see Fig. 2
τ_b	tangential shear stress, surface (b)
$\tilde{\tau}_b$	dimensionless shear stress, $r_0\tau_b/(Cp_0)$
$\vec{\tau}_b$	shear traction vector for surface (b), see Fig. 2
$\tilde{\tau}_c$	dimensionless tangential Couette shear stress, $(\tilde{\tau}_a + \tilde{\tau}_b)/2$
$\vec{\tau}_c$	Couette shear traction vector, $(\vec{\tau}_a + \vec{\tau}_b)/2$
$\tilde{\tau}_p$	dimensionless tangential Poiseuille shear stress, $(\tilde{\tau}_a - \tilde{\tau}_b)/2$
$\vec{\tau}_p$	Poiseuille shear traction vector, $(\vec{\tau}_a - \vec{\tau}_b)/2$
$\tilde{\tau}^*$	dimensionless effective shear stress, see Eq. (92)
$\tilde{\tau}_g^*, \tilde{\tau}_r^*$	values of $\tilde{\tau}^*$ obtained from first order solutions for grooves and ridges respectively
Φ, Ψ	turbulent shear functions, see Eqs. (14)-(15)
Φ^*, Ψ^*	global functions defined by Eqs. (42)-(43)
Φ_g, Ψ_g	turbulent shear functions over grooves, see Eq. (22)
Φ_r, Ψ_r	turbulent shear functions over ridges, see Eq. (23)
χ	function for predicting pressure change at jump in film thickness, see Eq. (17)
ψ	rotation about y axis, see Fig. 1
$\tilde{\psi}_0$	dimensionless amplitude, see Eq. (60)
Ω	angular velocity of oscillation

$\tilde{\Omega}$	dimensionless angular velocity, $\Omega r / V_0$
$\tilde{\Omega}^+, \tilde{\Omega}^-$	see Eq. (71)
ω	angular velocity of rotor
$\tilde{\omega}$	dimensionless angular velocity, $\omega r / V_0$

Subscripts

a,b	relating to surface (a),(b) shown in Fig. 2, generally (a) is moving, (b) is stationary
ex	exit
g	grooves
$\tilde{H}, \tilde{U}, \tilde{V}$	partial derivatives with respect to $\tilde{H}$, $\tilde{U}$ and $\tilde{V}$ respectively
in	inlet
J	jump discontinuity in global film thickness
k	index associated with displacements, see Eq. (64)
L	left or lower value of s
R	right or upper value of s
r	ridges
x	pertains to force or displacement in the x direction
y	pertains to force or displacement in the y direction
ϕ	pertains to moment or rotation about x axis
ψ	pertains to moment or rotation about y axis

1. Introduction

Spiral groove bearings and seals are used to provide stability, load support and pumping for both cylindrical and face seal geometries. In the case of a cylindrical bearing, grooves are usually designed to pump against each other in a symmetric arrangement to provide enhanced stability. A lightly loaded cylindrical seal operating at a low axial flow rate will produce a force that is nearly 90 degrees out of phase with the displacement which will tend to destabilize the rotating shaft. The introduction of spiral grooves can significantly increase the component of force in phase with the displacement and decrease the out of phase component thereby improving stability.

In the case of a face seal or thrust bearing, spiral grooves are often introduced as the primary means of load support. Since a symmetric arrangement is not possible in a radial geometry, the grooves are usually designed to pump towards an ungrooved dam region. The resistance of the dam region increases as the film thickness decreases hence the pumping pressure rise increases thereby giving rise to a positive axial stiffness. The spiral grooves can also be used to pump against an applied pressure gradient thereby resulting in either reduced or reversed leakage.

The computer codes developed here are oriented toward the prediction of performance characteristics of incompressible cylindrical and face seals with or without the inclusion of spiral grooves. Performance characteristics include load capacity (for face seals), leakage flow, power requirements and dynamic characteristics in the form of stiffness, damping and apparent mass coefficients in 4 degrees of freedom for cylindrical seals and 3 degrees of freedom for face seals. These performance characteristics are computed as functions of seal and groove geometry, load or film thickness, running and disturbance speeds, fluid viscosity, and boundary pressures.

The basic assumptions that have gone into the computer code are listed below:

1. The flow is assumed to be isothermal and incompressible.

2. Turbulence is treated with an extended form of the Hirs bulk flow model (reference 1), generalized to include separate and arbitrary friction factor - Reynolds number relationships for each surface.

3. Inertia effects (which throughout this report will refer to additional effects to those inherent in turbulence) associated with film discontinuities will be treated with the use of loss coefficients.

4. Circumferential and transient effects are treated with the use of small perturbations to a steady state first order solution for a concentric, aligned seal. These effects are characterized by either by

stiffness and damping coefficients that are dependent on the disturbance frequencies or by stiffness, damping, and apparent mass coefficients.

5. The film thickness is assumed to be small compared with seal lengths and diameters but large compared with surface roughness.

6. Narrow groove theory is used to characterize the effects of grooves by a global pressure distribution without requiring computations on a groove by groove basis. This has previously involved neglecting edge effects and local inertia effects associated with groove to groove pressure variations. In general, narrow groove theory is valid when there are a sufficiently large number of grooves so that $2\pi/N_g << 1$, where N_g is the number of grooves. This theory has been extended to account for the pressure jumps arising from the effects of local inertia associated with the sudden changes in cross section at the inlet to each groove and ridge which can be of the order of N_g larger than the other local inertia effects which have been neglected.

7. Although transverse (axial for cylindrical seals or radial for face seals) variations in the film thickness profiles are permitted, machined surfaces for seals are assumed to be axisymmetric with the exception of effects of spiral grooves.

The above assumptions still leave the code applicable to a broad range of cylindrical and face seal applications. Practical designs should contain a fairly large number of grooves to ensure smooth, isotropic operation. Elastic and thermal distortions as well as machining tolerances should also be estimated to validate the axisymmetric clearance assumption and may be characterized in part by inclusion of film variations in the transverse direction. The overall accuracy of the program will depend on the grid size used. Factors such as large film thickness variations in the transverse direction, inclusion of very small transverse inertia effects and large values of the length to diameter ratio could require an increased number of grid points.

A derivation of the equations governing the performance of turbulent, incompressible, spiral groove cylindrical and face seals along with a description of their solution is given in the next section. This will be followed by a description of the computer codes including an input description, sample cases and comparisons with results of other codes.

2. Formulation and Method of Solution

Coordinate variables will be used to make the equations developed here applicable to both cylindrical and face seals and may be defined with the aid of Figure 1. The circumferential coordinate, θ, is as shown in Figure 1. The transverse coordinate is described by the variable, **s**, which is taken to equal the radial coordinate, **r**, for a face seal and the axial coordinate, **z**, for a cylindrical seal. The quantity **r**, when it appears will denote radial position for a face seal and should be set equal to the shaft radius, $\mathbf{R_0}$ for a cylindrical seal. The symbols $\vec{i}, \vec{j}$ will be used to denote unit vectors in the θ and **s** directions respectively.

Formulation of bulk flow equations for turbulent lubrication

The equations for turbulent bulk flow to be presented here will be based on a generalization of the Hirs model. Figure 2 shows the velocities and forces associated with a differential element in the θ direction. The bulk flow integrated momentum equations for the θ and **s** directions are

$$\rho h\left(\frac{\partial u}{\partial t}+v\frac{\partial u}{\partial s}+\frac{u}{r}\frac{\partial u}{\partial \theta}+\frac{uvl_f}{r}\right)=-\frac{h}{r}\frac{\partial p}{\partial \theta}+(\vec{\tau}_b-\vec{\tau}_a)\cdot\vec{i}\quad , \tag{1}$$

$$\rho h\left(\frac{\partial v}{\partial t}+v\frac{\partial v}{\partial s}+\frac{u}{r}\frac{\partial v}{\partial \theta}-\frac{u^2 l_f}{r}\right)=-h\frac{\partial p}{\partial s}+(\vec{\tau}_b-\vec{\tau}_a)\cdot\vec{j}\quad . \tag{2}$$

The integrated continuity equation is

$$\frac{1}{r}\frac{\partial}{\partial s}(rvh)+\frac{1}{r}\frac{\partial}{\partial \theta}(uh)+\frac{\partial h}{\partial t}=0\quad . \tag{3}$$

In the above equations **u** and **v** represent the components of the velocity vector, $\vec{u}=u\vec{i}+v\vec{j}$, **p** denotes the pressure, $\vec{\tau}_a$ and $\vec{\tau}_b$ are the shear stresses acting on the fluid at surfaces (a) and (b) respectively as shown in Figure 2 and $\mathbf{l_f}$ is a flag parameter set equal to 1 for a face seal and 0 for a cylindrical seal.

Each of these shear stresses is assumed to act in the direction of the fluid velocity relative to the respective surface and is related to that velocity by means of a coefficient of resistance or friction factor as follows:

$$\vec{\tau}_a=\frac{1}{2}\rho|\vec{u}-\vec{u}_a|f_a\left(\frac{2h\rho|\vec{u}-\vec{u}_a|}{\mu}\right)(\vec{u}-\vec{u}_a)=\frac{1}{4}\frac{\mu}{h}R_a f_a(R_a)(\vec{u}-\vec{u}_a)\quad , \tag{4}$$

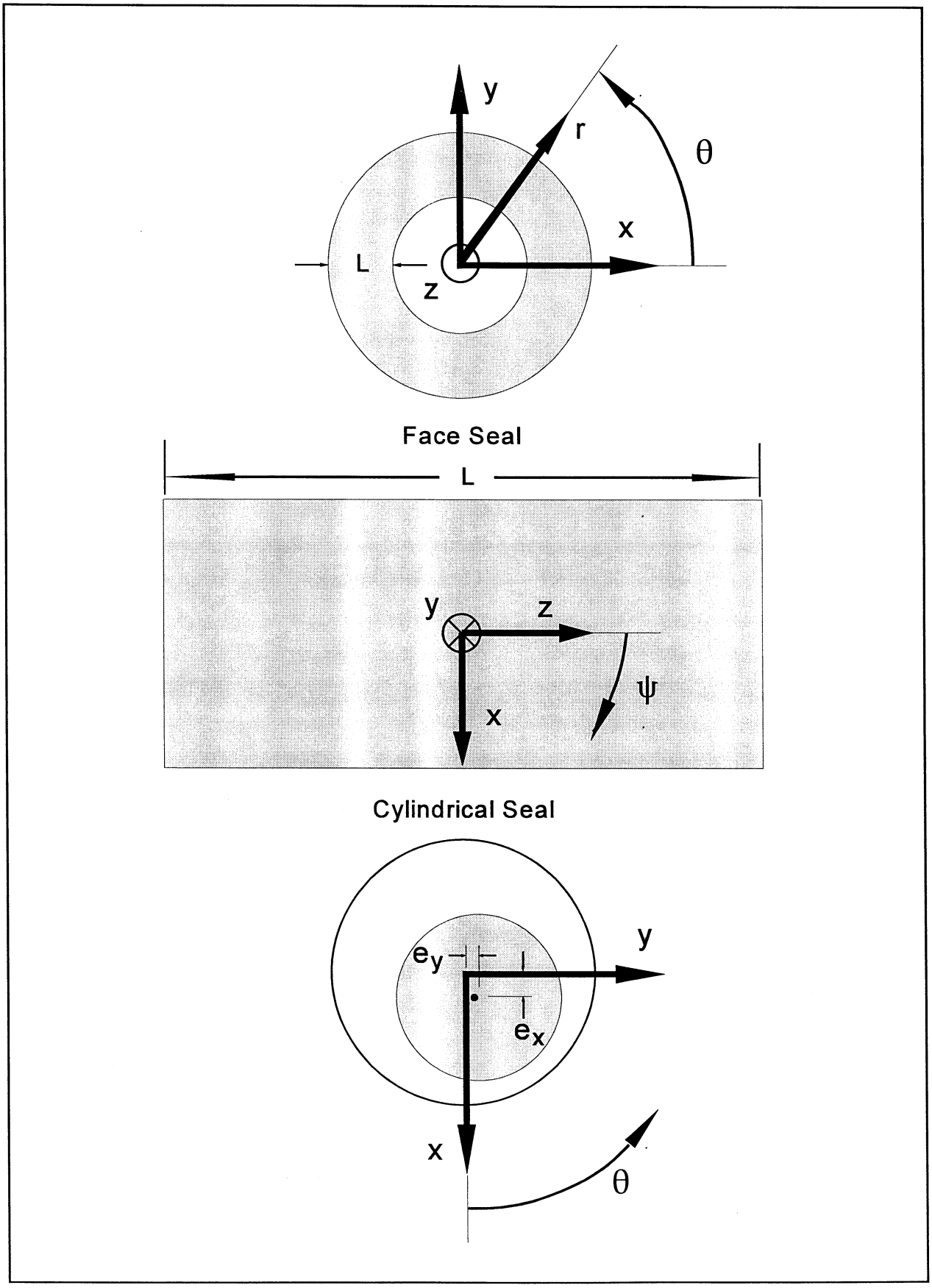


Figure 1 Coordinate system for spiral groove analysis.

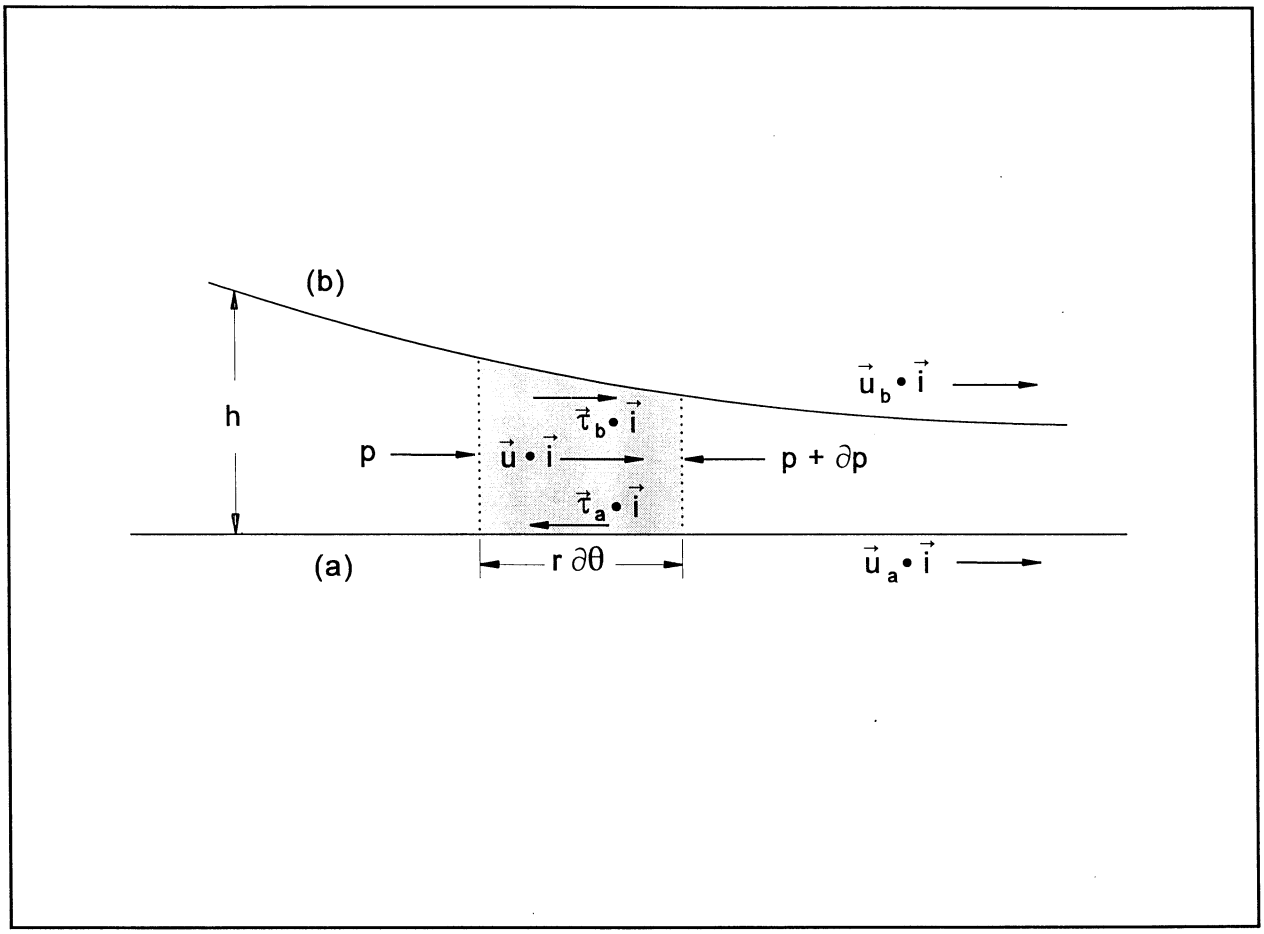


Figure 2 Velocities and forces on a differential element in the θ direction.

for surface (a) and for surface (b)

$$\vec{\tau}_b = -\frac{1}{2}\rho\,|\vec{u}-\vec{u}_b|\,f_b\left(\frac{2h\rho\,|\vec{u}-\vec{u}_b|}{\mu}\right)(\vec{u}-\vec{u}_b) = -\frac{1}{4}\frac{\mu}{h}R_b f_b(R_b)(\vec{u}-\vec{u}_b) \quad , \qquad \textbf{(5)}$$

where the shear factors $\mathbf{f_a}$ and $\mathbf{f_b}$ are one fourth of the resistance coefficients or friction factors for the respective surfaces (reference 2) and are functions of the respective Reynolds numbers $\mathbf{R_a}$ and $\mathbf{R_b}$ which are in turn defined as

$$R_a = 2h\,|\vec{u}-\vec{u}_a|\,\rho/\mu \quad , \qquad R_b = 2h\,|\vec{u}-\vec{u}_b|\,\rho/\mu \quad . \qquad \textbf{(6)}$$

The use of various shear functions in the prediction of turbulent behavior of bearings and seals may be found in references 3 - 6. Power law relationships of the form $\mathbf{f = nR^m}$ have been used in references 3 - 5 to characterize both smooth and rough surfaces. If both surfaces are smooth the relationship

$$f_a(R_a) = n_0 R_a^{m_0} \quad , \qquad f_b(R_b) = n_0 R_b^{m_0} \qquad \textbf{(7)}$$

may be used with n_0 and m_0 obtained from the Blasius Equation (reference 1) as $n_0 = 0.0751$, $m_0 = -.25$ for turbulent flow (Reynolds numbers ranging from 4,000 to 100,000). The corresponding values for laminar flow are $n_0 = 24$ and $m_0 = -1$.

Equations (1) - (3) may be expressed in dimensionless form with the use of the following dimensionless variables

$$\tilde{h} = \frac{h}{C}\ ,\quad \tilde{p} = \frac{p}{p_0}\ ,\quad \tilde{u} = \frac{u}{V_0}\ ,\quad \tilde{v} = \frac{v}{V_0}\ ,\quad \tilde{r} = \frac{r}{r_0}$$

$$S = \frac{s}{r_0}\ ,\quad \tilde{t} = \frac{V_0}{r_0}t\ ,\quad \tilde{\tau} = \frac{r_0}{C}\frac{\tau}{p_0} \tag{8}$$

and parameters

$$R = \frac{2CV_0\rho}{\mu}\ ,\quad R^* = \frac{2C}{r_0}R\ ,\quad \tilde{\omega} = \frac{\omega r_0}{V_0}\ ,\quad \tilde{p}^* = \frac{\mu V_0 r_0}{4C^2 p_0}\ . \tag{9}$$

In the above equations V_0 represents a characteristic velocity, p_0 a characteristic pressure, r_0 and C represent the radius and clearance for a cylindrical seal and the outside radius and characteristic film thickness for a face seal.

Henceforth surface (b) will be taken to be stationary and surface (a) will be taken to move with a circumferential velocity $r\omega$. The Reynolds numbers R_a and R_b given by Equation (6) then become

$$R_a = R\tilde{h}\sqrt{(\tilde{u} - \tilde{r}\tilde{\omega})^2 + \tilde{v}^2}\ ,\quad R_b = R\tilde{h}\sqrt{\tilde{u}^2 + \tilde{v}^2}\ . \tag{10}$$

The integrated momentum and continuity equations may now be expressed in the dimensionless form

$$-\frac{1}{\tilde{r}}\frac{\partial \tilde{p}}{\partial \theta} = \tilde{p}^*\Phi(\tilde{u},\tilde{v},\tilde{h}) + \tilde{p}^*R^*\left(\frac{\partial \tilde{u}}{\partial \tilde{t}} + \tilde{v}\frac{\partial \tilde{u}}{\partial S} + \frac{\tilde{u}}{\tilde{r}}\frac{\partial \tilde{u}}{\partial \theta} + l_f\frac{\tilde{u}\tilde{v}}{\tilde{r}}\right)\ , \tag{11}$$

$$-\frac{\partial \tilde{p}}{\partial S} = \tilde{p}^*\Psi(\tilde{u},\tilde{v},\tilde{h}) + \tilde{p}^*R^*\left(\frac{\partial \tilde{v}}{\partial \tilde{t}} + \tilde{v}\frac{\partial \tilde{v}}{\partial S} + \frac{\tilde{u}}{\tilde{r}}\frac{\partial \tilde{v}}{\partial \theta} - l_f\frac{\tilde{u}^2}{\tilde{r}}\right)\ , \tag{12}$$

$$\frac{1}{\tilde{r}}\frac{\partial(\tilde{r}\tilde{v}\tilde{h})}{\partial S} + \frac{1}{\tilde{r}}\frac{\partial(\tilde{u}\tilde{h})}{\partial\theta} + \frac{\partial\tilde{h}}{\partial\tilde{t}} = 0 \qquad \textbf{(13)}$$

where

$$\Phi(\tilde{u},\tilde{v},\tilde{h}) = \frac{(\tilde{u} - \tilde{r}\tilde{\omega})R_a f_a(R_a) + \tilde{u}R_b f_b(R_b)}{\tilde{h}^2}, \qquad \textbf{(14)}$$

and

$$\Psi(\tilde{u},\tilde{v},\tilde{h}) = \frac{R_a f_a(R_a) + R_b f_b(R_b)}{\tilde{h}^2}\tilde{v} . \qquad \textbf{(15)}$$

Equations (11) - (13) together with the functions defined by Equations (10), (14) and (15) constitute the dimensionless differential equations for the generalized Hirs bulk flow model under consideration. These equations require a prescribed film thickness profile, $\tilde{\mathbf{h}}(\mathbf{S},\theta,\tilde{\mathbf{t}})$, definitions of $\mathbf{f_a}$ and $\mathbf{f_b}$ such as those given by Equation (7) and boundary conditions which will be treated below.

Boundary and continuity conditions

This analysis is limited to essentially axisymmetric surface shapes and constant boundary pressures. Although spiral grooves will be considered, the groove angle, depth and spacing will be independent of θ. Individual pads and partial films are not treated here. As such, all θ (and time) dependence will be associated with displacements of the sealing surfaces. The only conditions on θ are the requirement of periodicity. That is, pressure and flow rates at $\theta + 2\pi$ must equal those at θ for all θ.

Variations of surface shapes in the **s** direction, including discontinuities are considered. The upstream values of **v** and **p** at discontinuities in **h** are denoted by $\mathbf{v_J}$ and $\mathbf{p_J}$ as shown below. The film thickness changes from the upstream value of $\mathbf{h - \Delta h}$ to the downstream value of **h** across the jump.

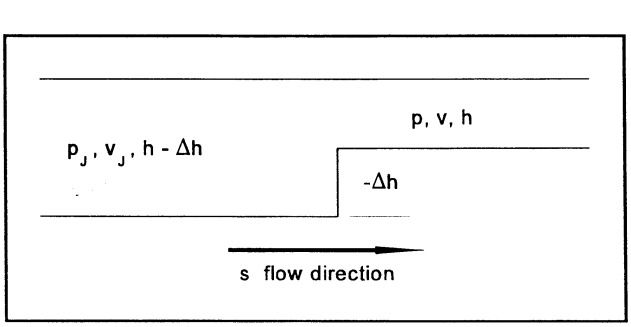


Figure 3 Jump in film thickness.

Since the flow rate normal to the jump must be continuous

$$(h - \Delta h)v_J = hv \quad @ \; s = s_J \quad ,$$

where $\mathbf{s}_J$ denotes the **s** coordinate at the jump.

The pressure change at $\mathbf{s}_J$ may be expressed in terms of a loss coefficient ξ, based on downstream conditions (reference 7) as follows:

$$p_J + \tfrac{1}{2}\rho v_J^2 = p + \tfrac{1}{2}\rho v^2(1 + \xi) \quad @ \; s = s_J \quad .$$

The preceding two equations may be rearranged and expressed in dimensionless form as

$$\tilde{v} = (1 - \tfrac{\Delta\tilde{h}}{\tilde{h}})\tilde{v}_J \; , \quad \Delta\tilde{p} = \tilde{p} - \tilde{p}_J = \tfrac{1}{2}\tilde{p}^* R^* \chi(\tilde{v},\tilde{h},\Delta\tilde{h}) \quad @S = S_J \quad , \qquad \textbf{(16)}$$

where

$$\chi(\tilde{v},\tilde{h},\Delta\tilde{h}) = -\left[1 - \left(\frac{\tilde{h}}{\tilde{h} - \Delta\tilde{h}}\right)^2 + \xi\right]\tilde{v}^2 \quad . \qquad \textbf{(17)}$$

The loss coefficient ξ, due to a contraction will in general be a function of the axial Reynolds number and will be denoted by the function $\zeta(\mathbf{R}\tilde{h}\tilde{v})$ but is frequently taken to be constant (references 3 - 5). The loss coefficient for an expansion may be found in reference 7 and is given together with the corresponding relationship for a contraction below:

$$\xi = \begin{cases} \zeta(R,\tilde{h},\tilde{v}) & , \; \Delta\tilde{h} < 0 \text{ (contraction)} \\ \left(1 - \dfrac{\tilde{h}}{\tilde{h} - \Delta\tilde{h}}\right)^2 & , \; \Delta\tilde{h} \geq 0 \text{ (expansion)} \end{cases} \quad . \qquad \textbf{(18)}$$

The above considerations together with the requirement that the tangential component of velocity is continuous at jumps across constant **s** boundaries provides sufficient information to prescribe the boundary conditions at the inlet and exit to the seal as well as the continuity conditions at jumps.

The tangential component of the velocity, $\mathbf{u}_{in}$ and the pressure, $\mathbf{p}_{in}$ are prescribed at the inlet side of the seal. The relationship between $\mathbf{p}_{in}$ and **v** at the inlet is obtained by setting $\tilde{p}_J = \tilde{p}_{in}$ and evaluating χ as $\Delta\tilde{h} \rightarrow -\infty$ in

Equations (16) - (18). These conditions may be written in dimensionless form as

$$\tilde{u} = \tilde{u}_{in} , \quad \tilde{p} = \tilde{p}_{in} + \frac{1}{2}\tilde{\rho}^* R^* \chi(\tilde{v},\tilde{h},-\infty) = \tilde{p}_{in} - \frac{1}{2}\tilde{\rho}^* R^* (1+\zeta)\tilde{v}^2 \quad @ \; S = S_{in} . \qquad \textbf{(19)}$$

The pressure at the exit from the seal will be taken to be continuous and equal to the exit side pressure, $\mathbf{p_{ex}}$.

$$\tilde{p} = \tilde{p}_{ex} \quad @ \; S = S_{ex} \quad . \qquad \textbf{(20)}$$

It should be noted that $\mathbf{S_{in}}$ may correspond to either the left or right hand sides of the seal (lower or upper values of **S**) depending on the direction of flow. $\mathbf{S_{ex}}$ will be the value of **S** at the opposite side of the seal from $\mathbf{S = S_{in}}$.

Narrow groove theory for spiral groove seals

The development of the narrow groove equations to be presented here will expand upon equations used in reference 8 which, in turn, contains a reformulation of the lubrication equations for laminar, compressible spiral groove seals presented in reference 9.

The purpose of narrow groove theory is to obtain equations and solutions for continuous, smooth global pressure and velocity distributions that approximate the limiting form of the solution to Equations (10) - (15) as the number of grooves becomes large, with the groove angle, β and the groove to pitch ratio, α, held constant. This process greatly reduces the complexity of the solution and eliminates the need for the large grid that would be required to adequately describe all of the grooves individually.

The discontinuities in film thickness associated with the grooves will give rise to discontinuities in the pressures, pressure gradients, and velocities at the ridge-groove interfaces. The relative discontinuities in the velocity components normal to the grooves will be of the same order as the relative film discontinuities. The predicted discontinuities in the local pressures at the interfaces would be of the order of the inertia ($\tilde{\rho}^* R^*$) terms on the right hand sides of Equations (11) and (12). It is important to note however, that as both the number of grooves and the inertia terms become large, flows will not be able to fully develop within or between grooves.

Figure 4 shows three conceptual states of flow development in the order of increasing significance of local fluid inertia and decreasing degree of flow development. These are Case a, where the local pressure changes at the inlet to each groove (or ridge) are negligible; Case b, where a wake forms at the inlet to a groove whose extent is small compared to the length of a groove and Case c, where a jet forms and prevails over most or

all of the length of the groove. These three cases are discussed individually below:

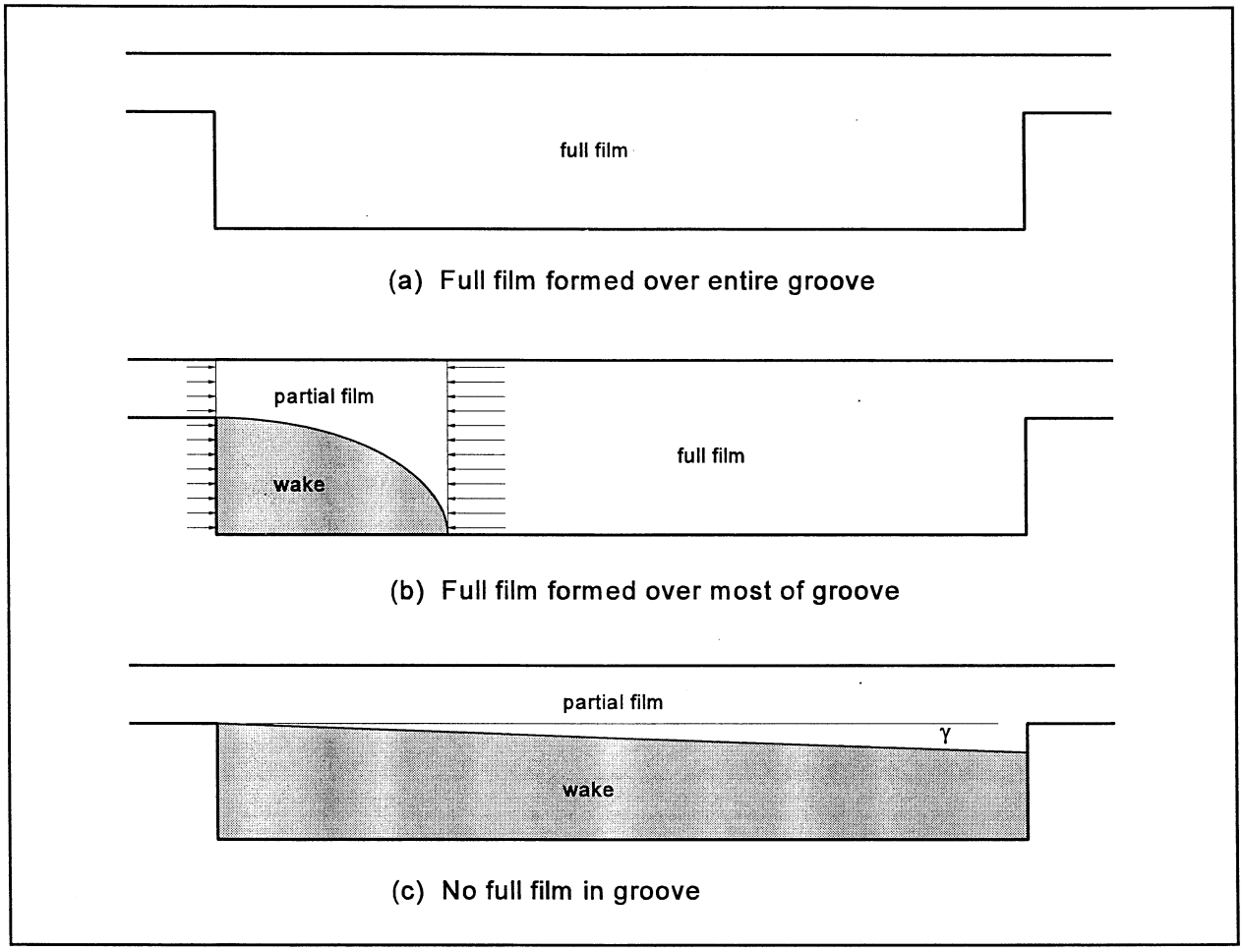


Figure 4 Examples of degrees of film formation in groove

a. **Negligible inlet pressure changes.** Spiral groove seals frequently operate at relatively small clearances (as opposed to labyrinth seals or even damping seals) and will pump at relatively low flow rates compared with those produced by imposed pressure gradients of sufficient magnitude to produce large inertia effects. Under these conditions, the flow can be treated as fully developed over the entire groove and inertia effects may be neglected in the analysis of the **local** pressures and velocities. All inertia effects in Equations (11) - (20) may, however, be included in the treatment of the global pressure and velocities. As such, pumping affected by turbulent shear in regions containing spiral grooves would be accounted for and global inertia effects due to circular steps and grooves and other axial clearance variations would still be included in all regions.

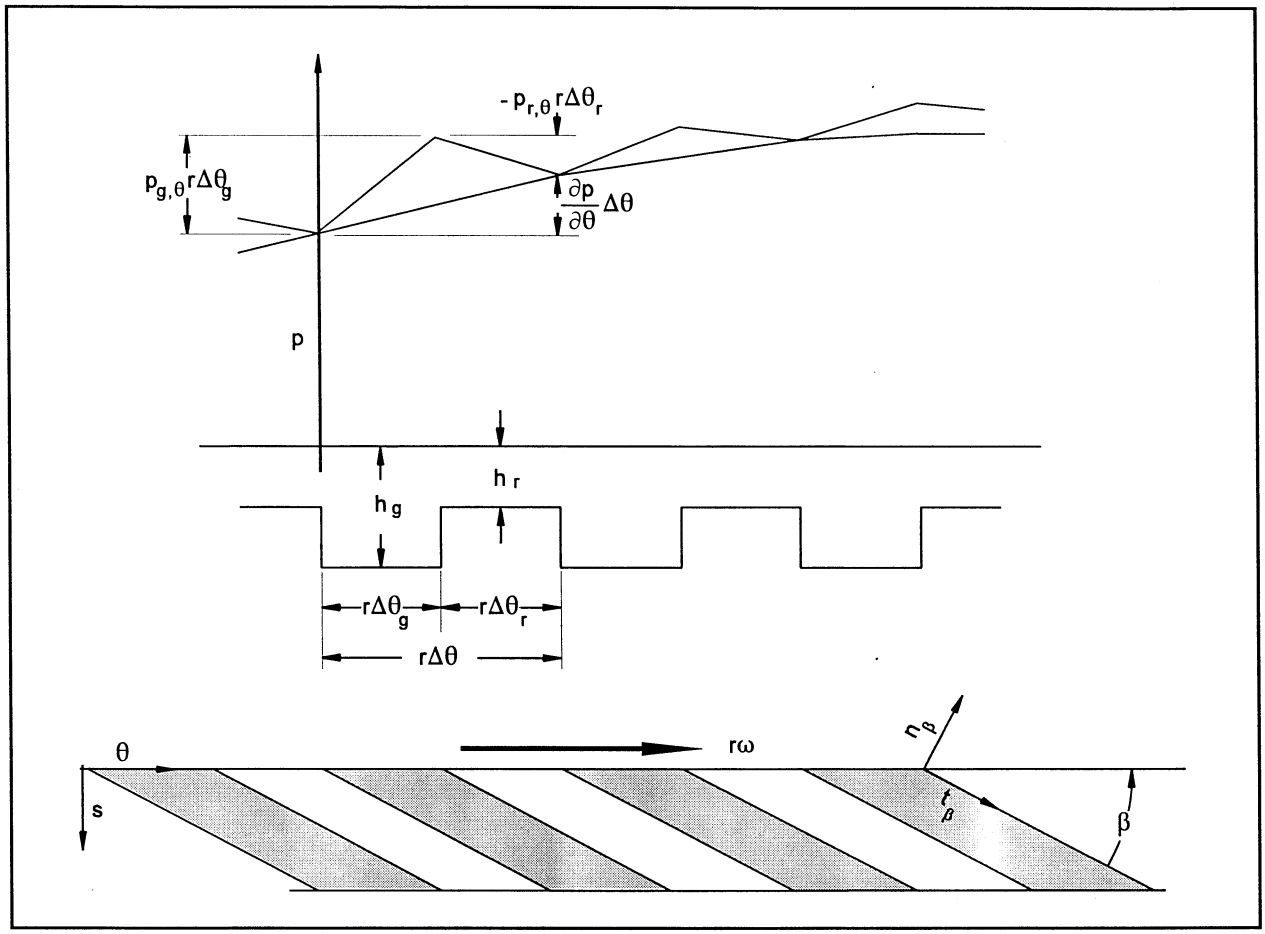


Figure 5 Schematic of spiral groove parameters, global and local pressures, Case a

A schematic showing a global and local pressure distribution for this case along with some of the spiral groove film variables under consideration is presented in Figure 5. The local pressure profile is shown by the sawtooth lines whose lower vertices, for purposes of illustration, are connected by the global pressure profile, **p**. The global pressure profile does not necessarily lie at the lower vertices of the local pressure profile but could lie anywhere between the lower and upper vertices. In the limit as the number of grooves becomes large, curves connecting the upper and lower vertices will approach each other (subject to the approximations discussed above). This limiting behavior is not true of **u**, **v**, **h** or the local pressure gradients which will have different values over lands and grooves no matter how large the number of grooves.

b. **Fully developed films with significant inlet pressure changes.** This case extends Case a by including local pressure changes at the inlet to each groove and ridge with the use of loss coefficients in a manner analogous to that used at the inlets to each region given by Equations (16) - (18). The treatment of these pressure changes as boundary pressure discontinuities assume that the length of the wake shown in Figure 4b is small compared with other relevant circumferential and transverse length dimensions. The relevant length for comparison with the wake length at the start of a region

would be the transverse length of the region. In the case of spiral grooves within a region, the relevant lengths would be the widths of the grooves and ridges.

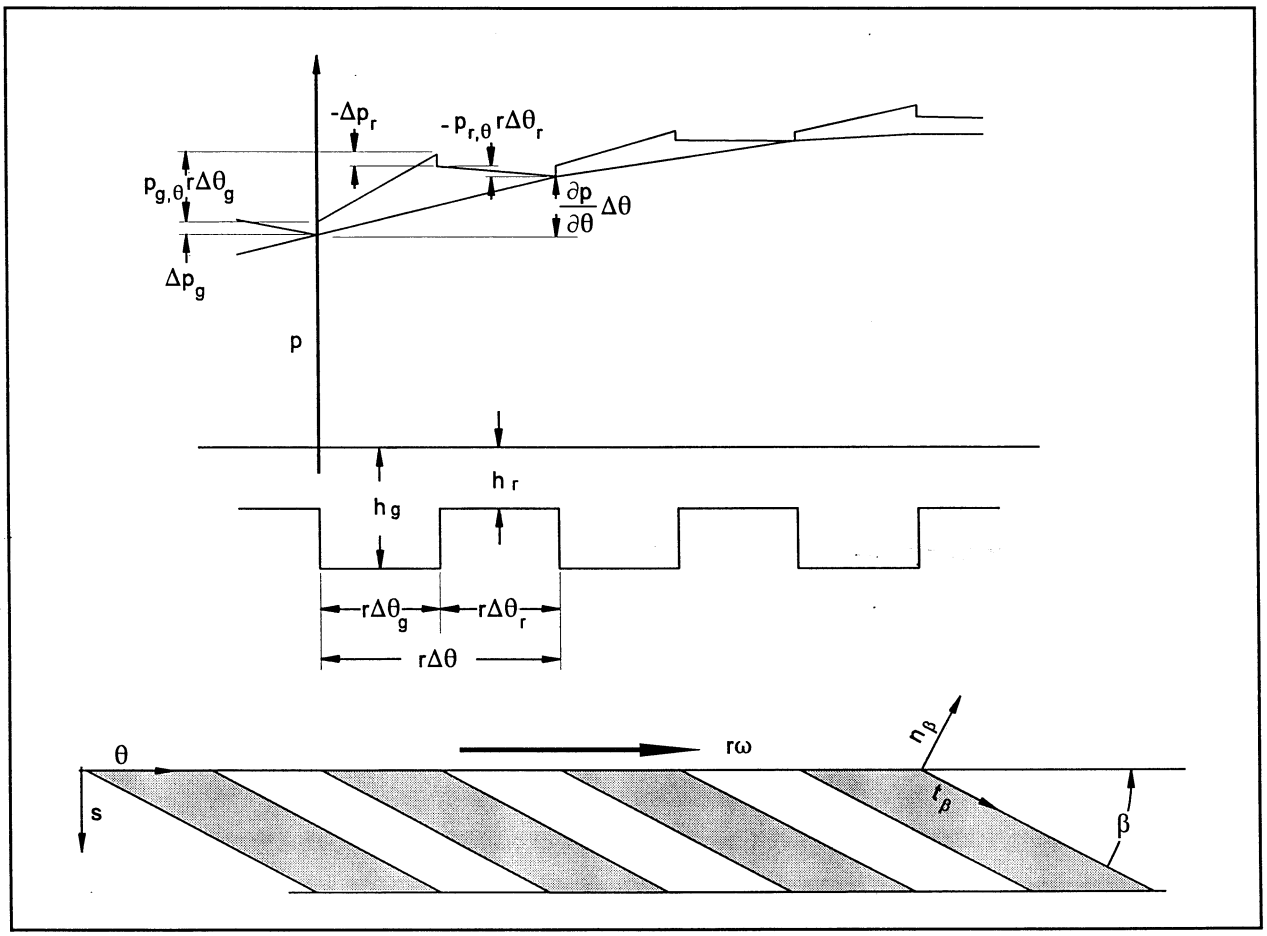


Figure 6 Schematic of spiral groove parameters, global and local pressures, Case b

The local pressures shown in Figure 6 are a generalization of those in Figure 5 to allow for local pressure jumps at the inlet to each groove and ridge. Unlike Case a, the upper and lower envelopes of the local pressure curves will not coalesce as the number of grooves becomes large since the magnitudes of the groove and ridge widths do not enter directly into the jump relationships given by Equations (16) - (18) and the magnitudes of the jumps will not approach 0 as long as Case b conditions prevail. The local pressure jumps for this case will be shown to give rise to a term of order $(\tilde{\mathbf{p}}^* \mathbf{R}^* \mathbf{N}_g)$ which will be retained in the analysis. As with case 1, the other inertia terms will be neglected in the local analysis but maintained in the global analysis. These assumptions will thus give rise to asymptotic relationships as the number of grooves becomes very large in contrast to the limiting relationships corresponding to the assumptions used in Case a.

c. **Jet extends over entire groove.** As the number of grooves becomes very large a limiting flow

should in fact occur as a jet forms that extends across the entire groove. The bulk flow theory which is based on the assumptions that the shear forces on the turbulent core arise directly from interactions between the core and the bounding surfaces break down at this point. A rigorous analysis would involve consideration of the jet, the wake, interactions between jet and wake, interactions between jet and wall etc. and would require three dimensional solutions to the momentum and continuity equations which is beyond the scope of the present effort. An alternative approach would involve the use of additional empirical relationships to characterize these interactions so that limiting behavior can be obtained. Examples of the use of such relationships are given in reference 10 for labyrinth seals and in reference 11 for straight through screw seals.

The narrow groove analysis contained in the rest of this section will refer to Case b unless otherwise specified. The theory requires the development of expressions for the local quantities in terms of continuous global quantities that become valid as the number of grooves becomes large. Local quantities will be denoted by the subscript **g** when referring to grooves and **r** when referring to ridges. Variables such as **p**,**u**,**v** appearing without **r** or **g** subscripts will henceforth denote global quantities. The subscript **r** denoting ridges has been used for consistency with existing literature and should not be confused with the radial position variable **r** which will not be used as a subscript.

Spiral groove patterns for a given region are characterized by three parameters which are defined in terms of quantities shown in Figure 6. These are the groove depth $\delta = h_g - h_r$, the groove to pitch ratio $\alpha = \Delta\theta_g/(\Delta\theta_g+\Delta\theta_r)$ and the groove angle β defined as the angle between the groove and the surface velocity direction, measured from the groove.

One may now introduce the dimensionless groove and ridge flows in the θ and **s** directions

$$\tilde{q}_{g\theta} = \tilde{u}_g\tilde{h}_g \ , \quad \tilde{q}_{gs} = \tilde{v}_g\tilde{h}_g \ , \quad \tilde{q}_{r\theta} = \tilde{u}_r\tilde{h}_r \ , \quad \tilde{q}_{rs} = \tilde{v}_r\tilde{h}_r \ , \tag{21}$$

and express the turbulent shear functions Φ and Ψ defined by Equations (14) and (15) for the grooves as

$$\Phi_g = \Phi\left(\frac{\tilde{q}_{g\theta}}{\tilde{h}_g}, \frac{\tilde{q}_{gs}}{\tilde{h}_g}, \tilde{h}_g\right) \ , \quad \Psi_g = \Psi\left(\frac{\tilde{q}_{g\theta}}{\tilde{h}_g}, \frac{\tilde{q}_{gs}}{\tilde{h}_g}, \tilde{h}_g\right) \tag{22}$$

and for the ridges as

$$\Phi_r = \Phi\left(\frac{\tilde{q}_{r\theta}}{\tilde{h}_r}, \frac{\tilde{q}_{rs}}{\tilde{h}_r}, \tilde{h}_r\right) \ , \quad \Psi_r = \Psi\left(\frac{\tilde{q}_{r\theta}}{\tilde{h}_r}, \frac{\tilde{q}_{rs}}{\tilde{h}_r}, \tilde{h}_r\right) \ . \tag{23}$$

One may now write Equations (11) and (12) for the groove regions as

$$-\tilde{p}_{g,\theta} = -\frac{1}{\tilde{r}}\frac{\partial \tilde{p}}{\partial \theta}\bigg|_g = \tilde{p}^* \Phi_g + \tilde{p}^* R^* \left(\frac{\partial \tilde{u}}{\partial \tilde{t}} + \tilde{v}\frac{\partial \tilde{u}}{\partial S} + \frac{\tilde{u}}{\tilde{r}}\frac{\partial \tilde{u}}{\partial \theta} + l_f \frac{\tilde{u}\tilde{v}}{\tilde{r}} \right) , \tag{24}$$

$$-\tilde{p}_{g,s} = -\frac{\partial \tilde{p}}{\partial S}\bigg|_g = \tilde{p}^* \Psi_g + \tilde{p}^* R^* \left(\frac{\partial \tilde{v}}{\partial \tilde{t}} + \tilde{v}\frac{\partial \tilde{v}}{\partial S} + \frac{\tilde{u}}{\tilde{r}}\frac{\partial \tilde{v}}{\partial \theta} - l_f \frac{\tilde{u}^2}{\tilde{r}} \right) \tag{25}$$

and for the ridge regions as

$$-\tilde{p}_{r,\theta} = -\frac{1}{\tilde{r}}\frac{\partial \tilde{p}}{\partial \theta}\bigg|_r = \tilde{p}^* \Phi_r + \tilde{p}^* R^* \left(\frac{\partial \tilde{u}}{\partial \tilde{t}} + \tilde{v}\frac{\partial \tilde{u}}{\partial S} + \frac{\tilde{u}}{\tilde{r}}\frac{\partial \tilde{u}}{\partial \theta} + l_f \frac{\tilde{u}\tilde{v}}{\tilde{r}} \right) , \tag{26}$$

$$-\tilde{p}_{r,s} = -\frac{\partial \tilde{p}}{\partial S}\bigg|_r = \tilde{p}^* \Psi_r + \tilde{p}^* R^* \left(\frac{\partial \tilde{v}}{\partial \tilde{t}} + \tilde{v}\frac{\partial \tilde{v}}{\partial S} + \frac{\tilde{u}}{\tilde{r}}\frac{\partial \tilde{v}}{\partial \theta} - l_f \frac{\tilde{u}^2}{\tilde{r}} \right) . \tag{27}$$

The unit tangent and normal vectors for the logarithmic spiral as shown in Figure 6 are given by

$$\vec{t}_\beta = \cos\beta\,\vec{i} + \sin\beta\,\vec{j} \ , \quad \vec{n}_\beta = \sin\beta\,\vec{i} - \sin\beta\,\vec{j} \tag{28}$$

If local inertia effects were neglected, the pressure would be continuous at each groove-ridge interface and the derivative of the pressure in the direction tangential to the interface, $\vec{\nabla}\mathbf{p}\cdot\vec{\mathbf{t}}_\beta$, would also be continuous. In keeping with the assumption that the only *local* inertia effect to be considered is the pressure jump normal to the interface, continuity of the tangential pressure derivative will be maintained even when this effect is considered. Continuity of the tangential derivative of pressure at the interface may be expressed as

$$\cos\beta\,\tilde{p}_{g,\theta} + \sin\beta\,\tilde{p}_{g,s} = \cos\beta\,\tilde{p}_{r,\theta} + \sin\beta\,\tilde{p}_{r,s} \ . \tag{29}$$

One may now substitute Equations (24) - (27) for the corresponding pressure derivatives in the above equation to obtain

$$\cos\beta\,\Phi_g + \sin\beta\,\Psi_g = \cos\beta\,\Phi_r + \sin\beta\,\Psi_r \ . \tag{30}$$

The flow rate relative to a groove-ridge interface in the direction normal to that interface, $\tilde{q}_n$, must be continuous. For grooves on the stationary surface (b), that flow rate would be $\mathbf{h}\vec{u}\cdot\vec{n}_\beta$ and for grooves on the moving surface (a), it would be $\mathbf{h}(\vec{u} - r\omega\vec{i})\cdot\vec{n}_\beta$. One may use the dimensionless groove and ridge flow rates defined by Equation (21) and perform the indicated dot products to express this continuity condition as

$$\tilde{q}_n = (\tilde{q}_{g\theta} - \tilde{r}\tilde{\omega}\tilde{h}_g I_\omega)\sin\beta - \tilde{q}_{gs}\cos\beta = (\tilde{q}_{r\theta} - \tilde{r}\tilde{\omega}\tilde{h}_r I_\omega)\sin\beta - \tilde{q}_{rs}\cos\beta \ , \qquad (31)$$

where I_ω is equal to **1** if the grooves are on the moving surface and **0** if the grooves are on the stationary surface. The two equalities on the right may be rearranged to obtain the relationship

$$\sin\beta\,\tilde{q}_{g\theta} - \cos\beta\,\tilde{q}_{gs} - \sin\beta\,\tilde{q}_{r\theta} + \cos\beta\,\tilde{q}_{rs} = \tilde{r}\tilde{\omega}\tilde{\delta} I_\omega \sin\beta \ . \qquad (32)$$

One may now equate flow the across a groove-ridge pair in the θ direction to the global flow in that direction and express the result in dimensionless form as

$$\alpha\tilde{q}_{g\theta} + (1-\alpha)\tilde{q}_{r\theta} = \tilde{u}\tilde{h} \ . \qquad (33)$$

A similar balance in the **s** direction results in the relationship

$$\alpha\tilde{q}_{gs} + (1-\alpha)\tilde{q}_{rs} = \tilde{v}\tilde{h} \ . \qquad (34)$$

The global film thickness, **h** is the value which results in the same flow area as that produced by the local film thickness variation and may be expressed in dimensionless form as

$$\tilde{h} = \alpha\tilde{h}_g + (1-\alpha)\tilde{h}_r = \tilde{h}_r + \alpha\tilde{\delta} \qquad (35)$$

Equations (30) and (32) - (34) represent four algebraic equations which may be solved for the four local flow rates $\tilde{q}_{g\theta}$, $\tilde{q}_{gs}$, $\tilde{q}_{r\theta}$ and $\tilde{q}_{rs}$. Iterative solutions are obtained numerically with the use of a Newton-Raphson procedure to linearize Equation (30).

The pressure changes (downstream - upstream) incurred at the entrance to a groove, Δp_g, and at the entrance to a ridge, Δp_r, may be expressed in dimensionless form with the aid of the jump function χ, defined by Equations (16) - (18), as follows:

$$\Delta\tilde{p}_g = \frac{1}{2}p^* R^* \chi\left(\frac{\tilde{q}_n}{\tilde{h}_g}, \tilde{h}_g, \tilde{\delta}\right) , \quad \Delta\tilde{p}_r = \frac{1}{2}p^* R^* \chi\left(\frac{\tilde{q}_n}{\tilde{h}_r}, \tilde{h}_r, -\tilde{\delta}\right) . \tag{36}$$

The normal flow component, $\tilde{q}_n$, may be expressed in terms of the global velocities and film thickness with the use of Equations (31) and (33) - (35) as

$$\tilde{q}_n = (\tilde{u}\tilde{h} - \tilde{r}\tilde{\omega}\tilde{h}l_\omega)\sin\beta - \tilde{v}\tilde{h}\cos\beta . \tag{37}$$

By equating the change in pressure over a groove-ridge pair to the changes in the global pressure, first in the θ direction, as shown in Figure 6, and then in the **s** direction and expressing the result in dimensionless form, the following equations are obtained:

$$\frac{1}{\tilde{r}}\frac{\partial\tilde{p}}{\partial\theta} = \alpha\tilde{p}_{g,\theta} + (1-\alpha)\tilde{p}_{r,\theta} + \frac{\Delta\tilde{p}_g + \Delta\tilde{p}_r}{\tilde{r}\Delta\theta}\,\mathrm{sign}(\tilde{q}_n\vec{n}_\beta\cdot\vec{i}) , \tag{38}$$

$$\frac{\partial\tilde{p}}{\partial S} = \alpha\tilde{p}_{g,s} + (1-\alpha)\tilde{p}_{r,s} + \frac{\Delta\tilde{p}_g + \Delta\tilde{p}_r}{\tilde{r}\Delta\theta\,|\tan\beta|}\,\mathrm{sign}(\tilde{q}_n\vec{n}_\beta\cdot\vec{j}) , \tag{39}$$

where the sign functions appearing in the above equations are either 1 or -1 depending on the direction of the normal component of flow with respect to the corresponding coordinate direction.

Finally, noting that $\Delta\theta = 2\pi/N_g$ and the definition of $\vec{n}_\beta$ given by Equation (28), one may substitute Equations (24) - (27) for the corresponding local pressure gradients and Equation (34) for the pressure jumps in Equations (38) and (39), and write the resulting equations in the form

$$-\frac{1}{\tilde{r}}\frac{\partial\tilde{p}}{\partial\theta} = \tilde{p}^*\Phi^*(\tilde{u},\tilde{v},\tilde{h},l_f) + \tilde{p}^* R^*\left(\frac{\partial\tilde{u}}{\partial\tilde{t}} + \tilde{v}\frac{\partial\tilde{u}}{\partial S} + \frac{\tilde{u}}{\tilde{r}}\frac{\partial\tilde{u}}{\partial\theta}\right) , \tag{40}$$

$$-\frac{\partial\tilde{p}}{\partial S} = \tilde{p}^*\Psi^*(\tilde{u},\tilde{v},\tilde{h},l_f) + \tilde{p}^* R^*\left(\frac{\partial\tilde{v}}{\partial\tilde{t}} + \tilde{v}\frac{\partial\tilde{v}}{\partial S} + \frac{\tilde{u}}{\tilde{r}}\frac{\partial\tilde{v}}{\partial\theta}\right) , \tag{41}$$

where

$$\Phi^* = \alpha\Phi_g + (1-\alpha)\Phi_r + R^*\left\{l_f\frac{\tilde{u}\tilde{v}}{\tilde{r}} - \frac{N_g}{4\pi\tilde{r}}\mathrm{sign}(\tilde{q}_n\sin\beta)\left[\chi\left(\frac{\tilde{q}_n}{\tilde{h}_g}, \tilde{h}_g, \tilde{\delta}\right) + \chi\left(\frac{\tilde{q}_n}{\tilde{h}_r}, \tilde{h}_r, -\tilde{\delta}\right)\right]\right\} \tag{42}$$

and

$$\Psi^* = \alpha\Psi_g + (1-\alpha)\Psi_r + R^*\left\{-l_f\frac{\tilde{u}^2}{\tilde{r}} + \frac{N_g}{4\pi\tilde{r}\,|\tan\beta|}\,\mathrm{sign}(\tilde{q}_n\cos\beta)\left[\chi\left(\frac{\tilde{q}_n}{\tilde{h}_g},\tilde{h}_g,\tilde{\delta}\right) + \chi\left(\frac{\tilde{q}_n}{\tilde{h}_r},\tilde{h}_r,-\tilde{\delta}\right)\right]\right\} \quad . \qquad \textbf{(43)}$$

The Coriolis and centrifugal inertia terms for face seals and the spiral groove local inertia term have been combined with the turbulent shear resistance terms in Equations (42) and (43). This has been done for convenience because of their algebraic nature and will simplify the development and solution of the first and second order flow equations to be discussed in the next section.

The actual number of grooves, $\mathbf{N_g}$, does not usually appear in a narrow groove analysis. It enters here only to characterize the cumulative effects of losses due to sudden changes in cross section between ridges and grooves. Formally setting $\mathbf{N_g=0}$ would therefore only eliminate the inclusion of these local inertia effects and would maintain all of the other spiral groove effects under consideration. Caution should be exercised when groove or ridge widths become the same order of magnitude as the clearance. This would invalidate one of the basic geometric assumptions of the bulk flow theory used throughout this analysis and could have a particularly pronounced affect on the validity of the above local inertia terms.

Equations (40) and (41) represent the generalization of Equations (11) and (12) to spiral groove seals and reduce to Equations (11) and (12) when both α and $\mathbf{N_g}$ are set equal to 0.. The continuity equation [Equation(13)], and the continuity and boundary conditions given by Equations (16) - (20) remain unchanged subject to the interpretation of $\tilde{\mathbf{u}}$, $\tilde{\mathbf{v}}$, $\tilde{\mathbf{p}}$ and $\tilde{\mathbf{h}}$ as their global values when $\alpha > 0$.

Development of first and second order equations for small displacements

The first order variables will be the global film thickness, pressure and tangential and transverse velocities for an undisplaced shaft. They will depend only on **s** and their dimensionless forms will be denoted by $\tilde{\mathbf{H}}$**(S)**, $\tilde{\mathbf{P}}$**(S)**, $\tilde{\mathbf{U}}$**(S)** and $\tilde{\mathbf{V}}$**(S)** respectively. Substitution of the above variables for $\tilde{\mathbf{h}}$**,** $\tilde{\mathbf{p}}$**,** $\tilde{\mathbf{u}}$**, and** $\tilde{\mathbf{v}}$ respectively, in Equations (40), (41), and (13) yields the following set of ordinary differential equations:

$$\Phi^*(\tilde{U},\tilde{V},\tilde{H},l_f) + R^*\tilde{V}\frac{d\tilde{U}}{dS} = 0 \quad , \qquad \textbf{(44)}$$

$$-\frac{d\tilde{P}}{dS} = \tilde{p}^*\Psi^*(\tilde{U},\tilde{V},\tilde{H},l_f) + \tilde{p}^*R^*\tilde{V}\frac{d\tilde{V}}{dS} \quad , \qquad \textbf{(45)}$$

$$\frac{d(\tilde{r}\tilde{H}\tilde{V})}{dS} = 0 \quad . \qquad \textbf{(46)}$$

The boundary and jump conditions for the first order variables are prescribed by Equations (16) - (20) with $\tilde{h}$, $\tilde{p}$, $\tilde{u}$, **and** $\tilde{v}$ replaced by the corresponding first order variables. The boundary conditions are given by

$$\tilde{U} = \tilde{u}_{in} \ , \quad \tilde{P} = \tilde{p}_{in} + \frac{1}{2}\tilde{\rho}^* R^* \chi(\tilde{V},\tilde{H},-\infty) = \tilde{p}_{in} - \frac{1}{2}\tilde{\rho}^* R^* (1+\zeta)\tilde{V}^2 \quad @ \ S = S_{in} \qquad \textbf{(47)}$$

and

$$\tilde{P} = p_{ex} \quad @ \ S = S_{ex} \ . \qquad \textbf{(48)}$$

One may now add a small displacement, $\mathbf{h'(s,\theta,t)}$ to $\mathbf{H(s)}$ and express the resulting film thickness, pressure and velocities in dimensionless form as

$$\begin{aligned} \tilde{h} &= \tilde{H}(S) + \tilde{h}'(S,\theta,\tilde{t}) \ , \quad \tilde{u} = \tilde{U}(S) + \tilde{u}'(S,\theta,\tilde{t}) \ , \\ \tilde{v} &= \tilde{V}(S) + \tilde{v}'(S,\theta,\tilde{t}) \ , \quad \tilde{p} = \tilde{P}(S) + \tilde{p}'(S,\theta,\tilde{t}) \ . \end{aligned} \qquad \textbf{(49)}$$

When above relationships are substituted for the corresponding variables in Equations (40), (41) and (13) and quadratic terms in second order (primed) quantities are neglected, the following second order, linearized momentum and continuity equations are obtained:

$$-\frac{1}{\tilde{r}\tilde{\rho}^*}\frac{\partial \tilde{p}'}{\partial \theta} = R^*\left(\frac{\partial \tilde{u}'}{\partial \tilde{t}} + \tilde{V}\frac{\partial \tilde{u}'}{\partial S} + \frac{d\tilde{U}}{dS}\tilde{v}' + \frac{\tilde{U}}{\tilde{r}}\frac{\partial \tilde{u}'}{\partial \theta}\right) + \Phi^*_{\tilde{U}}\tilde{u}' + \Phi^*_{\tilde{V}}\tilde{v}' + \Phi^*_{\tilde{H}}\tilde{h}' \ , \qquad \textbf{(50)}$$

$$-\frac{1}{\tilde{\rho}^*}\frac{\partial \tilde{p}'}{\partial S} = R^*\left(\frac{\partial \tilde{v}'}{\partial \tilde{t}} + \tilde{V}\frac{\partial \tilde{v}'}{\partial S} + \frac{d\tilde{V}}{dS}\tilde{v}' + \frac{\tilde{U}}{\tilde{r}}\frac{\partial \tilde{v}'}{\partial \theta}\right) + \Psi^*_{\tilde{U}}\tilde{u}' + \Psi^*_{\tilde{V}}\tilde{v}' + \Psi^*_{\tilde{H}}\tilde{h}' \ , \qquad \textbf{(51)}$$

$$\tilde{V}\frac{\partial(\tilde{r}\tilde{h}')}{\partial S} + \frac{d\tilde{V}}{dS}\tilde{r}\tilde{h}' + \tilde{r}\tilde{H}\frac{\partial v'}{\partial S} + \frac{d(\tilde{r}\tilde{H})}{dS}\tilde{v}' + \tilde{U}\frac{\partial \tilde{h}'}{\partial \theta} + \tilde{H}\frac{\partial \tilde{u}'}{\partial \theta} + \tilde{r}\frac{\partial \tilde{h}'}{\partial \tilde{t}} = 0 \ . \qquad \textbf{(52)}$$

The subscripts $\tilde{U}$, $\tilde{V}$ and $\tilde{H}$ are used to denote partial differentiation with respect to those variables.
The continuity requirements for $\tilde{p}'$ and $\tilde{v}'$ at values of **s** where **h** is discontinuous are obtained by performing a similar linearization on Equation (16) and are given below:

$$\tilde{v}' = \frac{\tilde{V}\Delta\tilde{h}}{\tilde{H}(\tilde{H}-\Delta\tilde{h})}\tilde{h}' + \frac{(\tilde{H}-\Delta\tilde{h})}{\tilde{H}}\tilde{v}_J' \;, \quad \Delta\tilde{p}' = \frac{1}{2}\tilde{p}^* R^* (\chi_{\tilde{V}}\tilde{v}' + \chi_{\tilde{H}}\tilde{h}') \quad @S = S_J \;. \tag{53}$$

The tangential velocity $\tilde{u}'$ will be continuous. The end conditions given below are obtained by linearizing Equations (19) and (20) and substituting the values of $\tilde{U}$, $\tilde{V}$ and $\tilde{P}$ prescribed by Equations (47) and (48):

$$\tilde{u}' = 0 \;, \quad \tilde{p}' = \frac{1}{2}\tilde{p}^* R^* (\chi_{\tilde{V}}\tilde{v}' + \chi_{\tilde{H}}\tilde{h}') \quad @S = S_{in} \tag{54}$$

and

$$\tilde{p}' = 0 \quad @ \; S = S_{ex} \;. \tag{55}$$

Solution to first order flow equations

The first order flow equations are solved by a fairly straight forward numerical procedure. To begin with one may integrate Equation (46) and express the result in the form

$$\tilde{V} = \frac{\tilde{r}_{in}\tilde{H}_{in}\tilde{V}_{in}}{\tilde{r}\tilde{H}} \;,$$

where the dimensionless transverse inlet velocity $\tilde{V}_{in}$, is unknown and must be initially assumed. One may compute $\tilde{V}(S)$, from the above equation, for the assumed value of $\tilde{V}_{in}$. The tangential velocity, $\tilde{U}(S)$, may now be determined by solving Equation (44) numerically subject the first boundary condition in Equation (47). Once $\tilde{U}(S)$ and $\tilde{V}(S)$ have been established, $\tilde{P}(S)$ may be determined by numerical integration of Equation (45) subject to the second boundary condition in Equation (47). The correct value of $\tilde{V}_{in}$ will be that which results in a pressure distribution that satisfies Equation (48) and is determined numerically by Newton's method. The transverse flow rate, Q, may then be calculated as $Q = 2\pi r_0 C V_0 \tilde{r}_{in}\tilde{H}_{in}\tilde{V}_{in}$.

A semi-implicit algorithm has been used for solving Equation (44). Examples of semi-implicit algorithms may be found in many texts on numerical methods such as reference 12. Although they are slightly more complex than some of the widely used explicit methods such as Runge-Kutta, they provide increased stability for "stiff" systems such as that which may occur here at small values of R^*. Although Equation (44) is a single first order differential equation, the algorithm is presented below for a system of N first order ordinary differential equations, as will occur later in the development of the second order solution.

The system of differential equations may be represented in the form

$$\frac{dY_i}{dS} = F_i(S,Y_1,Y_2,...,Y_N) \ , \quad i = 1,2,...,N \ , \tag{56}$$

where $\mathbf{Y_i}$ denotes the dependent variables. If the values of $\mathbf{Y_i}$ at the new position **(S + ΔS)** are denoted by the column vector **{Y^{new}}**, and the values at the old position by **{Y}**, the equation used for computing **{Y^{new}}** may be written as

$$\{Y^{new}\} = \{Y\} + \Delta S\,([I] - \frac{\Delta S}{2}[k])^{-1}\{F(S + \frac{\Delta S}{2},Y_1,Y_2,...,Y_N)\} \ , \tag{57}$$

where **[I]** is the unit diagonal matrix of order **N** and **[k]** is a matrix of derivatives whose components are

$$k_{ij} = \frac{\partial}{\partial Y_j}F_i(S + \frac{\Delta S}{2},Y_1,Y_2,...,Y_j,...,Y_N) \ , \quad i,j = 1,2,...,N \ . \tag{58}$$

Solution to second order flow equations

Although the global film thickness $\tilde{H}$, remains an arbitrary function of the transverse position **S**, the displacement of the center of the seal will be taken to have the form of a small oscillatory translation, $\mathbf{e_x}$, in the **x** direction, for a cylindrical seal or $\mathbf{e_z}$, in the **z** direction, for a face seal and a small oscillatory rotation about the **y** axis, ψ, for either type of seal. If the seal oscillates at speed Ω, the dimensionless film displacement, $-\tilde{h}'$, will take the form

$$-\tilde{h}' = \left[\Psi_0 S\cos\theta + l_c\tilde{e}_{x0}\cos\theta + l_f\tilde{e}_{z0}\right]\cos\tilde{\Omega}\tilde{t} \ , \tag{59}$$

where

$$l_c = 1 - l_f \ , \quad \tilde{\Omega} = \frac{\Omega r_0}{V_0} \ , \quad \Psi = \frac{r_0}{C}\Psi_0\cos\tilde{\Omega}\tilde{t} \ , \quad e_x = \frac{\tilde{e}_{x0}}{C}\cos\tilde{\Omega}\tilde{t} \ , \quad e_z = \frac{\tilde{e}_{z0}}{C}\cos\tilde{\Omega}\tilde{t} \ . \tag{60}$$

Each of the three terms on the right hand side of Equation (59) may be defined as component film displacements, δ_k and the equation may be rewritten as

$$-\tilde{h}' = \sum_{k=1}^{3}\delta_k \ . \tag{61}$$

The component film displacements may be expressed in complex form as

$$\delta_k = \frac{1}{2}\Re(\delta_k^+ + \delta_k^-) \quad , \tag{62}$$

where

$$\delta_k^{\pm} = \epsilon_k \eta_k(S)\, e^{i(J_k\theta \pm \tilde{\Omega}\tilde{t})} \quad . \tag{63}$$

The functions $\Re(Z)$ in the above equation and $\Im(Z)$ to be used later denote the real and imaginary parts of the complex variable Z respectively. The values of ϵ_k, η_k and J_k are given below:

$$\begin{aligned} k &= 1, \quad 2, \quad 3 \\ \epsilon_k &= \tilde{\Psi}_0, \quad \tilde{e}_{x0}, \quad \tilde{e}_{z0} \\ \eta_k &= S, \quad I_c, \quad I_f \\ J_k &= 1, \quad 1, \quad 0 \end{aligned} \tag{64}$$

Since the second order flow equations are linear one may superimpose component solutions obtained for $\tilde{h}'$ appearing in Equations (50) - (54) replaced by the various values of $-\delta_k^{\pm}$. If the component solutions for the dimensionless second order pressure and velocities are denoted by $\hat{p}_k^{\pm}$, $\hat{u}_k^{\pm}$ and $\hat{v}_k^{\pm}$ respectively, then the values of $\tilde{p}'$, $\tilde{u}'$ and $\tilde{v}'$ may be expressed as

$$\tilde{p}' = \sum_{k=1}^{3} \hat{p}_k \ , \quad \tilde{u}' = \sum_{k=1}^{3} \hat{u}_k \ , \quad \tilde{v}' = \sum_{k=1}^{3} \hat{v}_k \quad , \tag{65}$$

where

$$\hat{p}_k = \frac{1}{2}\Re(\hat{p}_k^+ + \hat{p}_k^-) \ , \quad \hat{u}_k = \frac{1}{2}\Re(\hat{u}_k^+ + \hat{u}_k^-) \ , \quad \hat{v}_k = \frac{1}{2}\Re(\hat{v}_k^+ + \hat{v}_k^-) \quad . \tag{66}$$

One may now attempt to separate variables by looking for component solutions in the form

$$\hat{p}_k^{\pm} = \overline{p}_k^{\pm}(S)\, e^{i(J_k\theta \pm \tilde{\Omega}\tilde{t})} \ , \quad \hat{u}_k^{\pm} = \overline{u}_k^{\pm}(S)\, e^{i(J_k\theta \pm \tilde{\Omega}\tilde{t})} \ , \quad \hat{v}_k^{\pm} = \overline{v}_k^{\pm}(S)\, e^{i(J_k\theta \pm \tilde{\Omega}\tilde{t})} \quad . \tag{67}$$

When the above expressions for $\hat{p}_k^{\pm}$, $\hat{u}_k^{\pm}$ and $\hat{v}_k^{\pm}$ are substituted for $\tilde{p}'$, $\tilde{u}'$ and $\tilde{v}'$ in Equations (50) - (53) a set of ordinary differential equations is obtained which may be arranged in the form

$$R^*\tilde{V}\frac{d\bar{u}_k^{\pm}}{dS} + (\Phi^*_{\tilde{U}} + iR^*\tilde{\Omega}^{\pm})\bar{u}_k^{\pm} + \left(\Phi^*_{\tilde{V}} + R^*\frac{d\tilde{U}}{dS}\right)\bar{v}_k^{\pm} + \frac{iJ_k}{\tilde{\rho}^*\tilde{r}}\bar{p}_k^{\pm} = \epsilon_k\eta_k\Phi^{\pm}_{\tilde{H}} \quad , \tag{68}$$

$$\frac{d\bar{v}_k^{\pm}}{ds} + i\frac{J_k}{\tilde{r}}\bar{u}_k^{\pm} + \frac{1}{\tilde{r}\tilde{H}}\frac{d(\tilde{r}\tilde{H})}{dS}\bar{v}_k^{\pm} = \frac{\epsilon_k}{\tilde{r}\tilde{H}}\left[\tilde{V}\frac{d(\tilde{r}\eta_k)}{dS} + \left(\frac{d\tilde{V}}{dS} + i\tilde{\Omega}^{\pm}\right)r\eta_k\right] \quad , \tag{69}$$

$$\begin{aligned}\frac{1}{\tilde{\rho}^*}\frac{d\bar{p}_k^{\pm}}{ds} + \left(\Psi^*_{\tilde{U}} - iR^*\frac{\tilde{V}}{\tilde{r}}\right)\bar{u}_k^{\pm} + \left[\Psi^*_{\tilde{V}} + R^*\left(\frac{d\tilde{V}}{dS} - \frac{\tilde{V}}{\tilde{r}\tilde{H}}\frac{d(\tilde{r}\tilde{H})}{dS} + i\tilde{\Omega}^{\pm}\right)\right]\bar{v}_k^{\pm} \\ = \epsilon_k\Psi^*_{\tilde{H}}\eta_k - \epsilon_k R^*\frac{\tilde{V}}{\tilde{r}\tilde{H}}\left[\tilde{V}\frac{d(\tilde{r}\eta_k)}{dS} + \left(\frac{d\tilde{V}}{dS} + i\tilde{\Omega}^{\pm}\right)r\eta_k\right] \quad ,\end{aligned} \tag{70}$$

where

$$\tilde{\Omega}^{\pm} = \pm\tilde{\Omega} + \frac{\tilde{U}}{\tilde{r}} \quad . \tag{71}$$

The transformations given in Equation (66) satisfy the periodicity requirements in θ. The remaining boundary and continuity conditions are obtained by substituting the variables defined in Equation (67) for the corresponding variables in Equations (53) - (55). The form of the equations remains unchanged and the results are given below:

$$\bar{v}_k^{\pm} = -\frac{\tilde{V}\Delta\tilde{h}}{\tilde{H}(\tilde{H} - \Delta\tilde{h})}\epsilon_k\eta_k + \frac{(\tilde{H} - \Delta\tilde{h})}{\tilde{H}}\bar{v}_{kJ}^{\pm} \quad , \quad \Delta\bar{p}_k^{\pm} = \tfrac{1}{2}\tilde{\rho}^*R^*(\chi_{\tilde{V}}\bar{v}_k^{\pm} - \chi_{\tilde{H}}\epsilon_k\eta_k) \quad @S = S_J \quad , \tag{72}$$

$$\bar{u}_k^{\pm} = 0 \quad , \quad \bar{p}_k^{\pm} = \tfrac{1}{2}\tilde{\rho}^*R^*(\chi_{\tilde{V}}\bar{v}_k^{\pm} - \chi_{\tilde{H}}\epsilon_k\eta_k) \quad @S = S_{in} \tag{73}$$

and

$$\bar{p}_k^{\pm} = 0 \quad @ \; S = S_{ex} \quad . \tag{74}$$

Equations (68) - (70) are solved numerically using the algorithm defined by Equations (56) - (58). Complimentary and particular solutions are constructed and combined so that the boundary conditions given by Equations (72) - (74) can be satisfied without having to iterate.

The real component pressures $\hat{p}_k$, can be expressed in terms of the real and imaginary parts of $\bar{p}_k^+$ and $\bar{p}_k^-$ by expanding the complex pressures, $\hat{p}_k^{\pm}$, substituting the result for the complex pressures in Equation (66) and extracting the real part as indicated. The result may be written as

$$\hat{p}_k = \frac{1}{2}\left[\Re(\bar{p}_k^+ + \bar{p}_k^-)\cos J_k\theta - \Im(\bar{p}_k^+ + \bar{p}_k^-)\sin J_k\theta\right]\cos\tilde{\Omega}\tilde{t} - \frac{1}{2}\left[\Im(\bar{p}_k^+ - \bar{p}_k^-)\cos J_k\theta + \Re(\bar{p}_k^+ - \bar{p}_k^-)\sin J_k\theta\right]\sin\tilde{\Omega}\tilde{t} \quad . \qquad \textbf{(75)}$$

The first term on the right in the above equation will be in phase with the displacement and related to the stiffness of the seal. The negative of the second term will be in phase with oscillatory velocity and related to the damping coefficient.

Forces, moments and dynamic coefficients

The dimensionless applied loads and moments obtained by integrating the pressure over the seal area are

$$\tilde{W}_x = l_c \int_0^{2\pi}\int_{S_L}^{S_R} \tilde{p}\cos\theta\, \check{r}\, dS\, d\theta, \quad \tilde{W}_y = l_c \int_0^{2\pi}\int_{S_L}^{S_R} \tilde{p}\sin\theta\, \check{r}\, dS\, d\theta, \quad \tilde{W}_z = l_f \int_0^{2\pi}\int_{S_L}^{S_R} \tilde{p}\, \check{r}\, dS\, d\theta,$$

$$\tilde{M}_x = -\int_0^{2\pi}\int_{S_L}^{S_R} \tilde{p}\sin\theta\, \check{r}S\, dS\, d\theta, \quad \tilde{M}_y = \int_0^{2\pi}\int_{S_L}^{S_R} \tilde{p}\cos\theta\, \check{r}S\, dS\, d\theta \quad . \qquad \textbf{(76)}$$

All first order applied loads and moments will be zero with the exception of the first order axial load acting on a face seal, W_z, which is given in dimensionless form by

$$\tilde{W}_z = 2\pi l_f \int_{S_L}^{S_R} \tilde{P}\, \check{r}\, dS \quad . \qquad \textbf{(77)}$$

The various stiffnesses can be obtained by substituting the first term on the right hand side of Equation (75) for the pressure, $\tilde{p}$, appearing in the force and moment integrals in Equation (76) and dividing the result by the associated displacement of the center of the seal. The dimensionless translations and rotations that have been included in Equation (59) are a rotation about the **y** axis of magnitude $\tilde{\psi}_0\cos\tilde{\Omega}\tilde{t}$ (corresponding to **k=1**), a translation in the **x** direction of magnitude $\tilde{e}_{x0}\cos\tilde{\Omega}\tilde{t}$ (corresponding to **k=2**) for a cylindrical seal and a translation in the axial direction of magnitude $\tilde{e}_{z0}\cos\tilde{\Omega}\tilde{t}$ (corresponding to **k=3**) for a face seal. The damping coefficients may be obtained in a similar manner by substituting the second term on the right hand side of Equation (75) for the pressure in Equation (76) and dividing the result by the velocity $-\tilde{\Omega}\tilde{t}\ \tilde{\psi}_0\sin\tilde{\Omega}\tilde{t}$ for **k=1**, $-\tilde{\Omega}\tilde{e}_{x0}\sin\tilde{\Omega}\tilde{t}$ for **k=2** and $-\tilde{\Omega}\tilde{e}_{z0}\sin\tilde{\Omega}\tilde{t}$ for **k=3**.

For small displacements about the centered position, stiffness and damping values associated with

translations in the **y** direction or rotations about the **x** axis may be obtained from symmetry considerations. For example, a displacement in the **y** direction will produce a force in that direction of the same magnitude as that which would be produced in the **x** direction for an equivalent displacement in that direction ($\mathbf{K_{yy}=K_{xx}}$). Similarly, a displacement in the **y** direction will produce a force at 90° from that direction (which would be the negative **x** direction) as would be produced in the positive **y** direction for an equivalent displacement in the **x** direction ($\mathbf{K_{xy}=-K_{yx}}$).

The symbols ϕ and ψ, when appearing as second subscripts on the dynamic coefficients, will denote rotations about the **x** and **y** axes respectively. When appearing as first subscripts they will denote moments about the **x** and **y** axes. The dimensionless stiffness and damping coefficients relating moments about the **x** and **y** axes to a rotation about the **y** axis (**k=1**) for both face and cylindrical seals are

$$\tilde{K}_{\phi\psi} = \frac{\pi}{2\epsilon_1}\int_{S_L}^{S_R} \Im(\bar{p}_1^{+} + \bar{p}_1^{-})S\,dS \;,\quad \tilde{K}_{\psi\psi} = \frac{\pi}{2\epsilon_1}\int_{S_L}^{S_R} \Re(\bar{p}_1^{+} + \bar{p}_1^{-})S\,dS \;,$$
$$\tilde{B}_{\phi\psi} = -\frac{\pi}{2\tilde{\Omega}\epsilon_1}\int_{S_L}^{S_R} \Re(\bar{p}_1^{+} - \bar{p}_1^{-})S\,dS \;,\quad \tilde{B}_{\psi\psi} = \frac{\pi}{2\tilde{\Omega}\epsilon_1}\int_{S_L}^{S_R} \Im(\bar{p}_1^{+} - \bar{p}_1^{-})S\,dS \;. \tag{78}$$

The corresponding coefficients for a rotation about the **x** axis obtained from symmetry considerations are

$$\tilde{K}_{\phi\phi} = \tilde{K}_{\psi\psi} \;,\quad \tilde{K}_{\psi\phi} = -\tilde{K}_{\phi\psi} \;,\quad \tilde{B}_{\phi\phi} = \tilde{B}_{\psi\psi} \;,\quad \tilde{B}_{\psi\phi} = -\tilde{B}_{\phi\psi} \;. \tag{79}$$

The dimensionless dynamic coefficients relating the **x** and **y** force components to a rotation about the **y** axis (**k=1**) for a cylindrical seal are

$$\tilde{K}_{x\psi} = \frac{\pi l_c}{2\epsilon_1}\int_{S_L}^{S_R} \Re(\bar{p}_1^{+} + \bar{p}_1^{-})dS \;,\quad \tilde{K}_{y\psi} = -\frac{\pi l_c}{2\epsilon_1}\int_{S_L}^{S_R} \Im(\bar{p}_1^{+} + \bar{p}_1^{-})dS \;,$$
$$\tilde{B}_{x\psi} = \frac{\pi l_c}{2\tilde{\Omega}\epsilon_1}\int_{S_L}^{S_R} \Im(\bar{p}_1^{+} - \bar{p}_1^{-})dS \;,\quad \tilde{B}_{y\psi} = \frac{\pi l_c}{2\tilde{\Omega}\epsilon_1}\int_{S_L}^{S_R} \Re(\bar{p}_1^{+} - \bar{p}_1^{-})dS \tag{80}$$

and the corresponding coefficients for a rotation about the **x** axis are

$$\tilde{K}_{x\phi} = \tilde{K}_{y\psi} \ , \quad \tilde{K}_{y\phi} = -\tilde{K}_{x\psi} \ , \quad \tilde{B}_{x\phi} = \tilde{B}_{y\psi} \ , \quad \tilde{B}_{y\phi} = -\tilde{B}_{x\psi} \ . \tag{81}$$

The dimensionless stiffness and damping coefficients relating moments about the **x** and **y** axes to a translation in the **x** direction (**k=2**) for a cylindrical seal are

$$\begin{aligned} \tilde{K}_{\phi x} &= \frac{\pi}{2\epsilon_2} \int_{S_L}^{S_R} \Im(\bar{p}_2^{\,+} + \bar{p}_2^{\,-}) S \, dS \ , \quad \tilde{K}_{\psi x} = \frac{\pi}{2\epsilon_2} \int_{S_L}^{S_R} \Re(\bar{p}_2^{\,+} + \bar{p}_2^{\,-}) S \, dS \ , \\ \tilde{B}_{\phi x} &= -\frac{\pi}{2\tilde{\Omega}\epsilon_2} \int_{S_L}^{S_R} \Re(\bar{p}_2^{\,+} - \bar{p}_2^{\,-}) S \, dS \ , \quad \tilde{B}_{\psi x} = \frac{\pi}{2\tilde{\Omega}\epsilon_2} \int_{S_L}^{S_R} \Im(\bar{p}_2^{\,+} - \bar{p}_2^{\,-}) S \, dS \end{aligned} \tag{82}$$

and the corresponding coefficients for a translation in the **y** direction are

$$\tilde{K}_{\phi y} = -\tilde{K}_{\psi x} \ , \quad \tilde{K}_{\psi y} = \tilde{K}_{\phi x} \ , \quad \tilde{B}_{\phi y} = -\tilde{B}_{\psi x} \ , \quad \tilde{B}_{\psi y} = \tilde{B}_{\phi x} \ . \tag{83}$$

The dimensionless dynamic coefficients relating the **x** and **y** force components to a translation in the **x** direction (**k=2**) for a cylindrical seal are

$$\begin{aligned} \tilde{K}_{xx} &= \frac{\pi l_c}{2\epsilon_2} \int_{S_L}^{S_R} \Re(\bar{p}_2^{\,+} + \bar{p}_2^{\,-}) dS \ , \quad \tilde{K}_{yx} = -\frac{\pi l_c}{2\epsilon_2} \int_{S_L}^{S_R} \Im(\bar{p}_2^{\,+} + \bar{p}_2^{\,-}) dS \ , \\ \tilde{B}_{xx} &= \frac{\pi l_c}{2\tilde{\Omega}\epsilon_2} \int_{S_L}^{S_R} \Im(\bar{p}_2^{\,+} - \bar{p}_2^{\,-}) dS \ , \quad \tilde{B}_{yx} = \frac{\pi l_c}{2\tilde{\Omega}\epsilon_2} \int_{S_L}^{S_R} \Re(\bar{p}_2^{\,+} - \bar{p}_2^{\,-}) dS \end{aligned} \tag{84}$$

and the corresponding coefficients for a translation in the **y** direction are

$$\tilde{K}_{xy} = -\tilde{K}_{yx} \ , \quad \tilde{K}_{yy} = \tilde{K}_{xx} \ , \quad \tilde{B}_{xy} = -\tilde{B}_{yx} \ , \quad \tilde{B}_{yy} = \tilde{B}_{xx} \ . \tag{85}$$

Finally, the stiffness and damping coefficients relating the axial force to an axial translation (**k=3**) for a face seal are

$$\tilde{K}_{zz} = \frac{\pi l_f}{\epsilon_3} \int_{S_L}^{S_R} \Re(\bar{p}_3^{+} + \bar{p}_3^{-}) dS \ , \quad \tilde{B}_{zz} = \frac{\pi l_f}{\tilde{\Omega}\epsilon_3} \int_{S_L}^{S_R} \Im(\bar{p}_3^{+} - \bar{p}_3^{-}) dS \ . \tag{86}$$

As a result of the assumption of small displacements about the centered position used in this analysis, the remaining dynamic coefficients for a face seal will all be zero:

$$\tilde{K}_{z\phi} = \tilde{K}_{\phi z} = \tilde{K}_{z\psi} = \tilde{K}_{\psi z} = \tilde{B}_{z\phi} = \tilde{B}_{\phi z} = \tilde{B}_{z\psi} = \tilde{B}_{\psi z} = 0 \ . \tag{87}$$

Relationships of the following type may be used to calculate the physical stiffness and damping coefficients from the dimensionless ones

$$K_{xx} = \frac{p_0 r_0^2}{C} \tilde{K}_{xx} \ , \quad K_{\phi\phi} = \frac{p_0 r_0^4}{C} \tilde{K}_{\phi\phi} \ , \quad K_{x\phi} = \frac{p_0 r_0^3}{C} \tilde{K}_{x\phi} \tag{88}$$

and

$$B_{xx} = \frac{p_0 r_0^3}{C V_0} \tilde{B}_{xx} \ , \quad B_{\phi\phi} = \frac{p_0 r_0^5}{C V_0} \tilde{B}_{\phi\phi} \ , \quad B_{x\phi} = \frac{p_0 r_0^4}{C V_0} \tilde{B}_{x\phi} \ . \tag{89}$$

The stiffness coefficients, which relate to forces in phase with the displacements and the damping coefficients, which relate to forces 90° out of phase with the displacements, are both, in general, functions of $\tilde{\Omega}$. For the case of incompressible flow under consideration, the damping coefficients and the cross coupled stiffness coefficients ($\tilde{K}_{xy}$, $\tilde{K}_{\phi\psi}$, $\tilde{K}_{yx}$, $\tilde{K}_{\psi\phi}$) are nearly independent of $\tilde{\Omega}$. Under these circumstances, it has been found that the frequency dependence may be described adequately with the introduction of an apparent mass matrix **[A]** such that **[K] = [K^0] - Ω^2[A]**, where **[K^0]** is the stiffness matrix evaluated at **Ω=0**. The components of **[A]** may be evaluated by computing **[K]** at a characteristic speed such as **$\Omega = V_0/r_0$** corresponding to **$\tilde{\Omega}$=1** or synchronous speed **($\Omega=\omega$)** and using the formula

$$A_{ij} = \frac{K_{ij} - K_{ij}^0}{\Omega^2} \tag{90}$$

The cross coupled components of **[A]** which have been included for completeness are not significant and the direct components are indeed found to be nearly independent of Ω.

Although the linearizations that have been used in obtaining the second order flow equations are only valid for small values of ϵ_k, once they have been performed the resulting equations for the dynamic coefficients may be shown, by rescaling variables, to be independent of the value ϵ_k actually used. Any convenient value such

as ϵ_k=1 may be used in computations.

Determination of power loss and flow

When the rotating surface (a) is ungrooved, the power loss will be proportional to the integral of $r\vec{\tau}_a \cdot \vec{i}$ over the surface of the seal. When the rotating surface is grooved, an additional term will be needed to correct for the pressures acting edges of the grooves. Although the solution to the equations based on bulk flow theory used here does provide for the prediction the shear stress on each surface, the validity of power loss predictions is somewhat doubtful. This is due to the difference in characterizing the bulk flow behavior for velocity distributions associated with Couette and Poiseuille flow.

One may write $\vec{\tau}_a$ as $\vec{\tau}_a = \vec{\tau}_c + \vec{\tau}_p$ where $\vec{\tau}_c$ denotes the Couette part of the shear stress defined as $\vec{\tau}_c = (\vec{\tau}_a + \vec{\tau}_b)/2$ and $\vec{\tau}_p$ denotes the Poiseuille portion of the shear stress defined as $\vec{\tau}_p = (\vec{\tau}_a - \vec{\tau}_b)/2$. It can be seen from Equations (1) and (2) that only $\vec{\tau}_p$ appears in the primary and secondary flow equations used to predict load, flow and dynamic coefficients. Comparisons between theory and experiments based on measurements of flow and dynamic coefficients alone may be used to validate or determine values of $\vec{\tau}_p$, but will not necessarily result in a bulk flow model that accurately predicts power loss. This weakness in the bulk flow model was recognized by Hirs (reference 1) who suggested the use of different friction factor representations based on measurements obtained from experiments based on Couette and Poiseuille flow. The method for predicting power loss used here will be a highly approximate one based on generalizations of an approach used by Hirs for cases where both surfaces were smooth and the flow was predominantly in the tangential direction.

If the scaler shear stress, τ, is used to represent the tangential shear stress, $(\tau=\vec{\tau}\cdot\vec{i})$, then the dimensionless forms of the tangential shear stresses τ_a and τ_b, can be obtained from Equations (4), (5), (8), and (10) as

$$\tilde{\tau}_a = \tilde{p}^* R_a f_a(R_a) \frac{\tilde{u} - \tilde{r}\tilde{\omega}}{\tilde{h}} \quad , \quad \tilde{\tau}_b = -\tilde{p}^* R_b f_b(R_b) \frac{\tilde{u}}{\tilde{h}} \quad . \tag{91}$$

One may attempt to compensate for the influence of the Couette portion of the shear stress by replacing $\tilde{\tau}_a$ with the effective shear stress, $\tilde{\tau}^*$, defined as

$$\tilde{\tau}^* = \frac{\tilde{\tau}_a + \tilde{\tau}_b}{2\lambda} + \frac{\tilde{\tau}_a - \tilde{\tau}_b}{2} = \frac{\tilde{\tau}_c}{\lambda} + \tilde{\tau}_p \tag{92}$$

in the integral used for determining power loss. The correct value of the "Couette reduction factor", λ, may

be shown to be λ=3 for laminar flow. A value of λ=1.2 will be used for turbulent flow. This value was suggested by Hirs based on one dimensional Couette flow measurements and provides power predictions that are in good agreement with those obtained with Ng and Pan theory (reference 13) over its range of validity.

The dimensionless power loss, $\tilde{\wp} = \wp/(Cp_0 r_0^2 \omega)$, obtained from the solution to the first order flow equations is given by

$$\tilde{\wp} = -2\pi \int_{S_L}^{S_R} \left[\alpha \tilde{\tau}_g^* + (1-\alpha)\tilde{\tau}_r^* + l_\omega \tilde{\delta} \left(\alpha \tilde{P}_{g,\theta} + \frac{N_g \tilde{p}^* R^*}{4\pi \tilde{r}} \chi\left(\frac{\tilde{q}_n}{\tilde{h}_g}, \tilde{h}_g, \tilde{\delta}\right) \mathrm{sign}(\tilde{q}_n \sin\beta) \right) \right] \tilde{r}^2 dS \quad . \quad \textbf{(93)}$$

The quantities $\tilde{\tau}_g^*$ and $\tilde{\tau}_r^*$ appearing in the above equation denote the values of the effective shear stress, $\tilde{\tau}^*$, based on the first order velocities and film thicknesses for the grooves and ridges respectively. The effective shear stress is defined by Equations (91) and (92) and the local velocities are obtained from the solution to Equations (30) and (32) - (34) and the definitions provided by Equation (21). The sum of the first two terms appearing inside the brackets of the integrand in Equation (93) represent the global value of $\tilde{\tau}^*$. The third term has been added to include the forces acting on the edges of the grooves when the grooves are on the rotor. The quantity $\tilde{P}_{g,\theta}$ is obtained by substituting first order variables for the corresponding quantities in Equation (24) and is given below:

$$\tilde{P}_{g,\theta} = -\tilde{p}^* \Phi_g - \tilde{p}^* R^* \left(\tilde{V} \frac{d\tilde{U}}{dS} + l_f \frac{\tilde{U}\tilde{V}}{\tilde{r}} \right) \quad . \quad \textbf{(94)}$$

3. Description of Computer Code SPIRALI

The FORTRAN computer program SPIRALI, has been written to implement the analysis that is contained in Section 2. The program has been compiled in its present form with Version 5.1 of the Microsoft® Fortran Compiler and should work with many other compilers with relatively little modification. SPIRALI uses two features that are supported by a wide variety of compilers that are extensions to FORTRAN 77. The first of these extensions is the use of NAMELIST input. The second extension relates to the implementation of complex double precision variables in the solution of the second order flow equations required to compute stiffness, damping and apparent mass values. It should be noted that NAMELIST is a VAX extension and COMPLEX DOUBLE PRECISION is part of IBM Systems Application Architecture, IBM VS and VAX extensions to Fortran 77.

The main program is system dependent in that it opens files and when compiled with the Microsoft compiler, allows placement of file names on the command line. It also reads the input data and generates the plot file. The supporting output routines either write to the standard output unit or take FORTRAN supported logical unit numbers as input, hence should not require significant modification with any FORTRAN 77 compiler. In particular, the subroutine INLIST writes the NAMELIST to the output file in a legible manner and the remainder of the output file is generated by the subroutine DIMOUT. Status and error messages are written to the standard output unit by the subroutines OUTSCR and EMSG respectively. There are no input or output statements in any of the other routines contained in SPIRALI.

Although SPIRALI is designed to run over a full range of conditions of laminar or turbulent flow, certain precautions need to be taken when the transverse flow rate is small. It can be seen, for example, that Equation (44) becomes singular as $\mathbf{R}^*\tilde{\mathbf{V}}$ approaches **0**. Numerical problems can be avoided here by setting $\mathbf{R}^*\tilde{\mathbf{V}}=\mathbf{0}$ and numerically solving Equation (44) as an algebraic equation rather than as a differential equation. SPIRALI provides an option for the user to exclude the transverse inertia effects arising from the terms $\tilde{v}\partial\tilde{u}/\partial S$ and $I_f\tilde{u}\tilde{v}/\tilde{r}$ in Equation (11) and $\tilde{v}\partial\tilde{v}/\partial S$ in Equation (12) and the associated discontinuities in pressure that occur at the inlet and at jump discontinuities in film thickness. This option, which is controlled by the input parameter NOI (see input description) is particularly useful for situations where the rotation speed is high but the seal pressure difference is low.

If transverse inertia is included, the location of the upstream or inlet boundary must be specified. When the seal pressure difference is sufficiently high, the upstream boundary will be at the high pressure side of the seal. At lower pressure differences the upstream boundary may depend on the rotor speed and the spiral groove parameters. The input parameter IFLOW is used to select the upstream boundary. If you are not sure of the flow direction, run the program with transverse inertia excluded. If you then wish to include transverse inertia, adjust IFLOW in accordance with the sign of the transverse flow rate given in the output and rerun the

program with transverse inertia included.

The analytical procedure contained in Section 2 has been oriented toward determining pressure distribution, load, flow, power loss, stiffness and damping for a given centered film thickness distribution. Face seals will, in general, have a non-zero first order axial load component and it is often desirable to determine the equilibrium film thickness from a prescribed load used to balance the seal. SPIRALI provides an iterative homing option for this purpose that is controlled by the input parameter IHOME. The homing option should be used with caution since convergence is sensitive to the starting film thickness which is determined from the input parameter C. It is recommended that the program be run for various values of C without the homing option so that a good starting value of C (one that produces an output value of the load to balance the face seal that is reasonably close to the prescribed load) can be obtained for the homing process.

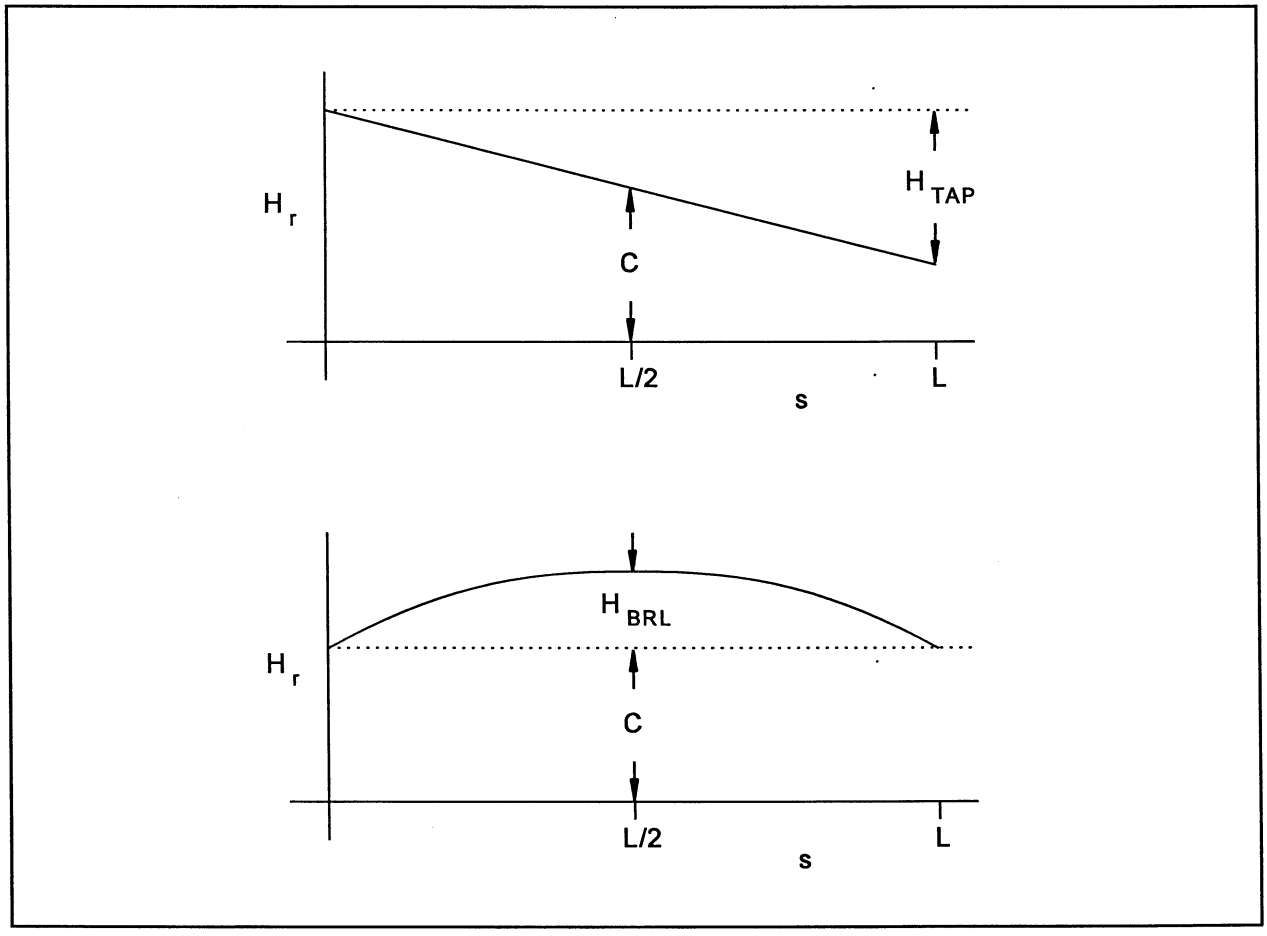


Figure 7 Parameters for characterizing quadratic film variation.

Although the analysis provides for an arbitrary transverse film thickness variation, SPIRALI is limited to a quadratic film variation with coefficients determined from the parameters $\mathbf{H_{TAP}}$, $\mathbf{H_{BRL}}$ and **C** as shown in Figure 7. These parameters may be positive, as shown or negative and should be able to characterize a fairly general film variation without the complexity of required inputs at every grid point.

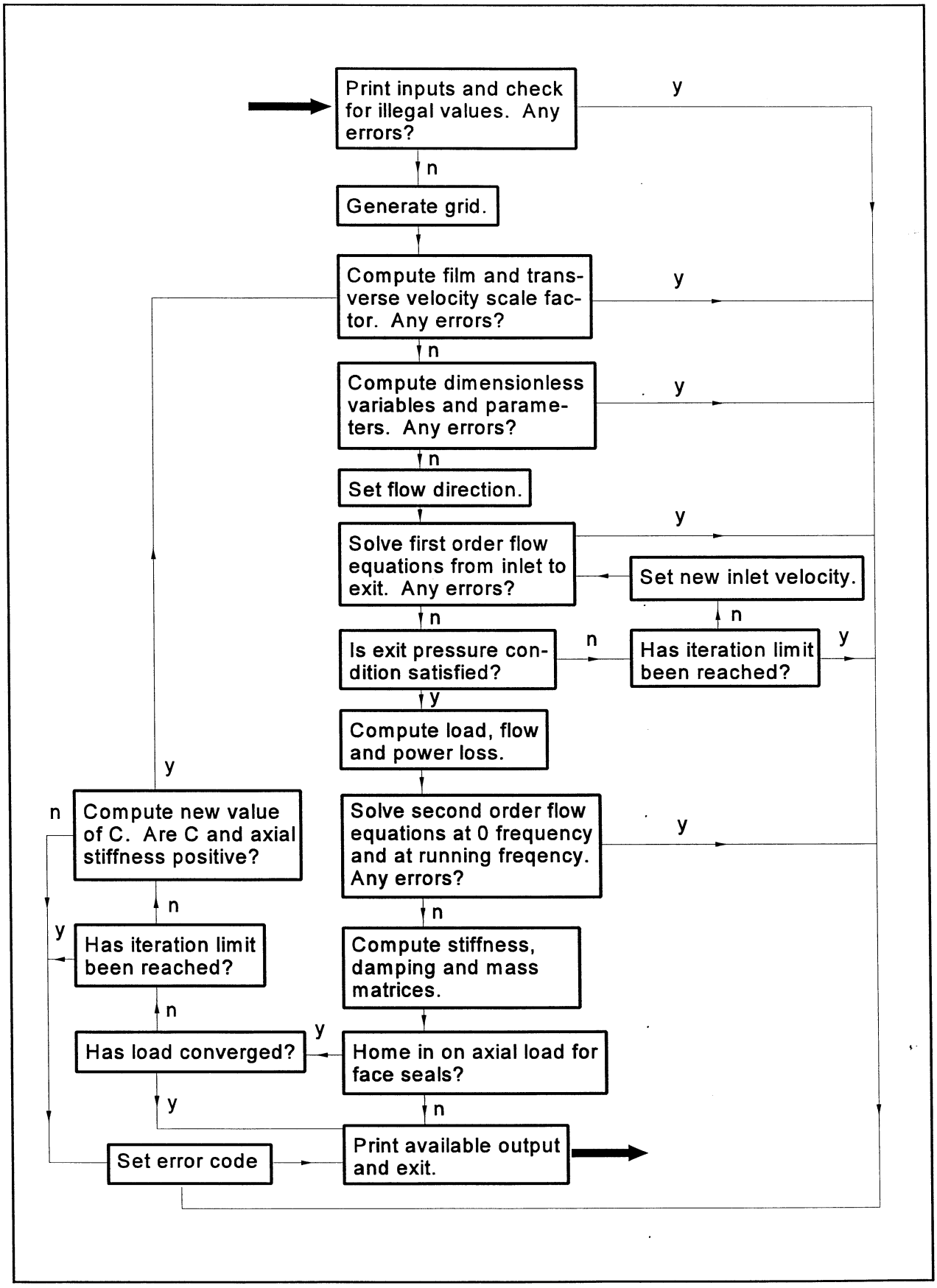


Figure 8 Flow diagram for overall logic used in computations

The logic used in SPIRALI for solving the first and second order flow equations, computing load, flow, power loss, stiffness, damping, apparent mass coefficients, etc. for a given case is shown in Figure 8. On completion, the program will look for a new NAMELIST and if found, will proceed to the next case.

The program SPIRALI may be run in its present form under either DOS or OS2 operating systems by entering the command

SPIRALI infile outfile plotfile

where infile and outfile are user supplied names of the input and output files respectively and plotfile is a data file containing first order film thickness, velocity and pressure profiles as functions of **S**. The contents of these files are described below.

Input description for SPIRALI

SPIRALI requires its input in NAMELIST form. The NAMELIST variables will be given below in the order that they are listed in the output. Units for dimensional inputs will be given in English units as required when ISIUN=0, followed by SI units required when ISIUN=1 in parentheses, where applicable. The NAMELIST name is INPUTS. The relationship between the NAMELIST variables and symbols appearing in the nomenclature will be given wherever possible.

TITLE any character string enclosed in quotes containing up to 64 characters

IFACE 0 for cylindrical seal, 1 for face seal

ISIUN 0 for English units, 1 for SI units

IGROT groove rotation flag, set to 1, if the rotating surface is grooved or 0, if ungrooved

NOI parameter which controls treatment of inertia effects with following values:

- -1 include all inertia effects
- 0 include tangential inertia effects, program decides on transverse inertia effects
- 1 include tangential inertia effects, exclude transverse inertia effects
- 2 exclude all inertia effects

IFLOW parameter which controls selection of inlet boundary with following values:

- -1 assume transverse flow rate to be negative, inlet boundary is at right ($\mathbf{s}_{in}=\mathbf{s}_R$)
- 0 assume that the sign of the transverse flow rate is the same as the sign of p_L-p_R and set inlet boundary accordingly
- 1 assume transverse flow rate to be positive, inlet boundary is at left ($\mathbf{s}_{in}=\mathbf{s}_L$)

R0 $\mathbf{r}_0$, radius of cylindrical seal (IFACE=0) or outside radius of face seal (IFACE=1), in. (m)

EL **L**, length of cylindrical seal (IFACE=0) or land width of face seal (IFACE=1) as shown in Figure 1, in. (m)

C	**C**, constant spacing between the two surfaces of the seal which would occur if δ, $\mathbf{H_{TAP}}$ and $\mathbf{H_{BRL}}$ were all equal to 0 (see Fig. 7). and is referred to as the clearance of a cylindrical seal (IFACE=0) or nominal film thickness of a face seal (IFACE=1), in. (m)
RPM	ω, angular speed of rotating surface converted to revolutions per minute
RPM0	$\mathbf{u_{in}/r_{in}}$, angular swirl speed of fluid at inlet to seal converted to revolutions per minute
RPMD	Ω, angular speed of disturbance converted to revolutions per minute. If Ω**>0**, the output file will contain a table of stiffness and damping values, evaluated at Ω followed by the static stiffnesses evaluated at 0 frequency. If Ω**=0**, the static stiffnesses will be replaced by apparent masses.
PLEG	$\mathbf{p_L}$, gage pressure at $\mathbf{s=s_L}$, psi (Pa)
PRIG	$\mathbf{p_R}$, gage pressure at $\mathbf{s=s_R}$, psi (Pa)
FZD	$\mathbf{W_z}$, applied load in z direction, used only if IHOME=1 and IFACE=1, lb. (N). It should be noted that the ambient pressure, $\mathbf{min(p_L,p_R)}$, does not contribute to the applied load and should be subtracted from all pressures when determining pressure induced loading.
VISC	μ, fluid viscosity, psi-sec (Pa-sec)
DENS	ρ, fluid density, lb-sec^2/in^4 (Kg/m^3)
EMA	$\mathbf{m_a}$, exponent in shear factor power law relationship for moving surface
ENA	$\mathbf{m_a}$, coefficient in shear factor power law relationship for moving surface
EMB	$\mathbf{m_b}$, exponent in shear factor power law relationship for stationary surface
ENB	$\mathbf{m_b}$, coefficient in shear factor power law relationship for stationary surface
HTAP	$\mathbf{H_{TAP}}$, film change defining linear taper, see Fig. 7, in. (m)
HBRL	$\mathbf{H_{BRL}}$, film change defining quadratic "barreling", see Fig. 7, in. (m)
TOLH	maximum allowable relative error in axial load (used only when IFACE=1 and IHOME=1) an error code is returned if this tolerance is not met in NITH iterations
TOLV	maximum allowable relative error in dimensionless first order transverse inlet velocity, $\mathbf{\nabla_{in}}$. An error code is returned if this tolerance is not met in NITV iterations.
DUT	relative increment used in numerical differentiation
IHOME	when set to 1 triggers computation of the nominal film thickness C for which the applied load prescribed by FZD is equal to the calculated load required to balance the face seal (used only if IFACE=1)
NITH	maximum number of iterations to be used for homing in on load for face seal (used only if IFACE=1 and IHOME=1)
NITV	maximum number of iterations to be used determination of first order transverse velocity component at inlet, $\mathbf{V_{in}}$
NREG	number of regions in axial direction (IFACE=0) or radial direction (IFACE=1)
NRSUB	vector of length NREG containing number of sub-intervals in each of the NREG regions
ELFR	vector of length NREG containing fractional extent of each of the NREG regions (length of region divided by **L**). The sum of the NREG values of ELFR must add up to 1.

ALPI vector of length NREG containing groove to pitch ratio, α, for each of the NREG regions. Set α**=0** in ungrooved regions. Set α**=1** for regions comprising circular steps or grooves. Spiral groove theory is not implemented when α**=0** or α**=1**.

BETI vector of length NREG containing groove angle, β (degrees), in the range -90° < BETI < 90°, for each of the NREG regions. Set to 0 in ungrooved regions. Spiral groove theory is not implemented when β**=0**.

DELT vector of length NREG containing groove depth, δ, for each of the NREG regions, in (m). If α**=1** but $\delta \neq$**0**, the region will be treated as a circular groove **(δ>0)** or step **(δ<0)**.

ZET vector of length NREG containing the contraction loss coefficient, ζ, at the inlet to each of the NREG regions

NSG vector of length NREG containing the number of spiral grooves in each region. This input is used solely for characterizing effects of local inertia on pressure jumps in regions where spiral groove theory is implemented. In regions where NG=0 effects of local inertia on spiral groove performance is ignored.

ZETG vector of length NREG containing the contraction loss coefficient, ζ, associated with the local pressure drop for flow going from grooves to ridges for each of the regions where spiral groove theory is implemented and NG>0.

The default values of the NAMELIST variables are given in Figure 9. These values correspond to a static, ungrooved, cylindrical seal with inputs in English units. The default case cannot be run until non-zero values are provided, at least, for R0, EL, C, VISC and either PLEG, PRIG or RPM.

Description of output from SPIRALI

Listings of output files generated by SPIRALI are given in Section 4 under sample problems. The output file starts with a reference case number and the title which is followed by a listing of the NAMELIST variables in a form suitable for extraction as an input file. The next line gives the seal type and a statement as to which (if any) inertia effects have been excluded. The next 4 lines provide a brief description of the seal geometry, operating data and fluid properties. When IHOME=0 and IFACE=1 the nominal film thickness will be the computed value rather than the input value of C. The next line contains an error code (see Section 7 for an explanation of non-zero error codes) and the number of iterations used in determining the transverse flow rate when solving the first order flow equations (iterations in primary flow). When IFACE=1 the axial load required to balance the face seal will be given which may be compared with the input value of FZD, when IHOME=1, to evaluate the accuracy of the homing process. The next two lines contain the transverse flow rate, **Q**, the torque and the power loss $\wp$. These are followed by the local Reynolds numbers at the left and right seal boundaries based on the absolute values of the transverse fluid velocities and the circumferential fluid velocities relative to the rotor respectively and may be used to estimate the degree of turbulence in the seal.

```
&INPUTS
   TITLE  =  ' '
   IFACE  =  0              ISIUN  =  0
   IGROT  =  0              NOI    =  0              IFLOW  =  0
   R0     =  0.0000E+00     EL     =  0.0000E+00     C      =  0.0000E+00
   RPM    =  0.0000E+00     RPM0   =  0.0000E+00     RPMD   =  0.0000E+00
   PLEG   =  0.0000E+00     PRIG   =  0.0000E+00     FZD    =  0.0000E+00
   VISC   =  0.0000E+00     DENS   =  0.0000E+00
   EMA    = -2.5000E-01     ENA    =  7.9100E-02
   EMB    = -2.5000E-01     ENB    =  7.9100E-02
   HTAP   =  0.0000E+00     HBRL   =  0.0000E+00
   TOLH   =  1.0000E-04     TOLV   =  1.0000E-05     DUT    =  1.0000E-06
   IHOME  =  0              NITH   =  10             NITV   =  30
   NREG   =  1              NRSUB  =  20
   ELFR   =  1.0000E+00
   ZET    =  0.0000E+00
   ALPI   =  0.0000E+00
   BETI   =  0.0000E+00
   DELT   =  0.0000E+00
   NSG    =  0
   ZETG   =  0.0000E+00
 /
```

Figure 9 Namelist defaults

A table of stiffness, K, damping, B, and apparent mass A, (if RPMD=0) or static stiffness, K0 (if RPMD>0) are given next, where the column corresponds to the displacement or rotation and the row corresponds to the force or moment. The units for any given stiffness, damping or mass value will be the force unit given at the end of its row divided by the displacement unit given at the top of its column.

The plot file corresponding to the third argument on the command line starts with a line containing the number of points in the data set to be plotted, NP. This is followed by a table of NP lines. The columns from left to right are values of the variables **S**, $\mathbf{H_r}$ [in. (m)], **U** [in/sec (m/sec)], **V** [in/sec (m/sec)] and **P** [psi (Pa)].

4. Sample Problems

Several sample problems have been prepared to show the use of the computer program for cylindrical and face seal applications. They are intended primarily for illustration and do not necessarily represent recommended seal designs. Separate input files are not given since the complete input NAMELIST is included in the output file for each case.

Cases 1 - 5 apply to the cylindrical seal geometry shown schematically in Figure 10. The seals for cases 1 - 4 are divided into two regions of equal length. The region at the left consists contains a spiral groove pattern for cases 1 and 2 and an ungrooved step of depth δ for cases 3 and 4. A plain cylindrical seal consisting of a single region at a constant film thickness, **C**, is used for comparison in case 5. The high pressure is at the left hand side of the seal for cases 1, 3 and 5 and at the right hand side for cases 2 and 4. A groove angle of β**=25**° has been used for cases 1 and 2, which will tend to pump from left to right. The flow produced by the pressure gradient should be in the same direction as groove pumping in case 1 and in the opposite direction in case 2. The pressure gradient will tend to dominate the flow in both cases. The parameters NOI and IFLOW have both been set to 0 for all of the above cases. Inertia effects have been included for all of the sample cases (otherwise the output file would state which effects were neglected) and the assumption that the flow direction is away from the high pressure side of the seal, which is employed when IFLOW=0, is validated by the sign of the flow rate for each of the cases.

Cases 6 - 8 correspond to a mechanical face seal with spiral grooves on the outside surface of the stator oriented to pump inward. The stator geometry is shown schematically in Figure 11. The high pressure is on the outside of the seal. A 1 mil (.0254 mm) nominal film thickness is used for case 6 and a value of 1.5 mils (.0381 mm) is used for case 7. IHOME is set equal to 1 for case 8 and a load of 1600 lb (7116.8 N) is applied to balance the seal. The load to balance the seal used in case 8 was bounded by the results of cases 6 and 7. This bounding procedure is recommended for all applications where IHOME will be set to 1. A finer grid was used in the inlet (outside) region for cases 6 - 8, to reduce truncation error resulting from the inclusion of inertia effects with the relatively low radial Reynolds number that occurs at the outside radius in case 6. It is particularly important to check accuracy by increasing the values of NRSUB when inertia effects are included.

Cases 9 - 10 correspond to a straight through helically grooved cylindrical seal of the type reported by Childs, Nolan and Kilgore in Reference 14. The input geometry for Case 9 corresponds to their Stator #2 which has 17 grooves, a groove angle of 15°and a gap of .376 mm. Case 10 is the same as Case 9 except that the value of $\mathbf{N_g}$ has been set equal to 0. Case 10 does not have any real physical significance and is presented solely for comparison with Case 9.

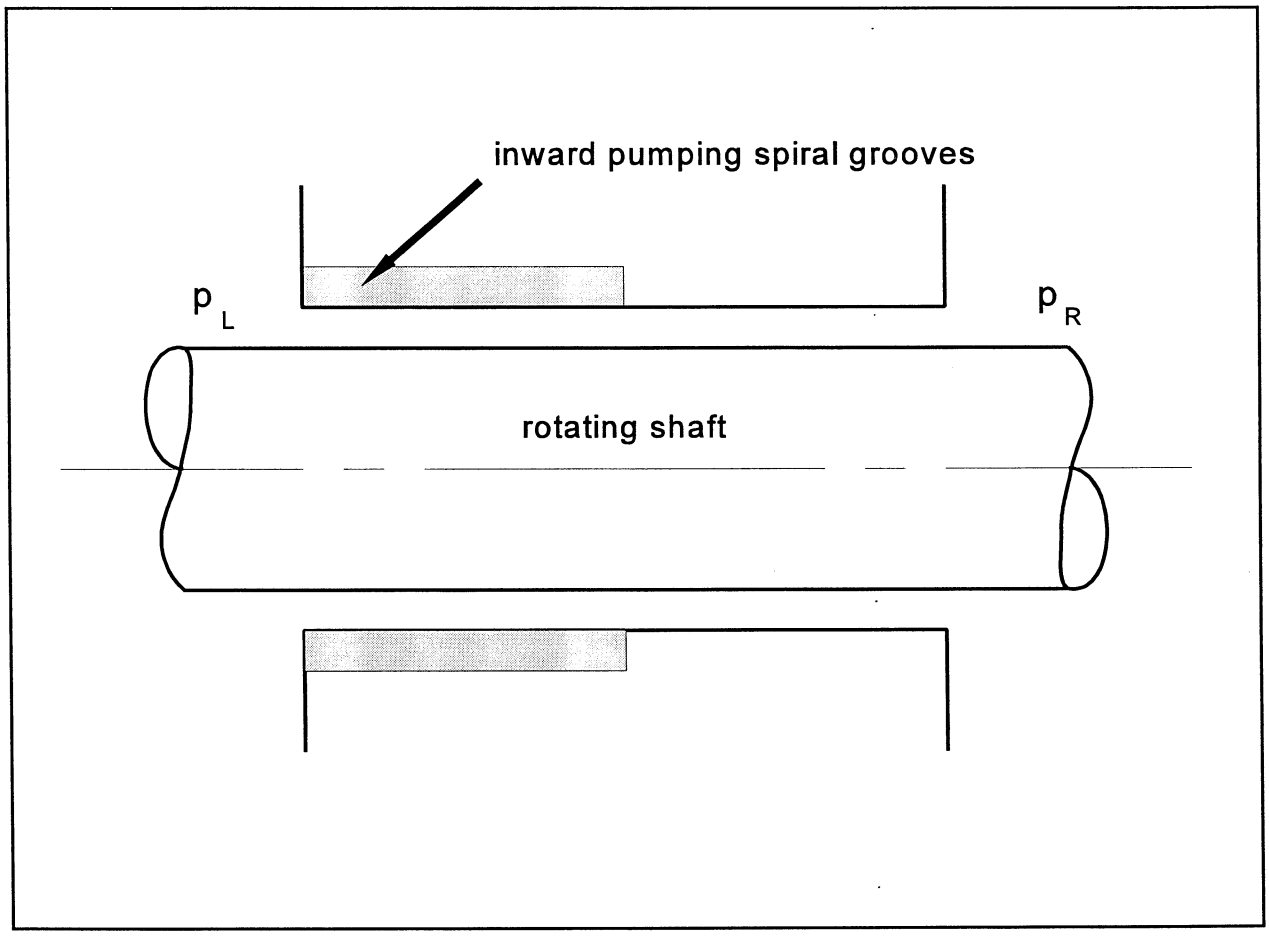


Figure 10 Schematic of cylindrical seal for cases 1 - 5

```
( CASE  1 )  Cylindrical seal, grooves pumping inward, high pres. at left

&INPUTS
   TITLE  =  'Cylindrical seal, grooves pumping inward, high pres. at left'
   IFACE  =  0              ISIUN  =  0
   IGROT  =  0              NOI    =  0              IFLOW  =  0
   R0     =  1.0000E+00     EL     =  5.0000E-01     C      =  1.0000E-03
   RPM    =  5.0000E+04     RPM0   =  2.5000E+04     RPMD   =  0.0000E+00
   PLEG   =  1.0000E+03     PRIG   =  0.0000E+00     FZD    =  0.0000E+00
   VISC   =  3.0000E-08     DENS   =  1.0000E-04
   EMA    = -2.5000E-01     ENA    =  7.9100E-02
   EMB    = -2.5000E-01     ENB    =  7.9100E-02
   HTAP   =  0.0000E+00     HBRL   =  0.0000E+00
   TOLH   =  1.0000E-04     TOLV   =  1.0000E-05     DUT    =  1.0000E-06
   IHOME  =  0              NITH   =  10             NITV   =  30
   NREG   =  2              NRSUB  =  50  50
   ELFR   =  5.0000E-01  5.0000E-01
   ZET    =  0.0000E+00  0.0000E+00
   ALPI   =  5.0000E-01  0.0000E+00
   BETI   =  2.5000E+01  0.0000E+00
   DELT   =  2.0000E-03  0.0000E+00
   NSG    =  16   0
   ZETG   =  0.0000E+00  0.0000E+00
/

CYLINDRICAL SEAL

LENGTH, DIAMETER, CLEARANCE =  5.0000E-01,  2.0000E+00,  1.0000E-03  (IN)

ROTOR, SWIRL AND DIST. SPEEDS =  5.0000E+04,  2.5000E+04,  0.0000E+00  (RPM)

PRESSURE AT START, END AXIAL BOUNDARIES =  1.0000E+03,  0.0000E+00  (PSI)

VISCOSITY =  3.0000E-08  (PSI-SEC),   DENSITY =  1.0000E-04  (LB-SEC/IN4)

ERROR CODE =  0,   ITERATIONS IN PRIMARY FLOW =  5

FLOW =  9.6718E+00  (IN**3/SEC)

TORQUE =  6.2612E+00  (IN-LB),   FILM POWER LOSS =  4.9672E+00  (HP)

AXIAL REYNOLDS NUMBER                          =  1.0262E+04
CIRC. REYNOLDS NUMBERS FOR ROTOR AT SEAL ENDS =  3.4907E+04,  1.7454E+04

        DYNAMIC COEFFICIENTS  ( FORCE UNIT / DISP. UNIT )

DISP.      x (IN)       y (IN)     phi (RAD)   psi (RAD)    FORCE UNIT
Kx       3.6100E+05  1.9342E+05 -1.6886E+04  1.2744E+05   LB
Ky      -1.9342E+05  3.6100E+05 -1.2744E+05 -1.6886E+04   LB
Kphi    -9.9981E+02  2.1794E+03  3.1907E+03  8.8432E+02   IN-LB
Kpsi    -2.1794E+03 -9.9981E+02 -8.8432E+02  3.1907E+03   IN-LB
Bx       6.8435E+01  1.2504E+01  8.1569E-03  5.6432E+00   LB-SEC
By      -1.2504E+01  6.8435E+01 -5.6432E+00  8.1569E-03   LB-SEC
Bphi     3.8905E-02 -1.4517E-01  4.4703E-01  6.3076E-02   IN-LB-SEC
Bpsi     1.4517E-01  3.8905E-02 -6.3076E-02  4.4703E-01   IN-LB-SEC
Ax       2.2877E-03 -7.4684E-05 -1.3827E-05  8.2668E-06   LB-SEC2
Ay       7.4684E-05  2.2877E-03 -8.2668E-06 -1.3827E-05   LB-SEC2
Aphi     8.8069E-07 -2.7002E-05  9.5112E-06 -4.5208E-07   IN-LB-SEC2
Apsi     2.7002E-05  8.8069E-07  4.5208E-07  9.5112E-06   IN-LB-SEC2
```

```
( CASE  2 )  Cylindrical seal, grooves pumping inward, high pres. at right

&INPUTS
   TITLE  =  'Cylindrical seal, grooves pumping inward, high pres. at right'
   IFACE  =  0              ISIUN  =  0
   IGROT  =  0              NOI    =  0              IFLOW  =  0
   R0     =  1.0000E+00     EL     =  5.0000E-01     C      =  1.0000E-03
   RPM    =  5.0000E+04     RPM0   =  2.5000E+04     RPMD   =  0.0000E+00
   PLEG   =  0.0000E+00     PRIG   =  1.0000E+03     FZD    =  0.0000E+00
   VISC   =  3.0000E-08     DENS   =  1.0000E-04
   EMA    = -2.5000E-01     ENA    =  7.9100E-02
   EMB    = -2.5000E-01     ENB    =  7.9100E-02
   HTAP   =  0.0000E+00     HBRL   =  0.0000E+00
   TOLH   =  1.0000E-04     TOLV   =  1.0000E-05     DUT    =  1.0000E-06
   IHOME  =  0              NITH   =  10             NITV   =  30
   NREG   =  2              NRSUB  =  50  50
   ELFR   =  5.0000E-01  5.0000E-01
   ZET    =  0.0000E+00  0.0000E+00
   ALPI   =  5.0000E-01  0.0000E+00
   BETI   =  2.5000E+01  0.0000E+00
   DELT   =  2.0000E-03  0.0000E+00
   NSG    =  16   0
   ZETG   =  0.0000E+00  0.0000E+00
/

CYLINDRICAL SEAL

LENGTH, DIAMETER, CLEARANCE =  5.0000E-01,  2.0000E+00,  1.0000E-03  (IN)

ROTOR, SWIRL AND DIST. SPEEDS =  5.0000E+04,  2.5000E+04,  0.0000E+00  (RPM)

PRESSURE AT START, END AXIAL BOUNDARIES =  0.0000E+00,  1.0000E+03  (PSI)

VISCOSITY =  3.0000E-08  (PSI-SEC),   DENSITY =  1.0000E-04  (LB-SEC/IN4)

ERROR CODE =  0,   ITERATIONS IN PRIMARY FLOW =  5

FLOW = -5.8701E+00  (IN**3/SEC)

TORQUE =  7.0124E+00  (IN-LB),   FILM POWER LOSS =  5.5631E+00  (HP)

AXIAL REYNOLDS NUMBER                          =  6.2283E+03
CIRC. REYNOLDS NUMBERS FOR ROTOR AT SEAL ENDS =  4.6032E+04,  1.7453E+04

        DYNAMIC COEFFICIENTS  ( FORCE UNIT / DISP. UNIT )

DISP.      x (IN)       y (IN)     phi (RAD)   psi (RAD)    FORCE UNIT
Kx       1.8559E+05  1.6560E+05  9.2632E+02 -1.2796E+05   LB
Ky      -1.6560E+05  1.8559E+05  1.2796E+05  9.2632E+02   LB
Kphi     4.0924E+03 -9.6714E+03 -1.7721E+03  1.0930E+03   IN-LB
Kpsi     9.6714E+03  4.0924E+03 -1.0930E+03 -1.7721E+03   IN-LB
Bx       5.9485E+01  1.0399E+01 -2.8343E-01 -2.8982E+00   LB-SEC
By      -1.0399E+01  5.9485E+01  2.8982E+00 -2.8343E-01   LB-SEC
Bphi    -4.0130E-02 -1.5876E+00  3.1133E-01  3.9026E-02   IN-LB-SEC
Bpsi     1.5876E+00 -4.0130E-02 -3.9026E-02  3.1133E-01   IN-LB-SEC
Ax       2.5027E-03 -8.4394E-05  6.3797E-06  9.3042E-05   LB-SEC2
Ay       8.4394E-05  2.5027E-03 -9.3042E-05  6.3797E-06   LB-SEC2
Aphi     5.0318E-06 -1.6707E-05  9.1049E-06  3.0227E-07   IN-LB-SEC2
Apsi     1.6707E-05  5.0318E-06 -3.0227E-07  9.1049E-06   IN-LB-SEC2
```

(CASE 3) Cylindrical step seal, high pressure at left

```
&INPUTS
   TITLE  =  'Cylindrical step seal, high pressure at left'
   IFACE  =  0              ISIUN  =  0
   IGROT  =  0              NOI    =  0              IFLOW  =  0
   R0     =  1.0000E+00     EL     =  5.0000E-01     C      =  1.0000E-03
   RPM    =  5.0000E+04     RPM0   =  2.5000E+04     RPMD   =  0.0000E+00
   PLEG   =  1.0000E+03     PRIG   =  0.0000E+00     FZD    =  0.0000E+00
   VISC   =  3.0000E-08     DENS   =  1.0000E-04
   EMA    = -2.5000E-01     ENA    =  7.9100E-02
   EMB    = -2.5000E-01     ENB    =  7.9100E-02
   HTAP   =  0.0000E+00     HBRL   =  0.0000E+00
   TOLH   =  1.0000E-04     TOLV   =  1.0000E-05     DUT    =  1.0000E-06
   IHOME  =  0              NITH   =  10             NITV   =  30
   NREG   =  2              NRSUB  =  50  50
   ELFR   =  5.0000E-01  5.0000E-01
   ZET    =  0.0000E+00  0.0000E+00
   ALPI   =  1.0000E+00  0.0000E+00
   BETI   =  0.0000E+00  0.0000E+00
   DELT   =  2.0000E-03  0.0000E+00
   NSG    =   0   0
   ZETG   =  0.0000E+00  0.0000E+00
/

CYLINDRICAL SEAL

LENGTH, DIAMETER, CLEARANCE =  5.0000E-01,  2.0000E+00,  1.0000E-03  (IN)

ROTOR, SWIRL AND DIST. SPEEDS =  5.0000E+04,  2.5000E+04,  0.0000E+00  (RPM)

PRESSURE AT START, END AXIAL BOUNDARIES =  1.0000E+03,  0.0000E+00  (PSI)

VISCOSITY =  3.0000E-08  (PSI-SEC),   DENSITY =  1.0000E-04  (LB-SEC/IN4)

ERROR CODE =  0,   ITERATIONS IN PRIMARY FLOW =  5

FLOW =  1.0041E+01  (IN**3/SEC)

TORQUE =  5.8581E+00  (IN-LB),   FILM POWER LOSS =  4.6474E+00  (HP)

AXIAL REYNOLDS NUMBER                          =  1.0654E+04
CIRC. REYNOLDS NUMBERS FOR ROTOR AT SEAL ENDS =  5.2360E+04,  1.7453E+04
```

DYNAMIC COEFFICIENTS (FORCE UNIT / DISP. UNIT)

DISP.	x (IN)	y (IN)	phi (RAD)	psi (RAD)	FORCE UNIT
Kx	1.4595E+05	1.0148E+05	-1.4038E+04	7.8450E+04	LB
Ky	-1.0148E+05	1.4595E+05	-7.8450E+04	-1.4038E+04	LB
Kphi	2.9812E+03	-2.2209E+03	5.0418E+03	9.7526E+02	IN-LB
Kpsi	2.2209E+03	2.9812E+03	-9.7526E+02	5.0418E+03	IN-LB
Bx	3.8776E+01	9.1961E+00	-1.1539E-01	5.3554E+00	LB-SEC
By	-9.1961E+00	3.8776E+01	-5.3554E+00	-1.1539E-01	LB-SEC
Bphi	1.6853E-01	-1.1378E+00	3.7298E-01	5.1546E-02	IN-LB-SEC
Bpsi	1.1378E+00	1.6853E-01	-5.1546E-02	3.7298E-01	IN-LB-SEC
Ax	1.7549E-03	-7.6310E-06	-3.8051E-06	2.2759E-05	LB-SEC2
Ay	7.6310E-06	1.7549E-03	-2.2759E-05	-3.8051E-06	LB-SEC2
Aphi	5.1596E-07	-3.2278E-05	9.7987E-06	-2.5418E-07	IN-LB-SEC2
Apsi	3.2278E-05	5.1596E-07	2.5418E-07	9.7987E-06	IN-LB-SEC2

```
( CASE  4 )  Cylindrical step seal, high pressure at right

&INPUTS
   TITLE  =  'Cylindrical step seal, high pressure at right'
   IFACE  =  0              ISIUN  =  0
   IGROT  =  0              NOI    =  0              IFLOW  =  0
   R0     =  1.0000E+00     EL     =  5.0000E-01     C      =  1.0000E-03
   RPM    =  5.0000E+04     RPM0   =  2.5000E+04     RPMD   =  0.0000E+00
   PLEG   =  0.0000E+00     PRIG   =  1.0000E+03     FZD    =  0.0000E+00
   VISC   =  3.0000E-08     DENS   =  1.0000E-04
   EMA    = -2.5000E-01     ENA    =  7.9100E-02
   EMB    = -2.5000E-01     ENB    =  7.9100E-02
   HTAP   =  0.0000E+00     HBRL   =  0.0000E+00
   TOLH   =  1.0000E-04     TOLV   =  1.0000E-05     DUT    =  1.0000E-06
   IHOME  =  0              NITH   =  10             NITV   =  30
   NREG   =  2              NRSUB  =  50  50
   ELFR   =  5.0000E-01  5.0000E-01
   ZET    =  0.0000E+00  0.0000E+00
   ALPI   =  1.0000E+00  0.0000E+00
   BETI   =  0.0000E+00  0.0000E+00
   DELT   =  2.0000E-03  0.0000E+00
   NSG    =   0   0
   ZETG   =  0.0000E+00  0.0000E+00
/

CYLINDRICAL SEAL

LENGTH, DIAMETER, CLEARANCE =  5.0000E-01,  2.0000E+00,  1.0000E-03  (IN)

ROTOR, SWIRL AND DIST. SPEEDS =  5.0000E+04,  2.5000E+04,  0.0000E+00  (RPM)

PRESSURE AT START, END AXIAL BOUNDARIES =  0.0000E+00,  1.0000E+03  (PSI)

VISCOSITY =  3.0000E-08  (PSI-SEC),   DENSITY =  1.0000E-04  (LB-SEC/IN4)

ERROR CODE =  0,   ITERATIONS IN PRIMARY FLOW =  3

FLOW = -1.0518E+01  (IN**3/SEC)

TORQUE =  5.8957E+00  (IN-LB),   FILM POWER LOSS =  4.6772E+00  (HP)

AXIAL REYNOLDS NUMBER                          =  1.1160E+04
CIRC. REYNOLDS NUMBERS FOR ROTOR AT SEAL ENDS =  5.2360E+04,  1.7453E+04

        DYNAMIC COEFFICIENTS  ( FORCE UNIT / DISP. UNIT )

DISP.       x (IN)       y (IN)     phi (RAD)    psi (RAD)     FORCE UNIT
Kx       6.6425E+04   2.0961E+04   7.3302E+03  -4.8304E+04    LB
Ky      -2.0961E+04   6.6425E+04   4.8304E+04   7.3302E+03    LB
Kphi     4.5219E+03  -1.8963E+04  -4.3335E+03   3.2326E+02    IN-LB
Kpsi     1.8963E+04   4.5219E+03  -3.2326E+02  -4.3335E+03    IN-LB
Bx       8.5715E+00   1.3879E+01  -5.6371E-01  -2.7546E+00    LB-SEC
By      -1.3879E+01   8.5715E+00   2.7546E+00  -5.6371E-01    LB-SEC
Bphi     4.7773E-01  -1.7618E+00   1.2625E-01   7.1479E-02    IN-LB-SEC
Bpsi     1.7618E+00   4.7773E-01  -7.1479E-02   1.2625E-01    IN-LB-SEC
Ax       2.5896E-03  -3.1050E-04   2.4906E-05   1.0278E-04    LB-SEC2
Ay       3.1050E-04   2.5896E-03  -1.0278E-04   2.4906E-05    LB-SEC2
Aphi    -1.9030E-05  -8.7620E-05   1.3360E-05  -1.5316E-06    IN-LB-SEC2
Apsi     8.7620E-05  -1.9030E-05   1.5316E-06   1.3360E-05    IN-LB-SEC2
```

```
( CASE  5 )  Plain cylindrical seal, high pressure at left

&INPUTS
   TITLE  =  'Plain cylindrical seal, high pressure at left'
   IFACE  =  0              ISIUN  =  0
   IGROT  =  0              NOI    =  0              IFLOW  =  0
   R0     =  1.0000E+00     EL     =  5.0000E-01     C      =  1.0000E-03
   RPM    =  5.0000E+04     RPM0   =  2.5000E+04     RPMD   =  0.0000E+00
   PLEG   =  1.0000E+03     PRIG   =  0.0000E+00     FZD    =  0.0000E+00
   VISC   =  3.0000E-08     DENS   =  1.0000E-04
   EMA    = -2.5000E-01     ENA    =  7.9100E-02
   EMB    = -2.5000E-01     ENB    =  7.9100E-02
   HTAP   =  0.0000E+00     HBRL   =  0.0000E+00
   TOLH   =  1.0000E-04     TOLV   =  1.0000E-05     DUT    =  1.0000E-06
   IHOME  =  0              NITH   =  10             NITV   =  30
   NREG   =  1              NRSUB  = 100
   ELFR   =  1.0000E+00
   ZET    =  0.0000E+00
   ALPI   =  0.0000E+00
   BETI   =  0.0000E+00
   DELT   =  2.0000E-03
   NSG    =   0
   ZETG   =  0.0000E+00
/

CYLINDRICAL SEAL

LENGTH, DIAMETER, CLEARANCE =  5.0000E-01,  2.0000E+00,  1.0000E-03  (IN)

ROTOR, SWIRL AND DIST. SPEEDS =  5.0000E+04,  2.5000E+04,  0.0000E+00  (RPM)

PRESSURE AT START, END AXIAL BOUNDARIES =  1.0000E+03,  0.0000E+00  (PSI)

VISCOSITY =  3.0000E-08  (PSI-SEC),   DENSITY =  1.0000E-04  (LB-SEC/IN4)

ERROR CODE =  0,   ITERATIONS IN PRIMARY FLOW =  4

FLOW =  6.2940E+00  (IN**3/SEC)

TORQUE =  6.4988E+00  (IN-LB),   FILM POWER LOSS =  5.1557E+00  (HP)

AXIAL REYNOLDS NUMBER                          =  6.6781E+03
CIRC. REYNOLDS NUMBERS FOR ROTOR AT SEAL ENDS =  1.7453E+04,  1.7453E+04

        DYNAMIC COEFFICIENTS  ( FORCE UNIT / DISP. UNIT )

DISP.      x (IN)       y (IN)     phi (RAD)   psi (RAD)    FORCE UNIT
Kx       5.8071E+04  2.2021E+05 -1.2728E+04  1.6392E+05   LB
Ky      -2.2021E+05  5.8071E+04 -1.6392E+05 -1.2728E+04   LB
Kphi    -3.7963E+03  6.7330E+03 -1.8147E+03  1.0783E+03   IN-LB
Kpsi    -6.7330E+03 -3.7963E+03 -1.0783E+03 -1.8147E+03   IN-LB
Bx       8.4163E+01  1.7148E+01  1.5180E-02  4.8601E+00   LB-SEC
By      -1.7148E+01  8.4163E+01 -4.8601E+00  1.5180E-02   LB-SEC
Bphi    -3.3856E-02  1.4540E+00  4.1202E-01  7.2269E-02   IN-LB-SEC
Bpsi    -1.4540E+00 -3.3856E-02 -7.2269E-02  4.1202E-01   IN-LB-SEC
Ax       3.2700E-03 -2.7182E-05 -9.7794E-07 -2.7117E-06   LB-SEC2
Ay       2.7182E-05  3.2700E-03  2.7117E-06 -9.7794E-07   LB-SEC2
Aphi     2.1509E-06  6.0562E-06  1.3787E-05 -8.3503E-08   IN-LB-SEC2
Apsi    -6.0562E-06  2.1509E-06  8.3503E-08  1.3787E-05   IN-LB-SEC2
```

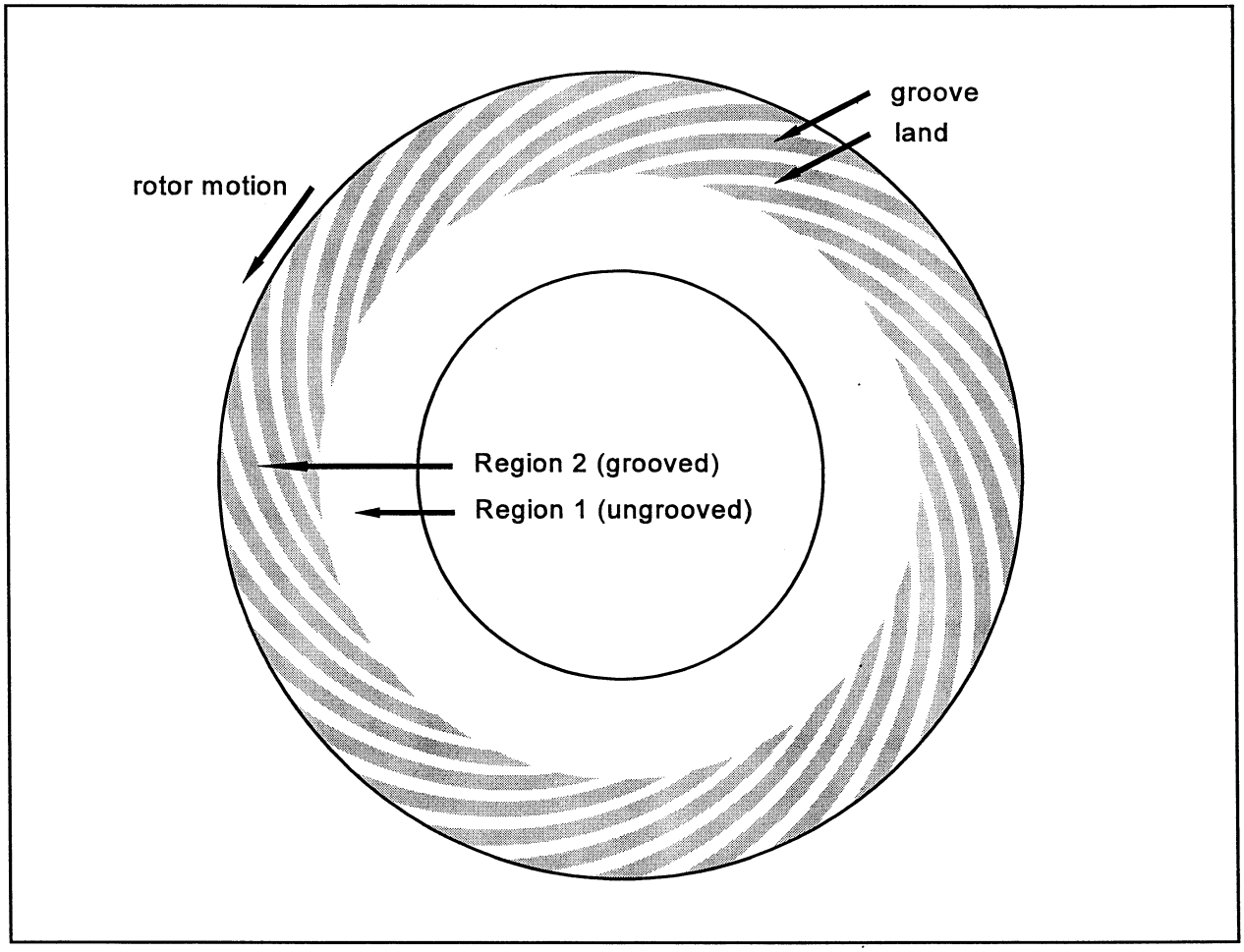


Figure 11 Stator with inward pumping grooves for cases 6 - 8

```
( CASE  6 )  Face seal, grooves pumping inward, high pressure outside

&INPUTS
   TITLE  =  'Face seal, grooves pumping inward, high pressure outside'
   IFACE  =  1              ISIUN  =  0
   IGROT  =  0              NOI    =  0              IFLOW  =  0
   R0     =  1.0000E+00     EL     =  5.0000E-01     C      =  1.0000E-03
   RPM    =  5.0000E+04     RPM0   =  2.5000E+04     RPMD   =  0.0000E+00
   PLEG   =  0.0000E+00     PRIG   =  1.0000E+03     FZD    =  0.0000E+00
   VISC   =  3.0000E-08     DENS   =  1.0000E-04
   EMA    = -2.5000E-01     ENA    =  7.9100E-02
   EMB    = -2.5000E-01     ENB    =  7.9100E-02
   HTAP   =  0.0000E+00     HBRL   =  0.0000E+00
   TOLH   =  1.0000E-04     TOLV   =  1.0000E-05     DUT    =  1.0000E-06
   IHOME  =  0              NITH   =  10             NITV   =  30
   NREG   =  2              NRSUB  =  50 200
   ELFR   =  5.0000E-01  5.0000E-01
   ZET    =  0.0000E+00  0.0000E+00
   ALPI   =  0.0000E+00  5.0000E-01
   BETI   =  0.0000E+00 -2.5000E+01
   DELT   =  0.0000E+00  2.0000E-03
   NSG    =   0  28
   ZETG   =  0.0000E+00  0.0000E+00
/

FACE SEAL

ID, OD, NOMINAL FILM THICKNESS =  1.0000E+00,  2.0000E+00,  1.0000E-03  (IN)

ROTOR, SWIRL AND DIST. SPEEDS =  5.0000E+04,  2.5000E+04,  0.0000E+00  (RPM)

INSIDE, OUTSIDE PRESSURE =  0.0000E+00,  1.0000E+03  (PSI)

VISCOSITY =  3.0000E-08  (PSI-SEC),   DENSITY =  1.0000E-04  (LB-SEC/IN4)

ERROR CODE =  0,   ITERATIONS IN PRIMARY FLOW =  5

AXIAL LOAD TO BALANCE FACE SEAL =  1.7443E+03  (LB)

FLOW = -5.5975E+00  (IN**3/SEC)

TORQUE =  2.2207E+00  (IN-LB),   FILM POWER LOSS =  1.7618E+00  (HP)

RADIAL REYNOLDS NUMBER AT ID, OD           =  1.1878E+04,  5.9391E+03
CIRC. REYNOLDS NUMBERS FOR ROTOR AT ID, OD =  5.8219E+03,  3.4907E+04

        DYNAMIC COEFFICIENTS  ( FORCE UNIT / DISP. UNIT )

DISP.      z (IN)     phi (RAD)    psi (RAD)    FORCE UNIT
Kz      5.2207E+05  0.0000E+00  0.0000E+00   LB
Kphi    0.0000E+00  9.0761E+04  9.7317E+04   IN-LB
Kpsi    0.0000E+00 -9.7317E+04  9.0761E+04   IN-LB
Bz      1.0792E+02  0.0000E+00  0.0000E+00   LB-SEC
Bphi    0.0000E+00  2.7303E+01  6.5037E+00   IN-LB-SEC
Bpsi    0.0000E+00 -6.5037E+00  2.7303E+01   IN-LB-SEC
Az      3.5278E-03  0.0000E+00  0.0000E+00   LB-SEC2
Aphi    0.0000E+00  9.0969E-04 -1.3478E-04   IN-LB-SEC2
Apsi    0.0000E+00  1.3478E-04  9.0969E-04   IN-LB-SEC2
```

```
( CASE  7 )  Same as case 6 but with 50% increase in nominal film clearance

&INPUTS
   TITLE  =  'Same as case 6 but with 50% increase in nominal film clearance'
   IFACE  =  1              ISIUN  =  0
   IGROT  =  0              NOI    =  0              IFLOW  =  0
   R0     =  1.0000E+00     EL     =  5.0000E-01     C      =  1.5000E-03
   RPM    =  5.0000E+04     RPM0   =  2.5000E+04     RPMD   =  0.0000E+00
   PLEG   =  0.0000E+00     PRIG   =  1.0000E+03     FZD    =  0.0000E+00
   VISC   =  3.0000E-08     DENS   =  1.0000E-04
   EMA    = -2.5000E-01     ENA    =  7.9100E-02
   EMB    = -2.5000E-01     ENB    =  7.9100E-02
   HTAP   =  0.0000E+00     HBRL   =  0.0000E+00
   TOLH   =  1.0000E-04     TOLV   =  1.0000E-05     DUT    =  1.0000E-06
   IHOME  =  0              NITH   =  10             NITV   =  30
   NREG   =  2              NRSUB  =  50 200
   ELFR   =  5.0000E-01  5.0000E-01
   ZET    =  0.0000E+00  0.0000E+00
   ALPI   =  0.0000E+00  5.0000E-01
   BETI   =  0.0000E+00 -2.5000E+01
   DELT   =  0.0000E+00  2.0000E-03
   NSG    =   0  28
   ZETG   =  0.0000E+00  0.0000E+00
/

FACE SEAL

ID, OD, NOMINAL FILM THICKNESS =  1.0000E+00,  2.0000E+00,  1.5000E-03  (IN)

ROTOR, SWIRL AND DIST. SPEEDS =  5.0000E+04,  2.5000E+04,  0.0000E+00  (RPM)

INSIDE, OUTSIDE PRESSURE =  0.0000E+00,  1.0000E+03  (PSI)

VISCOSITY =  3.0000E-08  (PSI-SEC),   DENSITY =  1.0000E-04  (LB-SEC/IN4)

ERROR CODE =  0,   ITERATIONS IN PRIMARY FLOW =  5

AXIAL LOAD TO BALANCE FACE SEAL =  1.5888E+03  (LB)

FLOW = -9.1255E+00  (IN**3/SEC)

TORQUE =  1.7426E+00  (IN-LB),   FILM POWER LOSS =  1.3825E+00  (HP)

RADIAL REYNOLDS NUMBER AT ID, OD           =  1.9365E+04,  9.6824E+03
CIRC. REYNOLDS NUMBERS FOR ROTOR AT ID, OD =  5.5391E+03,  4.3633E+04

        DYNAMIC COEFFICIENTS  ( FORCE UNIT / DISP. UNIT )

DISP.      z (IN)     phi (RAD)   psi (RAD)    FORCE UNIT
Kz      1.7409E+05  0.0000E+00  0.0000E+00   LB
Kphi    0.0000E+00  1.0475E+04  6.1962E+04   IN-LB
Kpsi    0.0000E+00 -6.1962E+04  1.0475E+04   IN-LB
Bz      6.2363E+01  0.0000E+00  0.0000E+00   LB-SEC
Bphi    0.0000E+00  1.5470E+01  4.4478E+00   IN-LB-SEC
Bpsi    0.0000E+00 -4.4478E+00  1.5470E+01   IN-LB-SEC
Az      2.3100E-03  0.0000E+00  0.0000E+00   LB-SEC2
Aphi    0.0000E+00  5.7624E-04 -7.2022E-05   IN-LB-SEC2
Apsi    0.0000E+00  7.2022E-05  5.7624E-04   IN-LB-SEC2
```

```
( CASE  8 )  Same as case 6 but with IHOME=1 and 1600 lb. balance load

&INPUTS
   TITLE  =  'Same as case 6 but with IHOME=1 and 1600 lb. balance load'
   IFACE  =  1              ISIUN  =  0
   IGROT  =  0              NOI    =  0              IFLOW  =  0
   R0     =  1.0000E+00     EL     =  5.0000E-01     C      =  1.0000E-03
   RPM    =  5.0000E+04     RPM0   =  2.5000E+04     RPMD   =  0.0000E+00
   PLEG   =  0.0000E+00     PRIG   =  1.0000E+03     FZD    =  1.6000E+03
   VISC   =  3.0000E-08     DENS   =  1.0000E-04
   EMA    = -2.5000E-01     ENA    =  7.9100E-02
   EMB    = -2.5000E-01     ENB    =  7.9100E-02
   HTAP   =  0.0000E+00     HBRL   =  0.0000E+00
   TOLH   =  1.0000E-04     TOLV   =  1.0000E-05     DUT    =  1.0000E-06
   IHOME  =  1              NITH   =  10             NITV   =  30
   NREG   =  2              NRSUB  =  50 200
   ELFR   =  5.0000E-01  5.0000E-01
   ZET    =  0.0000E+00  0.0000E+00
   ALPI   =  0.0000E+00  5.0000E-01
   BETI   =  0.0000E+00 -2.5000E+01
   DELT   =  0.0000E+00  2.0000E-03
   NSG    =   0  28
   ZETG   =  0.0000E+00  0.0000E+00
/

FACE SEAL

ID, OD, NOMINAL FILM THICKNESS =  1.0000E+00,  2.0000E+00,  1.4389E-03  (IN)

ROTOR, SWIRL AND DIST. SPEEDS =  5.0000E+04,  2.5000E+04,  0.0000E+00  (RPM)

INSIDE, OUTSIDE PRESSURE =  0.0000E+00,  1.0000E+03  (PSI)

VISCOSITY =  3.0000E-08  (PSI-SEC),   DENSITY =  1.0000E-04  (LB-SEC/IN4)

ERROR CODE =  0,   ITERATIONS IN PRIMARY FLOW =  5

AXIAL LOAD TO BALANCE FACE SEAL =  1.6001E+03  (LB)

FLOW = -8.6909E+00  (IN**3/SEC)

TORQUE =  1.7862E+00  (IN-LB),   FILM POWER LOSS =  1.4171E+00  (HP)

RADIAL REYNOLDS NUMBER AT ID, OD           =  1.8443E+04,  9.2213E+03
CIRC. REYNOLDS NUMBERS FOR ROTOR AT ID, OD =  5.7012E+03,  4.2566E+04

        DYNAMIC COEFFICIENTS  ( FORCE UNIT / DISP. UNIT )

DISP.      z (IN)     phi (RAD)    psi (RAD)     FORCE UNIT
Kz       1.9792E+05  0.0000E+00  0.0000E+00   LB
Kphi     0.0000E+00  1.5410E+04  6.4918E+04   IN-LB
Kpsi     0.0000E+00 -6.4918E+04  1.5410E+04   IN-LB
Bz       6.5903E+01  0.0000E+00  0.0000E+00   LB-SEC
Bphi     0.0000E+00  1.6391E+01  4.5984E+00   IN-LB-SEC
Bpsi     0.0000E+00 -4.5984E+00  1.6391E+01   IN-LB-SEC
Az       2.3918E-03  0.0000E+00  0.0000E+00   LB-SEC2
Aphi     0.0000E+00  5.9930E-04 -7.3444E-05   IN-LB-SEC2
Apsi     0.0000E+00  7.3444E-05  5.9930E-04   IN-LB-SEC2
```

(CASE 9) Childs,Nolan & Kilgore Stator 2, 25% swirl, 1000 RPM, NSG=17

```
&INPUTS
   TITLE  =  'Childs,Nolan & Kilgore Stator 2, 25% swirl, 1000 RPM, NSG=17'
   IFACE  =  0              ISIUN  =  1
   IGROT  =  0              NOI    =  0              IFLOW  =  0
   R0     =  5.0800E-02     EL     =  5.0800E-02     C      =  3.7600E-04
   RPM    =  1.0000E+03     RPM0   =  2.5000E+02     RPMD   =  0.0000E+00
   PLEG   =  2.0000E+06     PRIG   =  0.0000E+00     FZD    =  0.0000E+00
   VISC   =  1.5400E-04     DENS   =  1.5700E+03
   EMA    = -2.5000E-01     ENA    =  7.9100E-02
   EMB    = -2.5000E-01     ENB    =  7.9100E-02
   HTAP   =  0.0000E+00     HBRL   =  0.0000E+00
   TOLH   =  1.0000E-04     TOLV   =  1.0000E-05     DUT    =  1.0000E-06
   IHOME  =  0              NITH   =  10             NITV   =  30
   NREG   =  1              NRSUB  =  25
   ELFR   =  1.0000E+00
   ZET    =  1.0000E+00
   ALPI   =  4.9870E-01
   BETI   =  1.5000E+01
   DELT   =  3.8000E-04
   NSG    =  17
   ZETG   =  0.0000E+00
/

CYLINDRICAL SEAL

LENGTH, DIAMETER, CLEARANCE =  5.0800E-02,  1.0160E-01,  3.7600E-04  (m)

ROTOR, SWIRL AND DIST. SPEEDS =  1.0000E+03,  2.5000E+02,  0.0000E+00  (RPM)

PRESSURE AT START, END AXIAL BOUNDARIES =  2.0000E+06,  0.0000E+00  (Pa)

VISCOSITY =  1.5400E-04  (Pa-SEC),    DENSITY =  1.5700E+03  (Kg/m3)

ERROR CODE =  0,   ITERATIONS IN PRIMARY FLOW =  6

FLOW =  3.3398E-03  (m**3/SEC)

TORQUE =  2.9942E-02  (N-m),     FILM POWER LOSS =  3.1356E+00  (WATT)

AXIAL REYNOLDS NUMBER                          =  2.1335E+05
CIRC. REYNOLDS NUMBERS FOR ROTOR AT SEAL ENDS =  4.6004E+04,  7.6776E+04

        DYNAMIC COEFFICIENTS  ( FORCE UNIT / DISP. UNIT )

DISP.      x (m)        y (m)      phi (RAD)    psi (RAD)     FORCE UNIT
Kx       2.6765E+06 -3.4086E+05 -1.1729E+05  3.9721E+05   N
Ky       3.4086E+05  2.6765E+06 -3.9721E+05 -1.1729E+05   N
Kphi     6.1061E+02  4.1684E+04 -1.2753E+03 -4.4830E+02   N-m
Kpsi    -4.1684E+04  6.1061E+02  4.4830E+02 -1.2753E+03   N-m
Bx       1.3748E+04  3.9289E+03  5.5050E+01  1.6905E+02   N-SEC
By      -3.9289E+03  1.3748E+04 -1.6905E+02  5.5050E+01   N-SEC
Bphi    -1.3733E+01  5.9191E+01  7.6324E-01  2.8576E-01   N-m-SEC
Bpsi    -5.9191E+01 -1.3733E+01 -2.8576E-01  7.6324E-01   N-m-SEC
Ax       5.5942E+00 -1.3283E+00 -2.8954E-02 -3.1742E-02   N-SEC2
Ay       1.3283E+00  5.5942E+00  3.1742E-02 -2.8954E-02   N-SEC2
Aphi     4.7119E-03  7.4399E-03  3.3120E-04 -6.9730E-05   N-m-SEC2
Apsi    -7.4399E-03  4.7119E-03  6.9730E-05  3.3120E-04   N-m-SEC2
```

```
( CASE 10 )  Same as Case 9 except NSG=0

&INPUTS
   TITLE  =  'Same as Case 9 except NSG=0'
   IFACE  =  0              ISIUN  =  1
   IGROT  =  0              NOI    =  0              IFLOW  =  0
   R0     =  5.0800E-02     EL     =  5.0800E-02     C      =  3.7600E-04
   RPM    =  1.0000E+03     RPM0   =  2.5000E+02     RPMD   =  0.0000E+00
   PLEG   =  2.0000E+06     PRIG   =  0.0000E+00     FZD    =  0.0000E+00
   VISC   =  1.5400E-04     DENS   =  1.5700E+03
   EMA    = -2.5000E-01     ENA    =  7.9100E-02
   EMB    = -2.5000E-01     ENB    =  7.9100E-02
   HTAP   =  0.0000E+00     HBRL   =  0.0000E+00
   TOLH   =  1.0000E-04     TOLV   =  1.0000E-05     DUT    =  1.0000E-06
   IHOME  =  0              NITH   =  10             NITV   =  30
   NREG   =  1              NRSUB  =  25
   ELFR   =  1.0000E+00
   ZET    =  1.0000E+00
   ALPI   =  4.9870E-01
   BETI   =  1.5000E+01
   DELT   =  3.8000E-04
   NSG    =   0
   ZETG   =  0.0000E+00
/

CYLINDRICAL SEAL

LENGTH, DIAMETER, CLEARANCE =  5.0800E-02,  1.0160E-01,  3.7600E-04  (m)

ROTOR, SWIRL AND DIST. SPEEDS =  1.0000E+03,  2.5000E+02,  0.0000E+00  (RPM)

PRESSURE AT START, END AXIAL BOUNDARIES =  2.0000E+06,  0.0000E+00  (Pa)

VISCOSITY =  1.5400E-04  (Pa-SEC),    DENSITY =  1.5700E+03  (Kg/m3)

ERROR CODE =  0,   ITERATIONS IN PRIMARY FLOW =  5

FLOW =  5.2060E-03  (m**3/SEC)

TORQUE =  4.3118E-01  (N-m),     FILM POWER LOSS =  4.5153E+01  (WATT)

AXIAL REYNOLDS NUMBER                          =  3.3256E+05
CIRC. REYNOLDS NUMBERS FOR ROTOR AT SEAL ENDS =  4.6004E+04,  1.9099E+04

        DYNAMIC COEFFICIENTS  ( FORCE UNIT / DISP. UNIT )

DISP.      x (m)        y (m)      phi (RAD)   psi (RAD)    FORCE UNIT
Kx       5.7006E+06 -4.4186E+05 -3.8223E+04  4.7259E+05   N
Ky       4.4186E+05  5.7006E+06 -4.7259E+05 -3.8223E+04   N
Kphi     1.5121E+03  5.4046E+04 -2.9642E+03 -1.8965E+02   N-m
Kpsi    -5.4046E+04  1.5121E+03  1.8965E+02 -2.9642E+03   N-m
Bx       1.1165E+04  1.2289E+03  1.6233E+01  2.4667E+02   N-SEC
By      -1.2289E+03  1.1165E+04 -2.4667E+02  1.6233E+01   N-SEC
Bphi    -6.2979E+00  8.1492E+01  1.9357E-01  1.5111E-01   N-m-SEC
Bpsi    -8.1492E+01 -6.2979E+00 -1.5111E-01  1.9357E-01   N-m-SEC
Ax       6.3347E+00 -3.4209E-01 -7.1525E-03 -4.4958E-02   N-SEC2
Ay       3.4209E-01  6.3347E+00  4.4958E-02 -7.1525E-03   N-SEC2
Aphi     2.6813E-03  1.7398E-02  6.0569E-04 -5.3545E-05   N-m-SEC2
Apsi    -1.7398E-02  2.6813E-03  5.3545E-05  6.0569E-04   N-m-SEC2
```

5. Verification

An available MTI computer code has been used to obtain a partial check on the results of SPIRALI. This code implements a two dimensional finite difference solution to the spiral groove equations that is quite different from the perturbation methods used in SPIRALI. It does not treat inertia effects and uses the Ng and Pan (ref. 12) linearized turbulence theory which limits its validity to cases where turbulence is dominated by circumferential component of the flow. The assumptions used in the MTI code will be identical to those used in SPIRALI when the flow is laminar and inertia effects are neglected. The bulk flow model used in SPIRALI should also produce similar (although not identical) results to those obtained with the MTI code under turbulent conditions when inertia effects are neglected, there is no significant seal pressure difference, the circumferential Reynolds numbers are between 10^4 and 10^5 and the transverse Reynolds numbers are small compared with the circumferential ones.

Four test cases obtained with SPIRALI are presented for comparison with the MTI code on the following pages. Cases 1 and 3 correspond to laminar flow in a spiral grooved cylindrical and face seal respectively. It can be seen that the results of both cases agree extremely well with the results of the MTI code. The small discrepancies can easily be explained by truncation error associated with the finite difference solution used in the MTI code. Cases 2 and 4 provide comparisons similar to cases 1 and 3 under conditions of turbulent flow. It can be seen that the Reynolds numbers are in the general range of validity of the MTI code and all results agree to within 10% for both cases which is acceptable considering the differences in the turbulent flow models.

While the above cases provide a partial check on turbulent, spiral groove seals, they do not provide any validation on the treatment of inertia effects or seal behavior under high imposed pressure gradients. In order to obtain verification of the treatment of these effects, comparisons are presented between the results published by Childs in reference 4 and those obtained with SPIRALI for a plain ungrooved cylindrical seal. The output from SPIRALI is given as cases 5 - 8 on the following pages and comparisons of flow rates and rotordynamic coefficients with those published by Childs are given in Table 1. Although agreement is fairly good, discrepancies in results of up to 10%, such as that which occurs in the direct stiffness for case 6 where $u_{in}=r_0\omega/2$ and **L/D=1**, are somewhat surprising since the assumptions for that case are identical with those used by Childs. In order to obtain a further independent check on the results, a reduced form of the differential equations published by Childs for predicting the direct and cross stiffness coefficients when $u_{in}=r_0\omega/2$, were programmed and solved by the Runge-Kutta method. The program produced values of K_{xx}, K_{yy} and **Q** that agree to four places with the case 6 results produced by SPIRALI. It is thus likely that the small discrepancies between results obtained from SPIRALI and those published in reference 4 are due to truncation errors in the latter solution. Additional verification for helical groove seals is included in Appendix A.

```
( CASE  1 )  Cylindrical seal with grooves, laminar, no press. grad.

&INPUTS
   TITLE  =  'Cylindrical seal with grooves, laminar, no press. grad.'
   IFACE  =  0              ISIUN  =  0
   IGROT  =  0              NOI    =  2              IFLOW  =  1
   R0     =  1.0000E+00     EL     =  5.0000E-01     C      =  1.0000E-03
   RPM    =  5.0000E+04     RPM0   =  2.5000E+04     RPMD   =  0.0000E+00
   PLEG   =  0.0000E+00     PRIG   =  0.0000E+00     FZD    =  0.0000E+00
   VISC   =  3.0000E-08     DENS   =  0.0000E+00
   EMA    = -2.5000E-01     ENA    =  7.9100E-02
   EMB    = -2.5000E-01     ENB    =  7.9100E-02
   HTAP   =  0.0000E+00     HBRL   =  0.0000E+00
   TOLH   =  1.0000E-04     TOLV   =  1.0000E-05     DUT    =  1.0000E-06
   IHOME  =  0              NITH   =  10             NITV   =  30
   NREG   =  2              NRSUB  =  50  50
   ELFR   =  5.0000E-01  5.0000E-01
   ZET    =  0.0000E+00  0.0000E+00
   ALPI   =  5.0000E-01  0.0000E+00
   BETI   =  2.5000E+01  0.0000E+00
   DELT   =  2.0000E-03  0.0000E+00
   NSG    =   0   0
   ZETG   =  0.0000E+00  0.0000E+00
/

CYLINDRICAL SEAL, INERTIA NEGLECTED

LENGTH, DIAMETER, CLEARANCE =  5.0000E-01,  2.0000E+00,  1.0000E-03  (IN)

ROTOR, SWIRL AND DIST. SPEEDS =  5.0000E+04,  2.5000E+04,  0.0000E+00  (RPM)

PRESSURE AT START, END AXIAL BOUNDARIES =  0.0000E+00,  0.0000E+00  (PSI)

VISCOSITY =  3.0000E-08  (PSI-SEC),   DENSITY =  0.0000E+00  (LB-SEC/IN4)

ERROR CODE =  0,   ITERATIONS IN PRIMARY FLOW =  2

FLOW =  1.1506E+00  (IN**3/SEC)

TORQUE =  4.3909E-01  (IN-LB),   FILM POWER LOSS =  3.4835E-01  (HP)

AXIAL REYNOLDS NUMBER                          =  0.0000E+00
CIRC. REYNOLDS NUMBERS FOR ROTOR AT SEAL ENDS =  0.0000E+00,  0.0000E+00

        DYNAMIC COEFFICIENTS  ( FORCE UNIT / DISP. UNIT )

DISP.      x (IN)       y (IN)     phi (RAD)   psi (RAD)    FORCE UNIT
Kx       2.7021E+04  1.3511E+04 -6.3081E+02 -1.2959E+03   LB
Ky      -1.3511E+04  2.7021E+04  1.2959E+03 -6.3081E+02   LB
Kphi     2.3387E+02 -6.5242E+01  1.6699E+02  8.6419E+01   IN-LB
Kpsi     6.5242E+01  2.3387E+02 -8.6419E+01  1.6699E+02   IN-LB
Bx       5.1297E+00  7.8477E-11 -2.0242E-02  1.3973E-01   LB-SEC
By      -7.8477E-11  5.1297E+00 -1.3973E-01 -2.0242E-02   LB-SEC
Bphi    -2.0242E-02 -1.3973E-01  3.0437E-02  3.8319E-13   IN-LB-SEC
Bpsi     1.3973E-01 -2.0242E-02 -3.8319E-13  3.0437E-02   IN-LB-SEC
Ax       4.7708E-19  4.0552E-18  7.4544E-20 -1.7891E-19   LB-SEC2
Ay      -4.0552E-18  4.7708E-19  1.7891E-19  7.4544E-20   LB-SEC2
Aphi     1.1927E-19  5.4045E-20 -1.8636E-20  3.3545E-20   IN-LB-SEC2
Apsi    -5.4045E-20  1.1927E-19 -3.3545E-20 -1.8636E-20   IN-LB-SEC2
```

RESULTS OF MTI SPIRAL GROOVE CODE FOR COMPARISON WITH CASE 1

FLOW = 1.1506E+00 (IN**3/SEC)

TORQUE = 4.3909E-01 (IN-LB), FILM POWER LOSS = 3.4835E-01 (HP)

DYNAMIC COEFFICIENTS (FORCE UNIT / DISP. UNIT)

DISP.	x (IN)	y (IN)	phi (RAD)	psi (RAD)	FORCE UNIT
Kx	2.6996E+04	1.3497E+04	-6.2966E+02	-1.2947E+03	LB
Ky	-1.3497E+04	2.6996E+04	1.2947E+03	-6.2966E+02	LB
Kphi	2.3429E+02	-6.4947E+01	1.6666E+02	8.6250E+01	IN-LB
Kpsi	6.4947E+01	2.3429E+02	-8.6250E+01	1.6666E+02	IN-LB
Bx	5.1280E+00	2.4507E-07	-2.0178E-02	1.3967E-01	LB-SEC
By	9.3415E-09	5.1280E+00	-1.3967E-01	-2.0178E-02	LB-SEC
Bphi	-2.0178E-02	-1.3967E-01	3.0411E-02	3.0462E-09	IN-LB-SEC
Bpsi	1.3967E-01	-2.0178E-02	4.9311E-09	3.0411E-02	IN-LB-SEC

```
( CASE  2 )  Cylindrical seal with grooves, turbulent, no press. grad.

&INPUTS
   TITLE  =  'Cylindrical seal with grooves, turbulent, no press. grad.'
   IFACE  =  0              ISIUN  =  0
   IGROT  =  0              NOI    =  2              IFLOW  =  1
   R0     =  1.0000E+00     EL     =  5.0000E-01     C      =  1.0000E-03
   RPM    =  5.0000E+04     RPM0   =  2.5000E+04     RPMD   =  0.0000E+00
   PLEG   =  0.0000E+00     PRIG   =  0.0000E+00     FZD    =  0.0000E+00
   VISC   =  3.0000E-08     DENS   =  1.0000E-04
   EMA    = -2.5000E-01     ENA    =  7.9100E-02
   EMB    = -2.5000E-01     ENB    =  7.9100E-02
   HTAP   =  0.0000E+00     HBRL   =  0.0000E+00
   TOLH   =  1.0000E-04     TOLV   =  1.0000E-05     DUT    =  1.0000E-06
   IHOME  =  0              NITH   =  10             NITV   =  30
   NREG   =  2              NRSUB  =  50  50
   ELFR   =  5.0000E-01  5.0000E-01
   ZET    =  0.0000E+00  0.0000E+00
   ALPI   =  5.0000E-01  0.0000E+00
   BETI   =  2.5000E+01  0.0000E+00
   DELT   =  2.0000E-03  0.0000E+00
   NSG    =   0   0
   ZETG   =  0.0000E+00  0.0000E+00
/

CYLINDRICAL SEAL, INERTIA NEGLECTED

LENGTH, DIAMETER, CLEARANCE =  5.0000E-01,  2.0000E+00,  1.0000E-03  (IN)

ROTOR, SWIRL AND DIST. SPEEDS =  5.0000E+04,  2.5000E+04,  0.0000E+00  (RPM)

PRESSURE AT START, END AXIAL BOUNDARIES =  0.0000E+00,  0.0000E+00  (PSI)

VISCOSITY =  3.0000E-08  (PSI-SEC),   DENSITY =  1.0000E-04  (LB-SEC/IN4)

ERROR CODE =  0,   ITERATIONS IN PRIMARY FLOW =  3

FLOW =  1.7348E+00  (IN**3/SEC)

TORQUE =  6.1300E+00  (IN-LB),   FILM POWER LOSS =  4.8631E+00  (HP)

AXIAL REYNOLDS NUMBER                          =  1.8407E+03
CIRC. REYNOLDS NUMBERS FOR ROTOR AT SEAL ENDS =  3.8561E+04,  1.7453E+04

        DYNAMIC COEFFICIENTS  ( FORCE UNIT / DISP. UNIT )

DISP.      x (IN)       y (IN)     phi (RAD)    psi (RAD)     FORCE UNIT
Kx       2.0689E+05   1.0073E+05 -1.9681E+03 -9.2019E+03   LB
Ky      -1.0073E+05   2.0689E+05  9.2019E+03 -1.9681E+03   LB
Kphi     8.8445E+02  -2.4291E+02  1.1123E+03  4.9214E+02   IN-LB
Kpsi     2.4291E+02   8.8445E+02 -4.9214E+02  1.1123E+03   IN-LB
Bx       3.7161E+01   3.3996E-07 -6.9734E-02  5.2914E-01   LB-SEC
By      -3.3996E-07   3.7161E+01 -5.2914E-01 -6.9734E-02   LB-SEC
Bphi    -6.9734E-02  -5.2914E-01  1.7825E-01  2.1459E-12   IN-LB-SEC
Bpsi     5.2914E-01  -6.9734E-02 -2.1459E-12  1.7825E-01   IN-LB-SEC
Ax       3.8167E-18   7.6333E-18  2.3854E-18 -1.6698E-18   LB-SEC2
Ay      -7.6333E-18   3.8167E-18  1.6698E-18  2.3854E-18   LB-SEC2
Aphi     1.2076E-18  -3.5781E-19  1.4909E-19 -4.4727E-20   IN-LB-SEC2
Apsi     3.5781E-19   1.2076E-18  4.4727E-20  1.4909E-19   IN-LB-SEC2
```

RESULTS OF MTI SPIRAL GROOVE CODE FOR COMPARISON WITH CASE 2

FLOW = 1.7076E+00 (IN**3/SEC)

TORQUE = 5.8953E+00 (IN-LB), FILM POWER LOSS = 4.6770E+00 (HP)

DYNAMIC COEFFICIENTS (FORCE UNIT / DISP. UNIT)

DISP.	x (IN)	y (IN)	phi (RAD)	psi (RAD)	FORCE UNIT
Kx	2.1565E+05	1.0203E+05	-2.0751E+03	-9.8637E+03	LB
Ky	-1.0203E+05	2.1565E+05	9.8637E+03	-2.0751E+03	LB
Kphi	9.7231E+02	-2.4006E+02	1.1627E+03	5.0513E+02	IN-LB
Kpsi	2.4006E+02	9.7231E+02	-5.0513E+02	1.1627E+03	IN-LB
Bx	3.7602E+01	2.8881E-06	-6.8925E-02	5.6836E-01	LB-SEC
By	3.6843E-07	3.7602E+01	-5.6836E-01	-6.8930E-02	LB-SEC
Bphi	-6.8929E-02	-5.6836E-01	1.8265E-01	6.4583E-08	IN-LB-SEC
Bpsi	5.6836E-01	-6.8929E-02	-3.9709E-09	1.8265E-01	IN-LB-SEC

```
( CASE  3 )  Face seal with grooves, laminar, no press. grad.

&INPUTS
   TITLE  =  'Face seal with grooves, laminar, no press. grad.'
   IFACE  =  1              ISIUN  =  0
   IGROT  =  0              NOI    =  2              IFLOW  =  1
   R0     =  1.0000E+00     EL     =  5.0000E-01     C      =  1.0000E-03
   RPM    =  5.0000E+04     RPM0   =  2.5000E+04     RPMD   =  0.0000E+00
   PLEG   =  0.0000E+00     PRIG   =  0.0000E+00     FZD    =  0.0000E+00
   VISC   =  3.0000E-08     DENS   =  0.0000E+00
   EMA    = -2.5000E-01     ENA    =  7.9100E-02
   EMB    = -2.5000E-01     ENB    =  7.9100E-02
   HTAP   =  0.0000E+00     HBRL   =  0.0000E+00
   TOLH   =  1.0000E-04     TOLV   =  1.0000E-05     DUT    =  1.0000E-06
   IHOME  =  0              NITH   =  10             NITV   =  30
   NREG   =  2              NRSUB  =  50  50
   ELFR   =  5.0000E-01  5.0000E-01
   ZET    =  0.0000E+00  0.0000E+00
   ALPI   =  5.0000E-01  0.0000E+00
   BETI   =  2.5000E+01  0.0000E+00
   DELT   =  2.0000E-03  0.0000E+00
   NSG    =   0   0
   ZETG   =  0.0000E+00  0.0000E+00
/

FACE SEAL, INERTIA NEGLECTED

ID, OD, NOMINAL FILM THICKNESS =  1.0000E+00,  2.0000E+00,  1.0000E-03  (IN)

ROTOR, SWIRL AND DIST. SPEEDS =  5.0000E+04,  2.5000E+04,  0.0000E+00  (RPM)

INSIDE, OUTSIDE PRESSURE =  0.0000E+00,  0.0000E+00  (PSI)

VISCOSITY =  3.0000E-08  (PSI-SEC),   DENSITY =  0.0000E+00  (LB-SEC/IN4)

ERROR CODE =  0,   ITERATIONS IN PRIMARY FLOW =  2

AXIAL LOAD TO BALANCE FACE SEAL =  1.0391E+01  (LB)

FLOW =  5.7837E-01  (IN**3/SEC)

TORQUE =  2.1724E-01  (IN-LB),   FILM POWER LOSS =  1.7234E-01  (HP)

RADIAL REYNOLDS NUMBER AT ID, OD           =  0.0000E+00,  0.0000E+00
CIRC. REYNOLDS NUMBERS FOR ROTOR AT ID, OD =  0.0000E+00,  0.0000E+00

        DYNAMIC COEFFICIENTS  ( FORCE UNIT / DISP. UNIT )

DISP.      z (IN)     phi (RAD)   psi (RAD)    FORCE UNIT
Kz      2.3640E+04  0.0000E+00  0.0000E+00   LB
Kphi    0.0000E+00  6.2646E+03  7.0922E+03   IN-LB
Kpsi    0.0000E+00 -7.0922E+03  6.2646E+03   IN-LB
Bz      8.9011E+00  0.0000E+00  0.0000E+00   LB-SEC
Bphi    0.0000E+00  2.5921E+00  2.6323E-05   IN-LB-SEC
Bpsi    0.0000E+00 -2.6323E-05  2.5921E+00   IN-LB-SEC
Az      0.0000E+00  0.0000E+00  0.0000E+00   LB-SEC2
Aphi    0.0000E+00 -1.1927E-19  1.1927E-19   IN-LB-SEC2
Apsi    0.0000E+00 -1.1927E-19 -1.1927E-19   IN-LB-SEC2
```

RESULTS OF MTI SPIRAL GROOVE CODE FOR COMPARISON WITH CASE 3

AXIAL LOAD TO BALANCE FACE SEAL = 1.0391E+01 (LB)

FLOW = 5.7837E-01 (IN**3/SEC)

TORQUE = 2.1724E-01 (IN-LB), FILM POWER LOSS = 1.7234E-01 (HP)

DYNAMIC COEFFICIENTS (FORCE UNIT / DISP. UNIT)

DISP.	z (IN)	phi (RAD)	psi (RAD)	FORCE UNIT
Kz	2.3639E+04	7.1718E-03	7.1755E-03	LB
Kphi	5.8063E-06	6.2581E+03	7.0834E+03	IN-LB
Kpsi	1.1824E-05	-7.0834E+03	6.2581E+03	IN-LB
Bz	8.9022E+00	-2.7999E-07	-3.9768E-07	LB-SEC
Bphi	-6.6333E-08	2.5909E+00	2.9199E-06	IN-LB-SEC
Bpsi	-1.9181E-08	-2.9131E-06	2.5909E+00	IN-LB-SEC

```
( CASE  4 )  Face seal with grooves, turbulent, no press. grad.

&INPUTS
   TITLE  =  'Face seal with grooves, turbulent, no press. grad.'
   IFACE  =  1              ISIUN  =  0
   IGROT  =  0              NOI    =  2              IFLOW  =  1
   R0     =  1.0000E+00     EL     =  5.0000E-01     C      =  1.0000E-03
   RPM    =  5.0000E+04     RPM0   =  2.5000E+04     RPMD   =  0.0000E+00
   PLEG   =  0.0000E+00     PRIG   =  0.0000E+00     FZD    =  0.0000E+00
   VISC   =  3.0000E-08     DENS   =  1.0000E-04
   EMA    = -2.5000E-01     ENA    =  7.9100E-02
   EMB    = -2.5000E-01     ENB    =  7.9100E-02
   HTAP   =  0.0000E+00     HBRL   =  0.0000E+00
   TOLH   =  1.0000E-04     TOLV   =  1.0000E-05     DUT    =  1.0000E-06
   IHOME  =  0              NITH   =  10             NITV   =  30
   NREG   =  2              NRSUB  =  50  50
   ELFR   =  5.0000E-01  5.0000E-01
   ZET    =  0.0000E+00  0.0000E+00
   ALPI   =  5.0000E-01  0.0000E+00
   BETI   =  2.5000E+01  0.0000E+00
   DELT   =  2.0000E-03  0.0000E+00
   NSG    =   0   0
   ZETG   =  0.0000E+00  0.0000E+00
/

FACE SEAL, INERTIA NEGLECTED

ID, OD, NOMINAL FILM THICKNESS =  1.0000E+00,  2.0000E+00,  1.0000E-03  (IN)

ROTOR, SWIRL AND DIST. SPEEDS =  5.0000E+04,  2.5000E+04,  0.0000E+00  (RPM)

INSIDE, OUTSIDE PRESSURE =  0.0000E+00,  0.0000E+00  (PSI)

VISCOSITY =  3.0000E-08  (PSI-SEC),   DENSITY =  1.0000E-04  (LB-SEC/IN4)

ERROR CODE =  0,   ITERATIONS IN PRIMARY FLOW =  3

AXIAL LOAD TO BALANCE FACE SEAL =  5.8223E+01  (LB)

FLOW =  7.2459E-01  (IN**3/SEC)

TORQUE =  2.4948E+00  (IN-LB),   FILM POWER LOSS =  1.9792E+00  (HP)

RADIAL REYNOLDS NUMBER AT ID, OD           =  1.5376E+03,  7.6881E+02
CIRC. REYNOLDS NUMBERS FOR ROTOR AT ID, OD =  1.8985E+04,  1.7453E+04

        DYNAMIC COEFFICIENTS  ( FORCE UNIT / DISP. UNIT )

DISP.      z (IN)     phi (RAD)    psi (RAD)    FORCE UNIT
Kz      1.2740E+05  0.0000E+00  0.0000E+00   LB
Kphi    0.0000E+00  3.4989E+04  3.8692E+04   IN-LB
Kpsi    0.0000E+00 -3.8692E+04  3.4989E+04   IN-LB
Bz      4.8105E+01  0.0000E+00  0.0000E+00   LB-SEC
Bphi    0.0000E+00  1.4225E+01  6.4594E-05   IN-LB-SEC
Bpsi    0.0000E+00 -6.4594E-05  1.4225E+01   IN-LB-SEC
Az      0.0000E+00  0.0000E+00  0.0000E+00   LB-SEC2
Aphi    0.0000E+00  1.9083E-18 -9.5417E-19   IN-LB-SEC2
Apsi    0.0000E+00  9.5417E-19  1.9083E-18   IN-LB-SEC2
```

RESULTS OF MTI SPIRAL GROOVE CODE FOR COMPARISON WITH CASE 4

AXIAL LOAD TO BALANCE FACE SEAL = 5.8223E+01 (LB)

FLOW = 7.2032E-01 (IN**3/SEC)

TORQUE = 2.4013E+00 (IN-LB), FILM POWER LOSS = 1.9050E+00 (HP)

DYNAMIC COEFFICIENTS (FORCE UNIT / DISP. UNIT)

DISP.	z (IN)	phi (RAD)	psi (RAD)	FORCE UNIT
Kz	1.3685E+05	5.1323E-02	5.1174E-02	LB
Kphi	8.1427E-06	3.7351E+04	4.0251E+04	IN-LB
Kpsi	3.8131E-05	-4.0251E+04	3.7351E+04	IN-LB
Bz	4.9999E+01	-3.3078E-06	-3.4927E-06	LB-SEC
Bphi	9.6839E-07	1.4768E+01	7.7653E-06	IN-LB-SEC
Bpsi	2.8875E-07	-6.9217E-06	1.4768E+01	IN-LB-SEC

```
( CASE  5 )  Childs finite length solution, RPM0=RPM/2, L/D=.2

&INPUTS
   TITLE  =  'Childs finite length solution, RPM0=RPM/2, L/D=.2'
   IFACE  =  0              ISIUN  =  1
   IGROT  =  0              NOI    =  0              IFLOW  =  0
   R0     =  7.6200E-02     EL     =  3.0480E-02     C      =  1.9050E-04
   RPM    =  3.6000E+03     RPM0   =  1.8000E+03     RPMD   =  0.0000E+00
   PLEG   =  3.4400E+06     PRIG   =  0.0000E+00     FZD    =  0.0000E+00
   VISC   =  1.2950E-03     DENS   =  1.0000E+03
   EMA    = -2.5000E-01     ENA    =  7.9100E-02
   EMB    = -2.5000E-01     ENB    =  7.9100E-02
   HTAP   =  0.0000E+00     HBRL   =  0.0000E+00
   TOLH   =  1.0000E-04     TOLV   =  1.0000E-05     DUT    =  1.0000E-06
   IHOME  =  0              NITH   =  10             NITV   =  30
   NREG   =  1              NRSUB  = 200
   ELFR   =  1.0000E+00
   ZET    =  1.0000E-01
   ALPI   =  0.0000E+00
   BETI   =  0.0000E+00
   DELT   =  0.0000E+00
   NSG    =   0
   ZETG   =  0.0000E+00
/

CYLINDRICAL SEAL

LENGTH, DIAMETER, CLEARANCE =  3.0480E-02,  1.5240E-01,  1.9050E-04  (m)

ROTOR, SWIRL AND DIST. SPEEDS =  3.6000E+03,  1.8000E+03,  0.0000E+00  (RPM)

PRESSURE AT START, END AXIAL BOUNDARIES =  3.4400E+06,  0.0000E+00  (Pa)

VISCOSITY =  1.2950E-03  (Pa-SEC),    DENSITY =  1.0000E+03  (Kg/m3)

ERROR CODE =  0,   ITERATIONS IN PRIMARY FLOW =  4

FLOW =  4.0061E-03  (m**3/SEC)

TORQUE =  2.2528E+00  (N-m),     FILM POWER LOSS =  8.4929E+02  (WATT)

AXIAL REYNOLDS NUMBER                          =  1.2922E+04
CIRC. REYNOLDS NUMBERS FOR ROTOR AT SEAL ENDS =  4.2258E+03,  4.2258E+03

        DYNAMIC COEFFICIENTS  ( FORCE UNIT / DISP. UNIT )

DISP.      x (m)        y (m)      phi (RAD)   psi (RAD)    FORCE UNIT
Kx       1.8896E+07  4.1269E+06 -3.3389E+04  1.4185E+06   N
Ky      -4.1269E+06  1.8896E+07 -1.4185E+06 -3.3389E+04   N
Kphi    -1.2847E+04  9.8025E+04 -3.8943E+03  1.0298E+02   N-m
Kpsi    -9.8025E+04 -1.2847E+04 -1.0298E+02 -3.8943E+03   N-m
Bx       2.1895E+04  1.1396E+03 -7.0298E-01  1.7716E+02   N-SEC
By      -1.1396E+03  2.1895E+04 -1.7716E+02 -7.0298E-01   N-SEC
Bphi    -1.9373E-01  6.8162E+01  5.4617E-01  1.3431E-02   N-m-SEC
Bpsi    -6.8162E+01 -1.9373E-01 -1.3431E-02  5.4617E-01   N-m-SEC
Ax       3.0199E+00 -1.1981E-02  2.1688E-04  1.8092E-03   N-SEC2
Ay       1.1981E-02  3.0199E+00 -1.8092E-03  2.1688E-04   N-SEC2
Aphi     6.0437E-05  4.9833E-04  3.5919E-05  1.1575E-06   N-m-SEC2
Apsi    -4.9833E-04  6.0437E-05 -1.1575E-06  3.5919E-05   N-m-SEC2
```

```
( CASE  6 )  Childs finite length solution, RPM0=RPM/2, L/D=1

&INPUTS
   TITLE  =  'Childs finite length solution, RPM0=RPM/2, L/D=1'
   IFACE  =  0              ISIUN  =  1
   IGROT  =  0              NOI    =  0              IFLOW  =  0
   R0     =  7.6200E-02     EL     =  1.5240E-01     C      =  1.9050E-04
   RPM    =  3.6000E+03     RPM0   =  1.8000E+03     RPMD   =  0.0000E+00
   PLEG   =  3.4400E+06     PRIG   =  0.0000E+00     FZD    =  0.0000E+00
   VISC   =  1.2950E-03     DENS   =  1.0000E+03
   EMA    = -2.5000E-01     ENA    =  7.9100E-02
   EMB    = -2.5000E-01     ENB    =  7.9100E-02
   HTAP   =  0.0000E+00     HBRL   =  0.0000E+00
   TOLH   =  1.0000E-04     TOLV   =  1.0000E-05     DUT    =  1.0000E-06
   IHOME  =  0              NITH   =  10             NITV   =  30
   NREG   =  1              NRSUB  = 200
   ELFR   =  1.0000E+00
   ZET    =  1.0000E-01
   ALPI   =  0.0000E+00
   BETI   =  0.0000E+00
   DELT   =  0.0000E+00
   NSG    =   0
   ZETG   =  0.0000E+00
/

CYLINDRICAL SEAL

LENGTH, DIAMETER, CLEARANCE =  1.5240E-01,  1.5240E-01,  1.9050E-04  (m)

ROTOR, SWIRL AND DIST. SPEEDS =  3.6000E+03,  1.8000E+03,  0.0000E+00  (RPM)

PRESSURE AT START, END AXIAL BOUNDARIES =  3.4400E+06,  0.0000E+00  (Pa)

VISCOSITY =  1.2950E-03  (Pa-SEC),    DENSITY =  1.0000E+03  (Kg/m3)

ERROR CODE =  0,   ITERATIONS IN PRIMARY FLOW =  4

FLOW =  1.7711E-03  (m**3/SEC)

TORQUE =  6.9241E+00  (N-m),     FILM POWER LOSS =  2.6103E+03  (WATT)

AXIAL REYNOLDS NUMBER                          =  5.7131E+03
CIRC. REYNOLDS NUMBERS FOR ROTOR AT SEAL ENDS =  4.2258E+03,  4.2258E+03

        DYNAMIC COEFFICIENTS  ( FORCE UNIT / DISP. UNIT )

DISP.      x (m)        y (m)      phi (RAD)    psi (RAD)     FORCE UNIT
Kx       1.0794E+07   9.1778E+07 -1.5134E+06   1.5966E+07    N
Ky      -9.1778E+07   1.0794E+07 -1.5966E+07  -1.5134E+06    N
Kphi    -4.6942E+05   6.5852E+05 -4.7345E+04   5.3912E+04    N-m
Kpsi    -6.5852E+05  -4.6942E+05 -5.3912E+04  -4.7345E+04    N-m
Bx       4.8718E+05   1.0293E+05  1.1505E+02   8.0173E+03    N-SEC
By      -1.0293E+05   4.8718E+05 -8.0173E+03   1.1505E+02    N-SEC
Bphi    -6.5590E+01   2.4967E+03  2.8624E+02   5.1787E+01    N-m-SEC
Bpsi    -2.4967E+03  -6.5590E+01 -5.1787E+01   2.8624E+02    N-m-SEC
Ax       2.7261E+02  -2.1579E+00 -8.7333E-02  -2.8743E-01    N-SEC2
Ay       2.1579E+00   2.7261E+02  2.8743E-01  -8.7333E-02    N-SEC2
Aphi     4.7908E-02   1.6434E-01  1.3703E-01  -1.7189E-03    N-m-SEC2
Apsi    -1.6434E-01   4.7908E-02  1.7189E-03   1.3703E-01    N-m-SEC2
```

```
( CASE  7 )  Childs finite length solution, RPM0=0, L/D=.2

&INPUTS
   TITLE  =  'Childs finite length solution, RPM0=0, L/D=.2'
   IFACE  =  0              ISIUN  =  1
   IGROT  =  0              NOI    =  0              IFLOW  =  0
   R0     =  7.6200E-02     EL     =  3.0480E-02     C      =  1.9050E-04
   RPM    =  3.6000E+03     RPM0   =  0.0000E+00     RPMD   =  0.0000E+00
   PLEG   =  3.4400E+06     PRIG   =  0.0000E+00     FZD    =  0.0000E+00
   VISC   =  1.2950E-03     DENS   =  1.0000E+03
   EMA    = -2.5000E-01     ENA    =  7.9100E-02
   EMB    = -2.5000E-01     ENB    =  7.9100E-02
   HTAP   =  0.0000E+00     HBRL   =  0.0000E+00
   TOLH   =  1.0000E-04     TOLV   =  1.0000E-05     DUT    =  1.0000E-06
   IHOME  =  0              NITH   =  10             NITV   =  30
   NREG   =  1              NRSUB  = 200
   ELFR   =  1.0000E+00
   ZET    =  1.0000E-01
   ALPI   =  0.0000E+00
   BETI   =  0.0000E+00
   DELT   =  0.0000E+00
   NSG    =   0
   ZETG   =  0.0000E+00
/

CYLINDRICAL SEAL

LENGTH, DIAMETER, CLEARANCE =  3.0480E-02,  1.5240E-01,  1.9050E-04  (m)

ROTOR, SWIRL AND DIST. SPEEDS =  3.6000E+03,  0.0000E+00,  0.0000E+00  (RPM)

PRESSURE AT START, END AXIAL BOUNDARIES =  3.4400E+06,  0.0000E+00  (Pa)

VISCOSITY =  1.2950E-03  (Pa-SEC),    DENSITY =  1.0000E+03  (Kg/m3)

ERROR CODE =  0,   ITERATIONS IN PRIMARY FLOW =  4

FLOW =  3.9890E-03  (m**3/SEC)

TORQUE =  3.6677E+00  (N-m),     FILM POWER LOSS =  1.3827E+03  (WATT)

AXIAL REYNOLDS NUMBER                          =  1.2867E+04
CIRC. REYNOLDS NUMBERS FOR ROTOR AT SEAL ENDS =  8.4516E+03,  5.3357E+03

        DYNAMIC COEFFICIENTS  ( FORCE UNIT / DISP. UNIT )

DISP.      x (m)        y (m)      phi (RAD)    psi (RAD)     FORCE UNIT
Kx       1.8583E+07 -3.0274E+05 -3.0756E+04  1.4106E+06   N
Ky       3.0274E+05  1.8583E+07 -1.4106E+06 -3.0756E+04   N
Kphi     2.1014E+03  9.6616E+04 -3.8676E+03 -1.6999E+01   N-m
Kpsi    -9.6616E+04  2.1014E+03  1.6999E+01 -3.8676E+03   N-m
Bx       2.1892E+04  8.5184E+02  1.6580E+00  1.7615E+02   N-SEC
By      -8.5184E+02  2.1892E+04 -1.7615E+02  1.6580E+00   N-SEC
Bphi    -1.0540E+00  6.8066E+01  5.4479E-01  1.9870E-02   N-m-SEC
Bpsi    -6.8066E+01 -1.0540E+00 -1.9870E-02  5.4479E-01   N-m-SEC
Ax       3.0025E+00 -8.3743E-02 -5.4944E-04  1.8925E-03   N-SEC2
Ay       8.3743E-02  3.0025E+00 -1.8925E-03 -5.4944E-04   N-SEC2
Aphi     3.7677E-04  4.5070E-04  3.5698E-05 -2.5857E-06   N-m-SEC2
Apsi    -4.5070E-04  3.7677E-04  2.5857E-06  3.5698E-05   N-m-SEC2
```

```
( CASE  8 )  Childs finite length solution, RPM0=0, L/D=1

&INPUTS
   TITLE  =  'Childs finite length solution, RPM0=0, L/D=1'
   IFACE  =  0              ISIUN  =  1
   IGROT  =  0              NOI    =  0              IFLOW  =  0
   R0     =  7.6200E-02     EL     =  1.5240E-01     C      =  1.9050E-04
   RPM    =  3.6000E+03     RPM0   =  0.0000E+00     RPMD   =  0.0000E+00
   PLEG   =  3.4400E+06     PRIG   =  0.0000E+00     FZD    =  0.0000E+00
   VISC   =  1.2950E-03     DENS   =  1.0000E+03
   EMA    = -2.5000E-01     ENA    =  7.9100E-02
   EMB    = -2.5000E-01     ENB    =  7.9100E-02
   HTAP   =  0.0000E+00     HBRL   =  0.0000E+00
   TOLH   =  1.0000E-04     TOLV   =  1.0000E-05     DUT    =  1.0000E-06
   IHOME  =  0              NITH   =  10             NITV   =  30
   NREG   =  1              NRSUB  = 200
   ELFR   =  1.0000E+00
   ZET    =  1.0000E-01
   ALPI   =  0.0000E+00
   BETI   =  0.0000E+00
   DELT   =  0.0000E+00
   NSG    =   0
   ZETG   =  0.0000E+00
/

CYLINDRICAL SEAL

LENGTH, DIAMETER, CLEARANCE =  1.5240E-01,  1.5240E-01,  1.9050E-04  (m)

ROTOR, SWIRL AND DIST. SPEEDS =  3.6000E+03,  0.0000E+00,  0.0000E+00  (RPM)

PRESSURE AT START, END AXIAL BOUNDARIES =  3.4400E+06,  0.0000E+00  (Pa)

VISCOSITY =  1.2950E-03  (Pa-SEC),    DENSITY =  1.0000E+03  (Kg/m3)

ERROR CODE =  0,   ITERATIONS IN PRIMARY FLOW =  4

FLOW =  1.7673E-03  (m**3/SEC)

TORQUE =  7.8249E+00  (N-m),     FILM POWER LOSS =  2.9499E+03  (WATT)

AXIAL REYNOLDS NUMBER                          =  5.7007E+03
CIRC. REYNOLDS NUMBERS FOR ROTOR AT SEAL ENDS =  8.4516E+03,  4.2259E+03

        DYNAMIC COEFFICIENTS  ( FORCE UNIT / DISP. UNIT )

DISP.      x (m)        y (m)      phi (RAD)   psi (RAD)    FORCE UNIT
Kx       1.3250E+07  7.5182E+07 -1.8882E+06  1.5946E+07   N
Ky      -7.5182E+07  1.3250E+07 -1.5946E+07 -1.8882E+06   N
Kphi    -3.3283E+04  7.0821E+05 -4.8210E+04  4.1331E+04   N-m
Kpsi    -7.0821E+05 -3.3283E+04 -4.1331E+04 -4.8210E+04   N-m
Bx       4.8952E+05  8.9262E+04 -1.4507E+02  7.9030E+03   N-SEC
By      -8.9262E+04  4.8952E+05 -7.9030E+03 -1.4507E+02   N-SEC
Bphi     2.5693E+02  2.5639E+03  2.8825E+02  4.4699E+01   N-m-SEC
Bpsi    -2.5639E+03  2.5693E+02 -4.4699E+01  2.8825E+02   N-m-SEC
Ax       2.7214E+02 -3.2538E+00 -1.5739E-01 -2.5660E-01   N-SEC2
Ay       3.2538E+00  2.7214E+02  2.5660E-01 -1.5739E-01   N-SEC2
Aphi     6.4178E-02  1.5751E-01  1.3636E-01 -3.2263E-03   N-m-SEC2
Apsi    -1.5751E-01  6.4178E-02  3.2263E-03  1.3636E-01   N-m-SEC2
```

Table 1. Comparison of test cases 5 - 8 with data published by D. W. Childs (Ref. 4)

	$u_{in}=r_0\omega/2$, L/D=.2		$u_{in}=r_0\omega/2$, L/D=1		$u_{in}=0$, L/D=.2		$u_{in}=0$, L/D=1	
	SPIRALI	Childs	SPIRALI	Childs	SPIRALI	Childs	SPIRALI	Childs
Q (cm^3/s)	4006.	4019.	1771.	1779.	3989.	4019.	1767.	1779.
K_{xx} (MN/m)	18.90	18.65	10.79	9.756	18.58	18.52	13.25	12.48
K_{xy} (MN/m)	4.127	4.213	91.78	94.05	-.3027	-.3000	75.18	77.61
B_{xx} (KN-s/m)	21.89	22.35	487.2	500.6	21.89	22.47	489.5	502.2
B_{xy} (KN-s/m)	1.140	1.206	102.9	107.5	.8518	.8932	89.26	93.39
A_{xx} (kg)	3.020	3.200	272.6	285.3	3.003	3.189	272.1	285.3

6. Operating Environment

The computer code SPIRALI has been written to run under a variety of operating environments with very little modification. The extensions to ANSI Standard FORTRAN 77 that have been used are discussed at the start of Section 3. Executable versions of SPIRALI have been compiled with Version 5.1 of the Microsoft FORTRAN compiler and tested for use on IBM PC compatible computers with 80x87 floating point coprocessors. The source program listed in Appendix A has been compiled with the command:

```
FL /AH /Gt1024 /c SPIRALI.FOR
```

and linked with the appropriate large model, floating point libraries provided by Microsoft to run under either DOS or OS2 operating systems.

The memory required to run the program is controlled by the values of the parameters NDZ and NDREG in the one line parameter statement that appears in the main program and many of the supporting sub-programs. It currently has the form

```
PARAMETER (NDZ=201,NDREG=21)
```

permitting values of NRSUB of up to 200 in each of 21 regions and using approximately 500k of available memory.

The DOS version of the program should run on any IBM PC or compatible with a math coprocessor, sufficient memory and DOS 3.0 or higher. Mass storage requirements are minimal (a 360k diskette drive should be sufficient). The OS2 version will require sufficient additional resources to run OS2 (version 1.2 or higher).

7. Error Messages

1 Initial velocity computation diverged.

Occurs when the Newton iterative procedure for finding an initial scale factor for the velocity diverges. Check to see that reasonable values are used for C, DUT and NITV.

2 Primary flow computation diverged.

Occurs when the Newton iterative procedure for finding the transverse velocity at the inlet diverges in the primary flow solution. This error is likely to occur when transverse inertia effects are small but not neglected and the grid is too course. Try using a finer grid, particularly near the inlet. If that fails set NOI=1. Check to see that reasonable values are used for DUT and NITV.

3 Matrix inversion error encountered in second order solution.

This error occurs when the derivative matrix used in the semi-implicit solution algorithm becomes singular. If inputs are reasonable this error can be corrected by using a finer grid or setting NOI=1.

4 Spiral groove local flow computation diverged.

Occurs when the Newton-Raphson procedure for determining the global turbulent shear functions in grooved regions diverges. Check to see that the input spiral groove parameters are correct. If so, using a finer grid should eliminate this problem.

5 Face seal axial load iteration diverged.

This error can readily occur when IHOME=1 and a bad initial guess is used for the starting value of C. Try running with IHOME=0 to find a good starting value of C. Also make sure that the grid is fine enough to avoid excessive truncation error and that you have used a sufficiently large value for NITH.

6 Negative stiffness or film thickness in axial load iteration.

Causes and remedies same as error 5 above except changing NITH won't help.

7 Wrong inlet boundary was used with transverse inertia included.

Change value of IFLOW or set NOI=1.

8 Illegal length, clearance, viscosity, pressure or speed encountered.

Check inputs and correct error.

9 Maximum number of allowable grid points exceeded.

Reduce values of NRSUB.

10 Maximum number of allowable regions exceeded.

Reduce NREG.

11 Sum of length fractions are not equal to 1.

Adjust values of ELFR so that they add up to 1.

8. References

1. Hirs, G.G., *"A Bulk Flow Theory for Turbulence in Lubricant Films"*, ASME J. Lub. Tech., V 95, 2, (1973), pp. 137-146

2. Schlichting, H., *"Boundary-Layer Theory"*, Seventh Ed., McGraw-Hill, New York, (1987)

3. Childs, D.W., *"Dynamic Analysis of Turbulent Annular Seals Based on Hirs Lubrication Equation"*, ASME J. Lub. Tech., V 105, 3, (1983), pp. 429-436

4. Childs, D.W., *"Finite Length Solutions for Rotordynamic Coefficients of Turbulent Annular Seals"*, ASME J. Lub. Tech., V 105, 3, (1983), pp. 437-445

5. Childs, D.W. and Kim, C.H., *"Analysis and Testing for Rotordynamic Coefficients of Turbulent Annular Seals With Different, Directionally Homogeneous Surface Roughness Treatment for Rotor and Stator Elements"*, ASME J. Tribology, V 107, 3, (1985), pp. 296-306

6. San Andrés, L.A., *"Turbulent Hybrid Bearings With Fluid Inertia Effects"*, ASME J. Tribology, V 112, 4, (1990), pp. 699-707

7. Shames, I.H., *"Mechanics of Fluids"*, McGraw-Hill, New York, (1963)

8. Shapiro, W. et. al., *"Numerical, Analytical, Experimental Study of Fluid Dynamic Forces in Seals - Interim Report No. 1"*, MTI-92TR6, Mechanical Technology Incorporated, Latham, NY, (1991)

9. Vohr, J.H. and Pan, C.H.T., *"Design Data: Gas Lubricated Spin-Axis Bearings for Gyroscopes"*, MTI-68TR29, Mechanical Technology Incorporated, Latham, NY, (1968)

10. Tipton, D.L., Scott, T.E. and Vogel, R.E., *"Labyrinth Seals Analysis: Volume III -- Analytical and Expreimental Development of a Design Model for Labyrinth Seals"*, AFWAL-TR-85-2103, (1986)

11. Iwatsubo,T., Yang, B. and Ibaraki, R., *"Theoretical Approach to Obtaining Dynamic Characteristics of Noncontacting Spiral-Grooved Seals"*, NASA Conf. Pub. 2443, Rotordynamic Instability Problems in High-Performance Turbomachinery, (1986), pp 155-188

12. Press, W.H., Flannery, B.P., Teukolsky, S.A. and Vetterling, W.T., *"Numerical Recipes"*, Cambridge University Press, (1986)

13. Ng, C.W. and Pan, C.H.T., *"A Linearized Turbulent Lubrication Theory"*, ASME J. Bas. Eng., V 87, 3, (1965), pp. 675-688

14. Childs, D.W., Nolan, S.A. and Kilgore, J.J., *"Test Results for Turbulent Annular Seals, Using Smooth Rotors and Helically Grooved Stators"*, ASME J. Tribology, V 112, 2, (1990), pp. 254-258

APPENDIX A

Application to Parallel and Helical Grooved Seals

Parallel groove geometrics can be analyzed by using the separated region option of SPIRALI. Analysis was conducted of the parallel groove and stator 1 of Reference 1 by treating each groove and ridge as a separate region. The clearance and groove geometry are shown on Figure 1.

A total of 19 regions were used consisting of nine grooves, eight lands between grooves, an inlet land and an exit land. (The parameter statements in SPIRALI governing the maximum number of regions were enlarged appropriately). The inlet and exit land lengths were enlarged slightly to make the sum of the lengths of the individual regions equal to the total seal length (50.8 mm). The seal radius is 50.8 mm. The viscosity and density are 1.54 x 104 Pa-s and 1570 kg/m^3, respectively. The program default values for flow parameters of m = -0.25, n = 0.0791 (Hirs coefficients for smooth surfaces as given by Blasius theory), and loss coefficient of $\zeta = 0$ were used. Although it was stated in Reference 1 that no intentional swirl was provided, a swirl speed of 25% of the rotor speed was used in all computations to characterize the swirl that might naturally be present.

Comparison of Flow Rates and Force Coefficients

Experimental flow rates are presented in terms of a discharge coefficient, C_D, defined by Equation (3) of Reference 1. The value of $C_D^{-1/2}$ for stator 1 is shown in Figure 6 of Reference 1 to have a constant value of approximately 0.5 for all measured pressures. A comparison between that value and those predicted by SPIRALI is shown in Figure 2. The agreement is good and the results are predicted to be relatively insensitive to the rotating speed over the range of conditions covered, as indicated in Reference 1.

The dynamic coefficients presented in Table 1 of Reference 1 are computed from measured force coefficients based on the assumption that the coefficients are independent of speed. For purposes of comparison, the measured force coefficients, f_θand f_r, were retrieved with the use of Equation 6 in Reference 1. The seal pressure drops, ΔP, were calculated from the axial Reynolds number, R_a, using Equation (3) of Reference 1 with $C_D^{-1/2} = 0.5$. Values of f_θ versus ΔP obtained in this manner and those predicted by SPIRALI appear to be in good agreement, as shown in Figure 3. The predicted variation in f_r with rotating speed (Figure 4) is somewhat weaker than that obtained by experiment. Discrepancies in f_r can, in part, be due to sensitivity to the input values to SPIRALI provided for the friction factor and loss coefficients. Also, the effective mass, M_{ef}, in Table 1 of Reference 1 shows a significant jump at a Reynolds number of 200,000 that may be suspect.

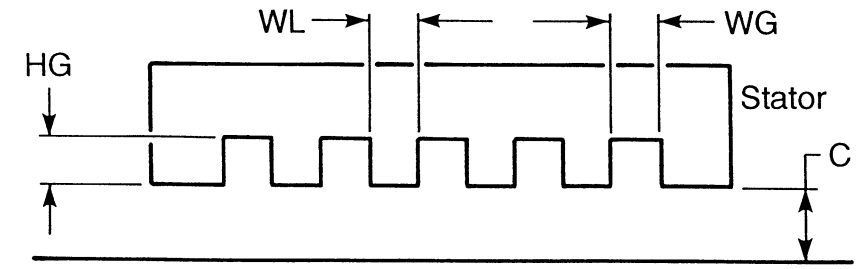
Effective stiffness values are compared in Figure 5. The experimental stiffnesses are based on extrapolations to zero speed. Stiffness is assumed to be caused principally by the pressure gradient and inlet Bernoulli effect which causes a circumferential pressure gradient and positive stiffness if the rotor goes eccentric. As Figure 5 indicates, the predicted values approach the experimental values as the speed is reduced. The predicted decrease in K with increasing rotating speed is to be expected due to the Bernoulli effect associated with fluid rotation. A corresponding comparison of C_{ef} with C - k/ω is given in Figure 6. In both cases, the agreement improves as the rotational speed is decreased and the physical interpretation of the data becomes valid.

Effect of Local Pressure Discontinuities on Predicted Flow

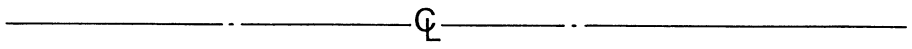
As described above, the effects of pressure jumps at the grooves are accounted for by SPIRALI in the prediction of flow and force coefficients. An estimate of these terms can be obtained by comparing the flow rate for circular grooves with that which would be predicted to occur if the effects of pressure jumps at the groove interfaces were neglected. This comparison is made at 1000 rpm in Figure 7. The large discrepancies between the two curves indicate a significant effect of local inertia that must be accounted for.

Check cases were also run against the helical groove results of Reference 1. Figure 8 shows comparisons of the flow coefficient for varying groove angles at a loss coefficient equal to 1, and the theory predicts results accurately. Cross-coupled force comparisons are shown on Figure 9. Cross-coupled effects are important because they are a measure of the stability of the seal and in some cases cross-coupled forces cause subsynchronous whirling of the rotor. The comparative results are very good. It is noted that cross-coupled forces were compared rather than the stiffnesses indicated in Reference 1. The experimental procedure measures forces and computes stiffness and damping based on the assumption that the cross-coupled coefficients vary directly with speed. The assumption of zero cross coupling at zero speed is suspect for helical grooves because the grooves apply a pressure-driven tangential flow at zero speed opposite the direction of rotation. As shown on Figure 10, the comparisons of direct stiffness, K_{ef}, were not as good as the parameters presented above. This may be due to the experimental assumptions or code assumptions.

The net results of these studies is that SPIRALI is an effective tool for analyzing many parallel and helical groove seals. The principal limitation is the bulk flow model that does not treat flow variations across gaps. If large gaps are used, then more sophisticated CFD analysis is required.



Rotor



N.G	WL	WG	HG	C
9 Grooves	2.38 mm	2.38 mm	0.38 mm	0.356 mm

94144

Figure 1 Parallel-groove pressure breakdown seal

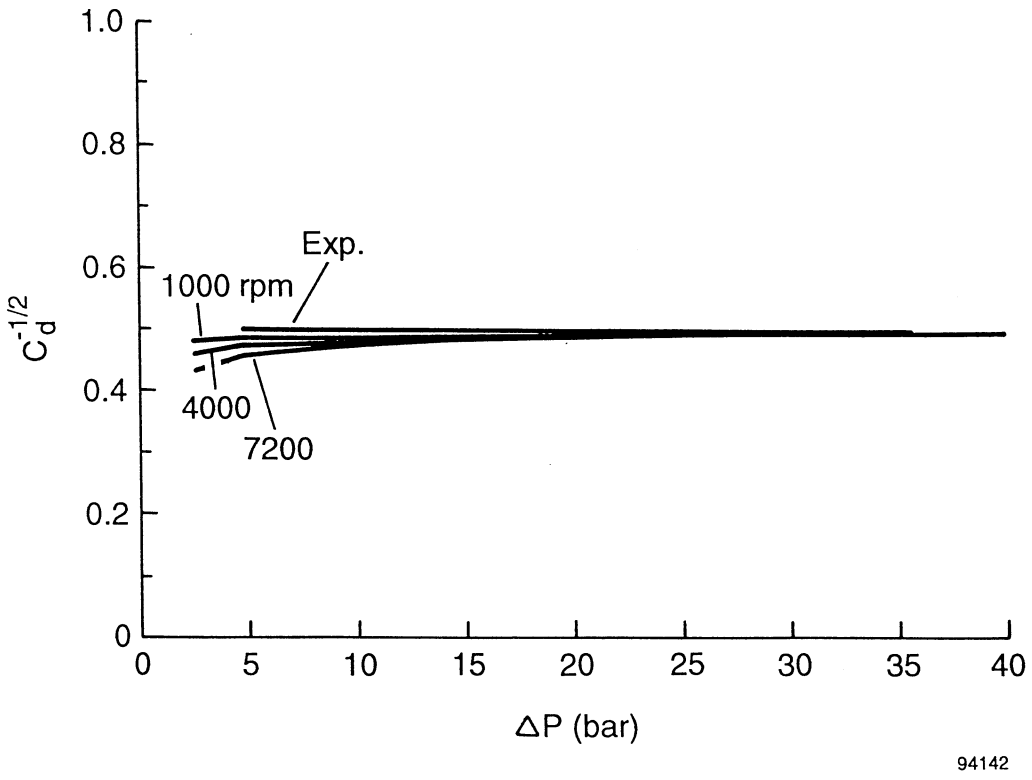


Figure 2 Parallel-groove seal flow coefficient

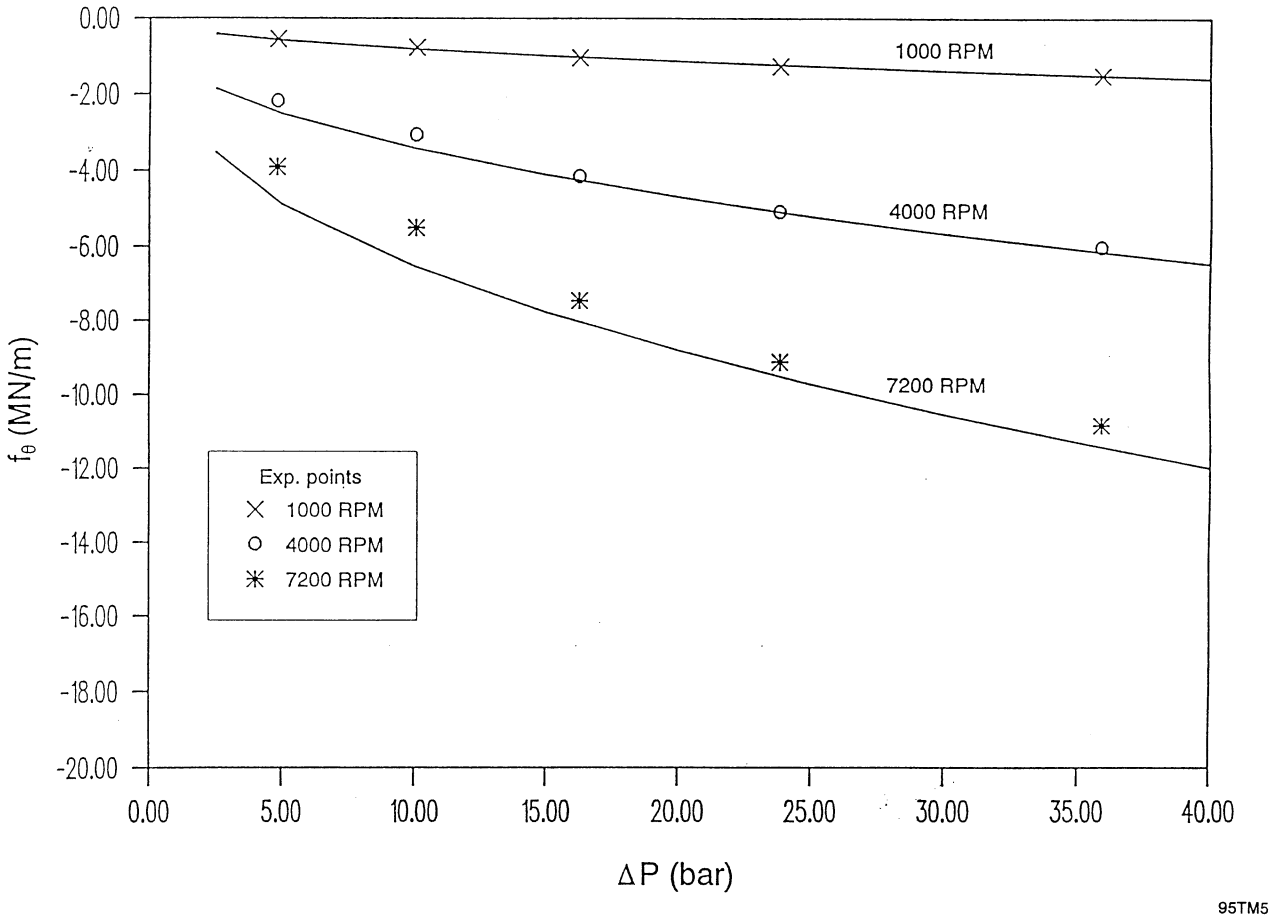


Figure 3 Tangential force coefficients

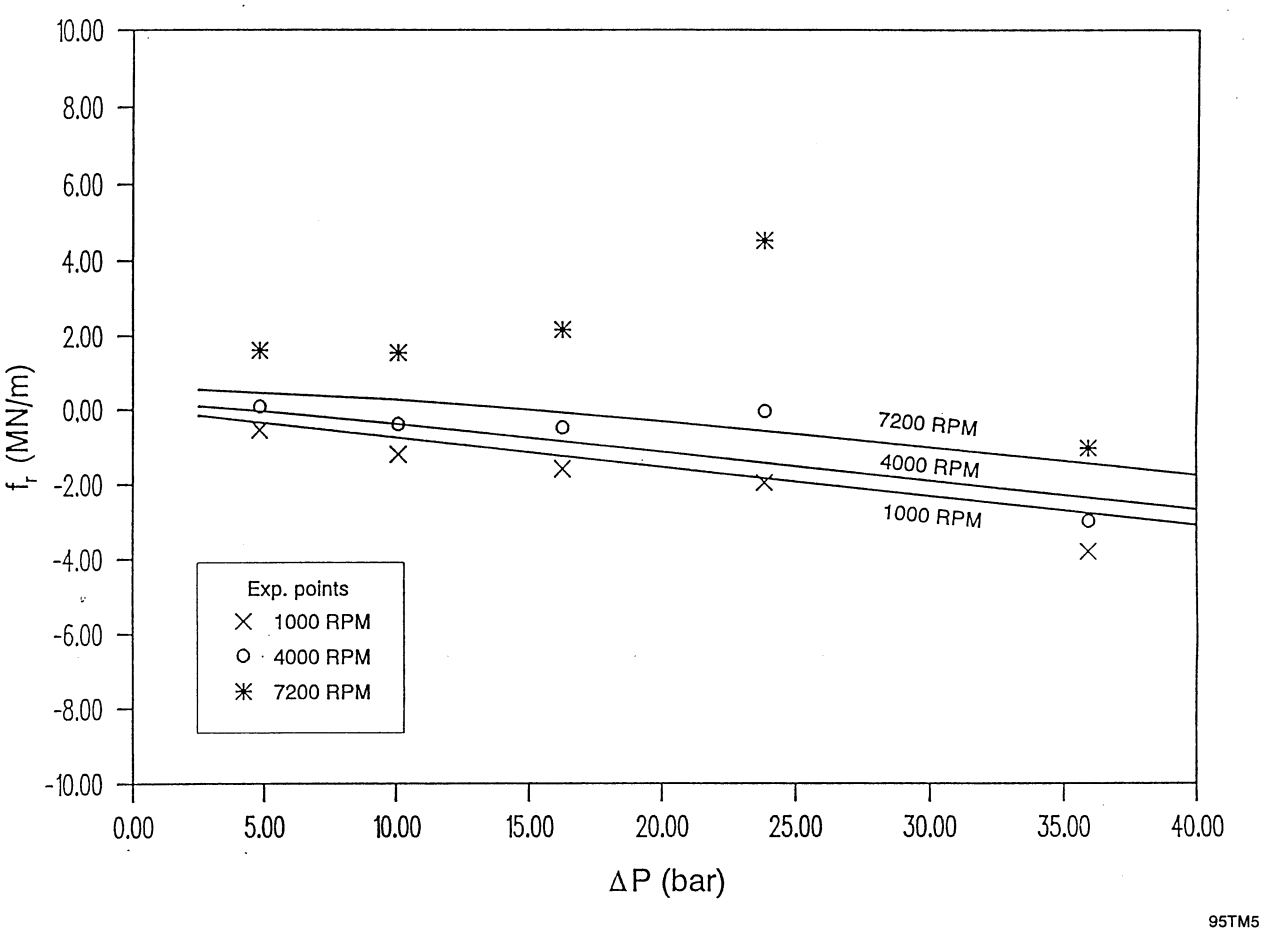
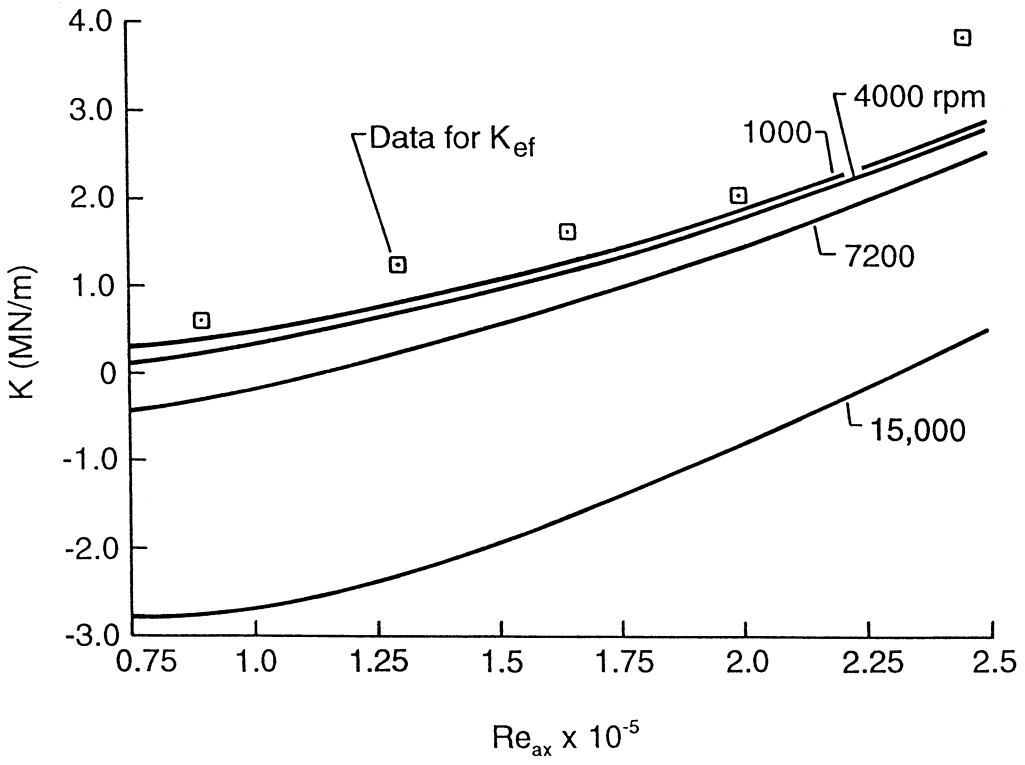


Figure 4 Normal force coefficients



Comparison between K and K_{ef} at Various Rotating Speeds

94141-1

Figure 5 Parallel-groove seal effective stiffness

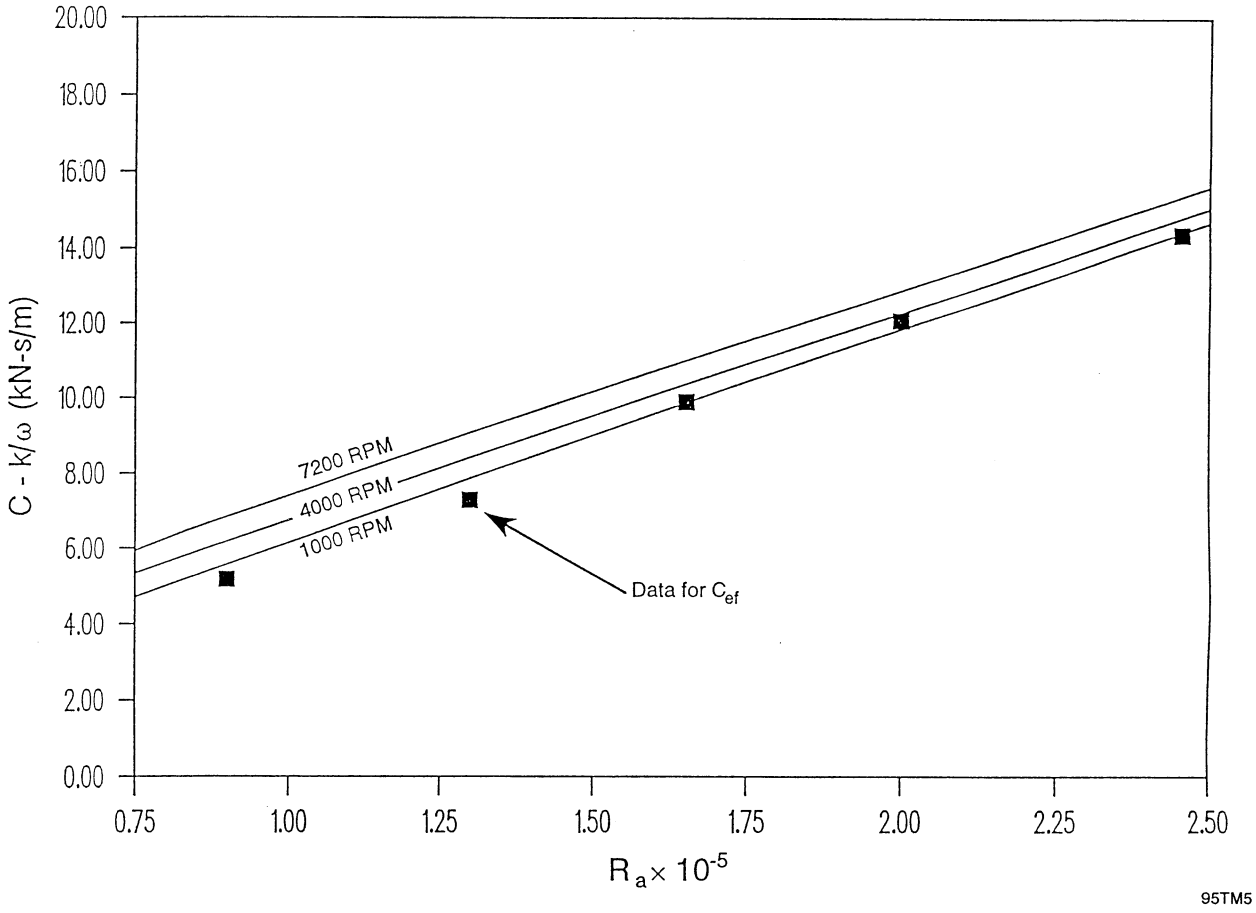


Figure 6 Comparison between C - k/ω and C_{ef} at various rotating speeds

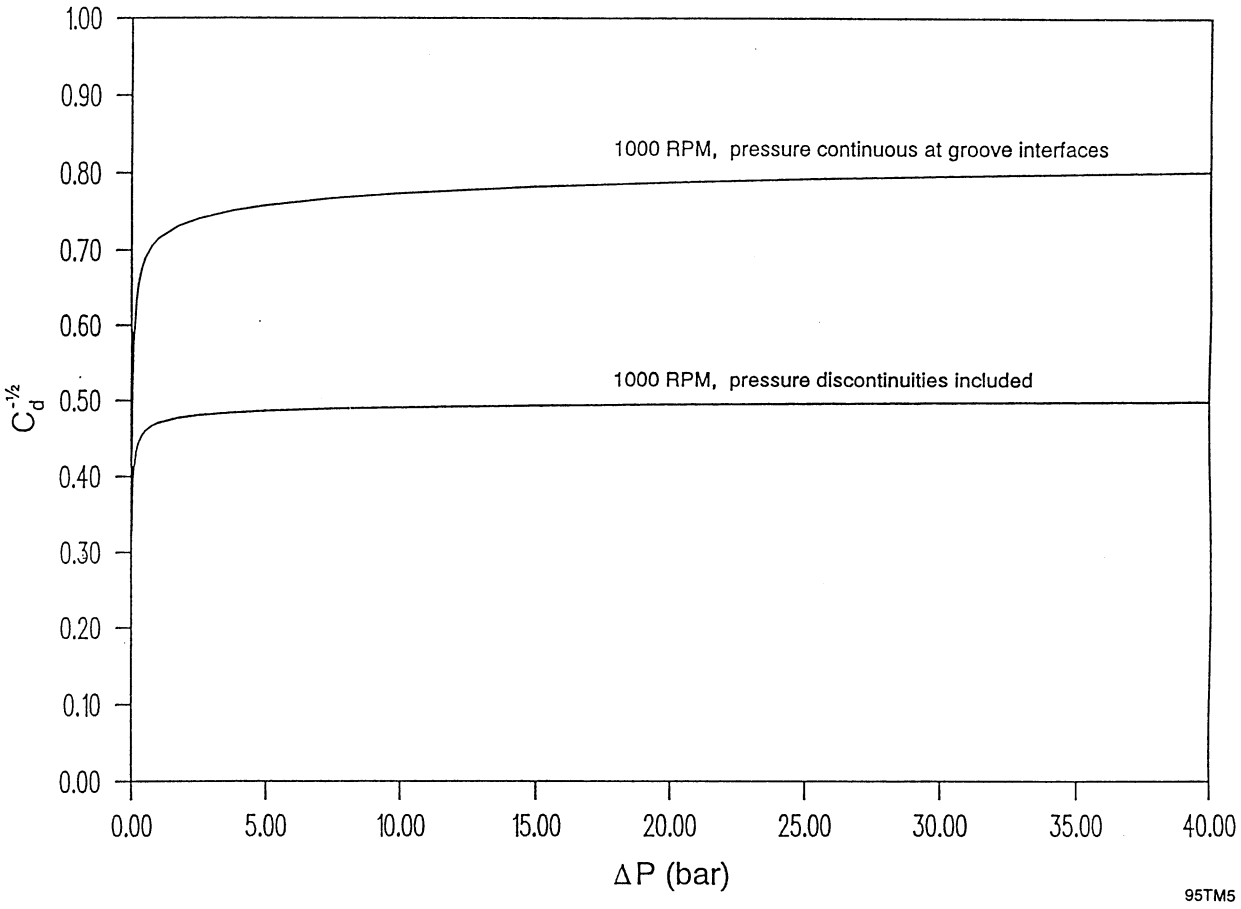


Figure 7 Effect of local pressure discontinuities on predicted axial flow rates

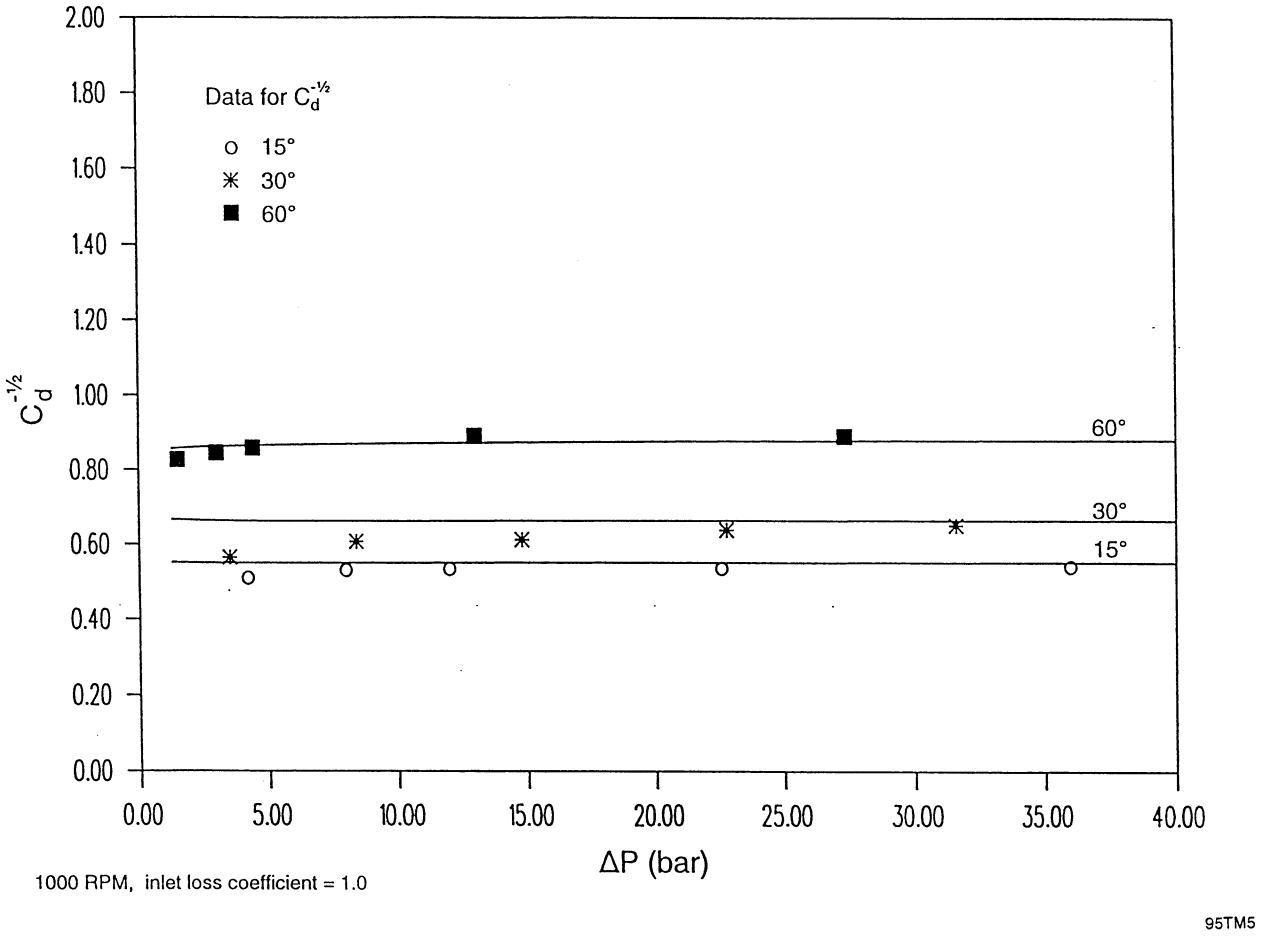


Figure 8 Flow coefficient: SPIRALI compared to reference 1

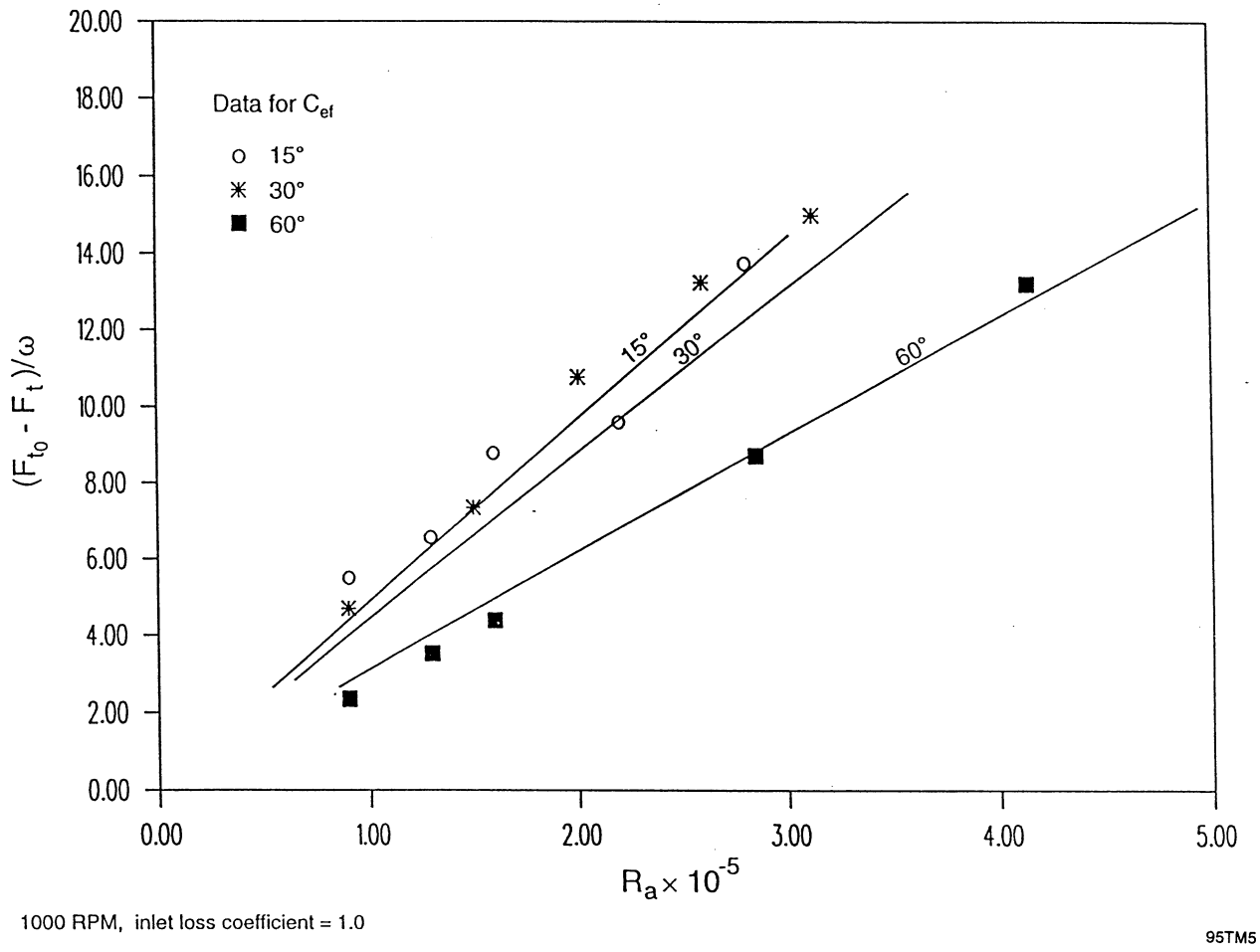


Figure 9 Effective damping: SPIRALI compared to reference 1

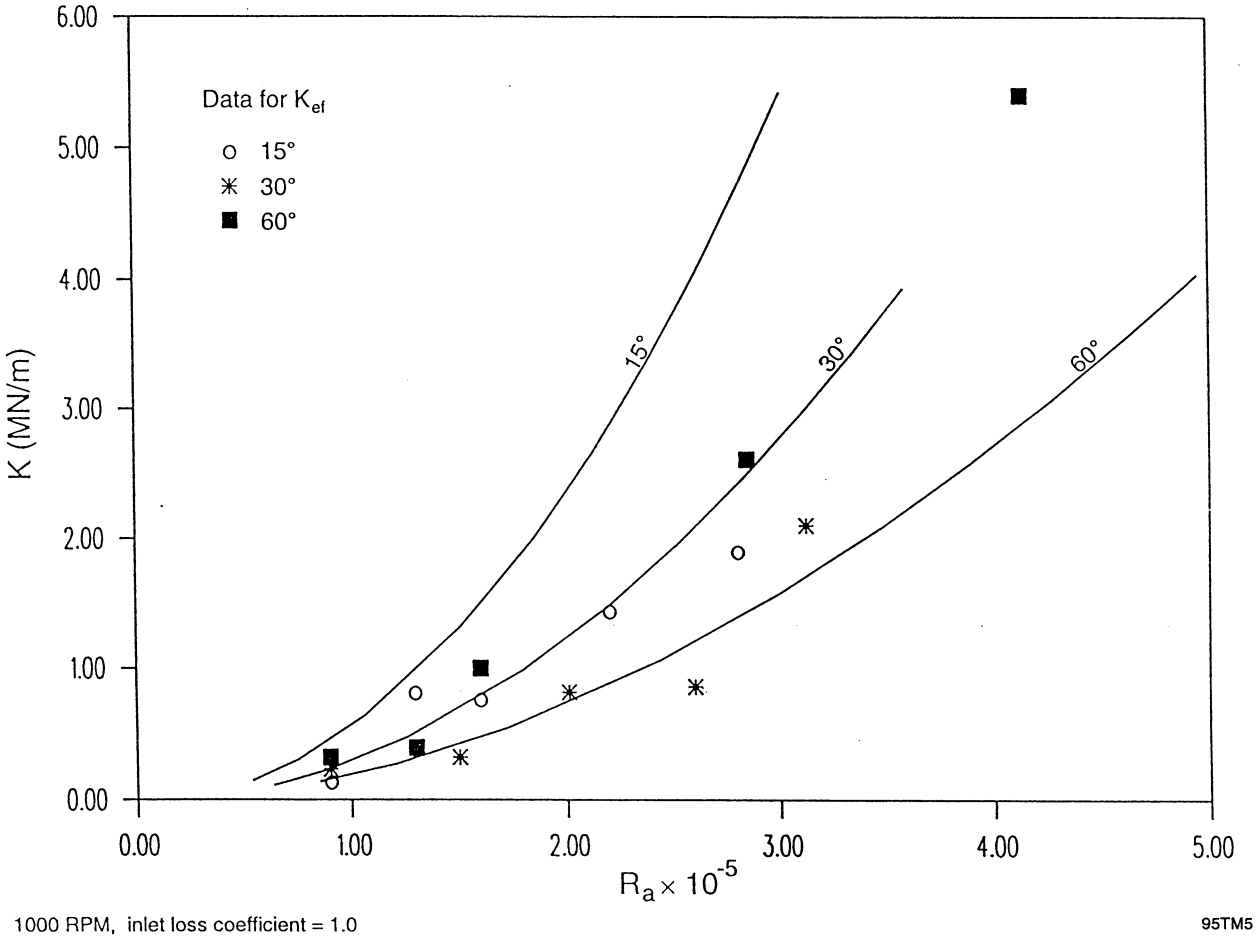


Figure 10 Direct stiffness: SPIRALI compared to reference 1

REPORT DOCUMENTATION PAGE

Form Approved
OMB No. 0704-0188

Public reporting burden for this collection of information is estimated to average 1 hour per response, including the time for reviewing instructions, searching existing data sources, gathering and maintaining the data needed, and completing and reviewing the collection of information. Send comments regarding this burden estimate or any other aspect of this collection of information, including suggestions for reducing this burden, to Washington Headquarters Services, Directorate for Information Operations and Reports, 1215 Jefferson Davis Highway, Suite 1204, Arlington, VA 22202-4302, and to the Office of Management and Budget, Paperwork Reduction Project (0704-0188), Washington, DC 20503.

1. AGENCY USE ONLY (*Leave blank*)	2. REPORT DATE	3. REPORT TYPE AND DATES COVERED
	October 2005	Final Contractor Report

4. TITLE AND SUBTITLE

Users' Manual for Computer Code SPIRALI

Incompressible, Turbulent Spiral Grooved Cylindrical and Face Seals

5. FUNDING NUMBERS

WU–506–42–31–00
WU–590–21–11–00
NAS3–25644

6. AUTHOR(S)

Jed A. Walowit and Wilbur Shapiro

7. PERFORMING ORGANIZATION NAME(S) AND ADDRESS(ES)

Mechanical Technology, Inc.
968 Albany Shaker Road
Latham, New York 12110

8. PERFORMING ORGANIZATION REPORT NUMBER

E–13615

9. SPONSORING/MONITORING AGENCY NAME(S) AND ADDRESS(ES)

National Aeronautics and Space Administration
Washington, DC 20546–0001

10. SPONSORING/MONITORING AGENCY REPORT NUMBER

NASA CR—2003-212359
MTI 95TM5

11. SUPPLEMENTARY NOTES

Jed A. Walowit, Jed A. Walowit, Inc., 4 Cypress Point, Clifton Park, New York 12065; and Wilbur Shapiro, Mechanical Technology, Inc., Latham, New York. Project Manager, Anita D. Liang, Aeropropulsion Projects Office, NASA Glenn Research Center, organization code P, 216–977–7439.

12a. DISTRIBUTION/AVAILABILITY STATEMENT

Restriction changed to Unclassified/Unlimited on July 27, 2005, by authority of the NASA Glenn Research Center, Structures Division.

Export Administration Regulations (EAR) Notice

This document contains information within the purview of the Export Administration Regulations (EAR), 15 CFR 730–774, and is export controlled. It may not be transferred to foreign nationals in the U.S. or abroad without specific approval of a knowledgeable NASA export control official, and/or unless an export license/license exception is obtained/available from the Bureau of Industry and Security, United States Department of Commerce. Violations of these regulations are punishable by fine, imprisonment, or both.

Unclassified-Unlimited
Subject Category: 34
Available electronically at http://gltrs.grc.nasa.gov
This publication is available from the NASA Center for AeroSpace Information, 301–621–0390.

12b. DISTRIBUTION CODE

13. ABSTRACT ***(Maximum 200 words)***

The SPIRALI code predicts the performance characteristics of incompressible cylindrical and face seals with or without the inclusion of spiral grooves. Performance characteristics include load capacity (for face seals), leakage flow, power requirements and dynamic characteristics in the form of stiffness, damping and apparent mass coefficients in 4 degrees of freedom for cylindrical seals and 3 degrees of freedom for face seals. These performance characteristics are computed as functions of seal and groove geometry, load or film thickness, running and disturbance speeds, fluid viscosity, and boundary pressures. A derivation of the equations governing the performance of turbulent, incompressible, spiral groove cylindrical and face seals along with a description of their solution is given. The computer codes are described, including an input description, sample cases, and comparisons with results of other codes.

14. SUBJECT TERMS

Face seals; Seals; Cylindrical seals; Leakage; Incompressible; Spiral-grooved; Turbulent; Users' manual

15. NUMBER OF PAGES

98

16. PRICE CODE

17. SECURITY CLASSIFICATION OF REPORT	18. SECURITY CLASSIFICATION OF THIS PAGE	19. SECURITY CLASSIFICATION OF ABSTRACT	20. LIMITATION OF ABSTRACT
Unclassified	Unclassified	Unclassified	